Washington University in St. Louis
Washington University Open Scholarship

All Theses and Dissertations (ETDs)

1-1-2011

Real-Time Bioluminescence Imaging Of Salmonella-Neoplastic Cell Interactions

Kelly Flentie
Washington University in St. Louis

Follow this and additional works at: https://openscholarship.wustl.edu/etd

Recommended Citation
Flentie, Kelly, "Real-Time Bioluminescence Imaging Of Salmonella-Neoplastic Cell Interactions" (2011). *All Theses and Dissertations (ETDs)*. 575.
https://openscholarship.wustl.edu/etd/575

This Dissertation is brought to you for free and open access by Washington University Open Scholarship. It has been accepted for inclusion in All Theses and Dissertations (ETDs) by an authorized administrator of Washington University Open Scholarship. For more information, please contact digital@wumail.wustl.edu.

Washington University

Division of Biology and Biomedical Sciences

Program in Molecular Microbiology and Microbial Pathogenesis

Dissertation Examination Committee

David Piwnica-Worms, Chairperson

Michael Caparon

Daniel Goldberg

David Haslam

David Hunstad

Jeffrey McKinney

REAL-TIME BIOLUMINESCENCE IMAGING OF *SALMONELLA*-NEOPLASTIC CELL INTERACTIONS

By

Kelly Flentie

A dissertation presented to the

Graduate School of Arts and Sciences of Washington University

in partial fulfillment of the requirements for the degree of

Doctor of Philosophy

August 2011

Saint Louis, Missouri

ABSTRACT OF THE DISSERTATION

Real-Time Bioluminescence Imaging of *Salmonella*-Neoplastic Cell Interactions

by

Kelly Flentie

Doctor of Philosophy in Molecular Microbiology and Microbial Pathogenesis
Washington University in Saint Louis, 2011

Dr. David Piwnica-Worms, Chairperson

Salmonella Typhimurium is a Gram-negative bacterial pathogen and a common cause of gastroenteritis in humans. The organism utilizes a multitude of well-studied virulence factors to invade and replicate in host intestinal epithelial cells and macrophages. Interestingly, *Salmonella* is also capable of localizing to tumors in *in vivo* model systems, and while the typical route of *Salmonella* infection and pathogenesis has been thoroughly investigated, the behavior of *Salmonella* in the tumor microenvironment has not. Therefore, to investigate *Salmonella* and host behavior during bacterial-neoplastic cell interactions, I utilized two high-throughput screens. In the first, I designed a bioluminescent transposon-reporter trap to identify specific *Salmonella* genes activated in the context of cancer cell co-culture conditions. Through this work, I identified five *Salmonella* genes reproducibly activated by co-culture with cancer cells, and further isolated the activating stimulus to low pH. Because low pH is a common characteristic of the tumor microenvironment, I also demonstrated the pH inducibility and reversibility of *Salmonella* gene activation in tumors *ex vivo* and *in vivo.* In a separate study, to better

understand how host neoplastic cells respond to *Salmonella*, I investigated the ability of *Salmonella* to induce pro-inflammatory responses in HCT116 colon carcinoma cells, specifically, NF-κB activation. Then, I performed a high-throughput siRNA screen to identify novel host kinases and phosphatases involved in detection of *Salmonella* and activation of NF-κB signaling. For this work, I used a reporter construct consisting of an IκBα-firefly luciferase fusion protein transcriptionally activated by NF-κB. The reporter permitted imaging of both degradation of the NF-κB negative inhibitor IκBα and its resynthesis, which is dependent on NF-κB activation, following stimulus with *Salmonella*. The host kinase, NME3, was identified in the screen as a specific modulator of NF-κB. Knockdown of NME3 prevents proper activation of NF-κB signaling pathways in HCT116 cells exposed to *Salmonella*, demonstrating the role of this kinase as a positive regulator of NF-κB pro-inflammatory signaling in colon carcinoma cells.

Acknowledgements

Dr. David Piwnica-Worms for all of his patience and guidance throughout my training. He is a wonderful scientist and mentor, and I consider myself fortunate to have worked with him. I will always be grateful for accepting me, a fourth-year microbiologist, into his lab with open arms. He has given me the opportunity to study microbiology in a unique setting, where I have received a truly diverse education.

Everyone in the Piwnica-Worms lab, past, present, and future. The discussions, advice, reagents, lessons, laughs and fun have all been needed and appreciated.

Dr. Jeffrey McKinney for providing me with amazing mentorship in the first few years of my career as a graduate student. His motivation and optimism are inspiring.

Everyone from the McKinney lab for their patience with a fresh, new graduate student.

My committee for their helpful advice and discussions.

My family and friends for all of their patience over the past seven years. Graduate school can be a demoralizing place, and I certainly would not have finished without their unending support.

The National Institutes of Health for the funding. (Molecular Imaging Center at Washington University (P50 CA94056) and NIH Training Grant T32 GM007067 for stipend support)

Table of Contents

Table of Tables

Table of Figures

CHAPTER 1

Introduction

1.1 Introduction to *Salmonella*

The genus *Salmonella* represents a large and diverse collection of Gram-negative bacteria belonging to the family Enterobacteriaceae [1]. It consists of two species of facultatively anaerobic bacilli, *S enterica* and *S bongori* [1]. Six subspecies exist within the species *Salmonella enterica* of which one, *Salmonella enterica* enterica, accounts for 59% of all *Salmonella* isolates, are the only strains regularly found in warm-blooded animals, and include 99% of disease-associated isolates [1]. This subspecies is further divided into multiple serovars based on antigenic determinants of the bacterium, such as its flagellin protein and outer polysaccharide structure [1]. *Salmonella enterica* enterica includes the pathogenic serovars *Salmonella* Typhimurium, *Salmonella* Enteritidis and *Salmonella* Typhi [1].

In the environment, *Salmonella* are maintained as normal flora in multiple diverse vertebrate animals including chickens, cattle and reptiles [2]. Perhaps due to its ubiquity in the environment, *Salmonella* is one of the leading causes of food poisoning in the United States each year [3]. The organism typically causes 30,000-40,000 confirmed infections in the United States annually, approximately 400 of which are fatal, although the true number of *Salmonella* infections is likely much higher [3]. When transmitted to humans, typically by contaminated food and water, *Salmonella* cause an infection termed

Salmonellosis, which most commonly results in a self-limiting gastroenteritis [4]. *S.* Typhimurium is also capable of more severe sequelae and can cause endocardidits and vascular infections by adhering to endothelial cells. In the most severe cases, *Salmonella* can progress to a systemic bacteremia in infected hosts by replicating and surviving within macrophages.

1.2 The Pathogenesis of Salmonella Typhimurium

Invasion

The pathogenesis of *Salmonella* Typhimurium has been studied in detail and much is known about its virulence factors and the molecular mechanisms used during infection of its host (**Figure 1-1**). During the typical route of infection, *Salmonella* bacteria travel through the stomach to the intestine following ingestion [4]. Once in the intestinal lumen, the bacteria utilize type 1 fimbrae to attach to enterocytes [5]. Local environmental conditions in the distal small intestine, the preferred site of *Salmonella* invasion, induce bacteria to activate the *Salmonella* pathogenicity island 1 (SPI-1) genes [6, 7]. SPI-1 refers to one of multiple clusters of virulence genes in the *Salmonella* genome and encodes multiple important virulence genes, including those encoding a type three secretion system (TTSS) and effector proteins that target the host cell [8-14]. The SPI-1 TTSS is a needle-like apparatus with structural similarity to bacterial flagellin [15, 16]. It consists of a basal body, anchoring the structure to the bacterial cell membrane, an ATPase motor and a translocon made of repeating filament protein, capable of delivering effector proteins directly from the bacterial cytosol into the eukaryotic cell [15, 16]. The SPI-1 TTSS has been shown to translocate at least 13 proteins [14]. Many of the secreted

effectors are involved in modulating host actin to induce *Salmonella* uptake into the host cell, indicating an essential role for the SPI1 in bacterial invasion [14]. One of these effectors, SipC, has two important functions. SipC acts both as an outer structural component of the TTSS translocon by forming a pore in the target cell membrane, as well as a nucleator of host actin filaments [17, 18]. As the first secreted effector, SipC therefore begins the host cytoskeletal filamentation process. The second secreted effector protein, SipA, promotes and enhances the actin filamentation process set into motion by SipC [19]. In addition to the initial actin filamentation steps induced by SipC and SipA, *Salmonella* utilizes additional effectors to further induce branching of actin filaments, which fuels the host cell membrane ruffling that promotes bacterial uptake. Two of these effectors, SopE and SopE2, act as guanine exchange factors (GEFs) for host Rac and Cdc42 GTPase proteins [20-22]. The GEF activity of SopE and SopE2 enhances the activity of these host cell molecular switch GTPases, which induce actin branching and cytoskeleton assembly [20-22]. The cooperative actions of SipC and SipA with SopE and SopE2 cause drastic host actin filamentation that results in full uptake of the bacteria into a *Salmonella* Containing Vacuole (SCV) within the host intracellular space.

Following bacterial entry, *Salmonella* effector proteins are also responsible for restoring the host cell actin cytoskeleton to its normal architecture. SptP acts as a GTPase-activating protein (GAP), and reverses the action of SopE by inactivating the host GTPases Rho and Cdc42 [23]. By taking advantage of the different stabilities of the SopE and SptP proteins, *Salmonella* can cover their tracks and reduce the possibility of alerting the immune system of their presence in the newly infected host cell[24]. SopE, as mentioned previously, is a GEF, promoting actin filamentation in target cells. While

SopE and SptP are injected by the SPI-1 TTSS in similar amounts, SopE is quickly targeted and degraded by the host proteasome [24]. Meanwhile, SptP persists to return the host cell membranes to their normal architecture [24].

Intracellular Survival

When *Salmonella* reach the intracellular compartment during infection, they utilize an additional set of effectors to modulate host cell trafficking and preserve the SCV. Within the host cell cytosol, *Salmonella* employ diverse mechanisms to control the composition, environment and intracellular location of the SCV. In general, *Salmonella* within intestinal epithelial cells and those engulfed by infiltrating macrophages during an intestinal infection respond similarly, by modulating intracellular trafficking and replicating within their host cell [25]. Immediately after bacterial entry, the SCV is enriched in early endosome membrane markers [26]. Later, the SCV gains late endosomal and lysosomal markers, localizes to a juxtanuclear position, and acidifies [27, 28]. Acidification of the SCV promotes activation of virulence genes and a second TTSS encoded by the SPI-2 pathogenicity island, while simultaneously repressing the previously used invasion genes of SPI-1 [29, 30]. SPI-2 virulence factors have been implicated in *Salmonella* modulation of host intracellular trafficking and signaling pathways as well as bacterial replication. SPI-2 knockouts are capable of invading host cells, but cause a much less severe disease *in vivo*, showing that these activities are required for a productive systemic infection [31]. It is unclear exactly how *Salmonella* modulate host cell trafficking while in the SCV, but, like the invasion process, the host cytoskeletal membrane dynamics are largely involved. Sixteen effectors have been identified as secreted products of the SPI-2 TTSS and at least half of these have been

known to associate with the endosomal membrane system [32]. Within four to six hours of bacterial invasion of host cells, Sif (*Salmonella* induced filament) formation is observed [33, 34]. These membrane extensions of the SCV are enriched in lysosomal proteins and may form along microtubules [33, 34]. While Sif formation and function are not fully understood, *Salmonella* dedicates multiple effector proteins (SseF, SseG, SseJ and SifA) to their maintenance and robustly induces their formation *in vitro*, indicating their relevance to bacterial virulence and intracellular replication.

1.3 Host Immunity to Salmonella

The Innate Immune Response to Salmonella

To detect and control *Salmonella* infection, hosts rely on the rapid response of innate immunity mechanisms. Innate immunity is considered the first line of defense against a pathogenic organism such as *Salmonella* and consists of extracellular secreted defense molecules, host cell receptors and intracellular signaling pathways. Human cells display multiple receptors designed to recognize pathogen associated molecular patterns (PAMPs) and alert the host as to the presence of a foreign organism. PAMPs include bacterial lipospolyssacharide (LPS), peptidoglycan and flagellin. PAMP receptors are referred to as pattern recognition receptors (PRRs) and those expressed in humans include Toll-like receptors (TLRs) and nucleotide oligomerization domain receptors (NODs). Binding of a PAMP to one of these receptors causes activation of multiple host cell signaling pathways responsible for inducing inflammation, recruiting immune cells and releasing cytokines.

Toll-Like Receptors

One of the major PRRs in the innate immunity system is the Toll-like receptor. The first Toll receptor was discovered in *Drosophila* as a necessary player in proper development, but was later linked to immunity when Toll mutant flies were shown to be more susceptible to fungal infection. To date, 10 different TLRs have been identified in mammalian cells (1-9 pictured in **Figure 1-2**) [35]. TLRs are type 1 transmembrane proteins consisting of an N-terminal extracellular (or intra-endosomal) region of leucine-rich repeats involved in recognizing PAMPs and a cytoplasmic domain necessary for downstream signal transduction [35]. The cytoplasmic domain of TLRs closely resembles the IL-1 receptor cytoplasmic domain, and therefore both of these are called TIR or Toll/interleukin receptor domains [36]. All TLRs are similar in their structures and respond to foreign antigens. However, TLRs are diverse in ligand specificity, subcellular location, required adapter proteins and induction of downstream signaling pathways. TLR3, TLR7, TLR8, and TLR9 respond to intracellular stimuli and are located on endosomal membranes [35]. TLR3 is activated by double-stranded RNA while TLR7 and TLR8 have been shown to respond to single-stranded RNA, both of which are formed during a viral infection. TLR7 and TLR8 have also been demonstrated to respond to synthetic imidazoquinolines, which are small antiviral compounds [37]. TLR9 reacts to viral and bacterial CpG DNA. The remaining TLRs: TLR2, TLR1, TLR6, TLR4 and TLR5 are typically found on the cell membrane and bind extracellular stimuli [35]. TLR2 alone recognizes peptidoglycan, but it also may heterodimerize with TLR1 or TLR6 to respond to bacterial lipopeptides. TLR4 and TLR5 are activated by

bacterial lipopolysaccharide(LPS) and flagellin, respectively. TLR10 has been discovered recently, and its specific ligand is not yet known [38].

Once a TLR is activated, the timing of signal transmission and downstream effects are dependent on adapter proteins recruited to the cytoplasmic TIR domain of the TLR. In general, TLRs can be described as either MyD88-dependent or MyD88–independent based on the TIR-domain adapters utilized. All TLRs except TLR3 and TLR4 require MyD88, though TLR4 can signal through a MyD88-dependent or MyD88-independent pathway [39, 40]. Some TLRs signal directly to MyD88, but TLR1, TLR2, TLR4 and TLR6 use a bridge adapter protein called TIRAP [40]. Once activated, MyD88 first recruits IRAK4 (IL-1R associated kinase), which in turn recruits IRAK1 and TRAF6 [41, 42]. This leads to recruitment and activation of the TAK1/TAB kinase complex [43, 44]. The TAK1/TAB kinase complex activates downstream targets including both MAPK (mitogen-activated protein kinase) pathways and the NF-κB **(**nuclear factor kappa-light-chain-enhancer of activated B cells) pathway through IKK (inhibitor of κB kinase) [44]. In the case of TLR3 and TLR4, which can signal independently of the MyD88 adapter, TRIF binds directly to the TIR domain of TLR3 to transduce the signal, or TRAM serves as an adapter to TRIF in the case of TLR4 [40, 45]. TRIF activates TRAF6 and RIP1, leading to IKK activation, and downstream NF-κB signaling as in MyD88-dependent TLR activation, but on a much different timescale than MyD88 dependent TLR signaling [42, 46]. In addition to NF-κB, IRF3 (interferon regulator factor 3) is a key transcription factor activated in the MyD88-independent pathway [47]. In this signaling node, TLR3 and TLR4 are both capable of activating non-canonical IKKs through TRAF3 [48]. The non-canonical IKKs (TBK1 and Ikke/IKKi) activate IRF3, which can then dimerize and

translocate to the nucleus, where it activates transcription at IFN-stimulated response elements (ISRE) [48]. IRF3 has also been shown to form a complex with NF-κB and ATF2/C-Jun called the enhanceasome, which activates interferon beta transcription [48]. Although different TLRs have similar structures, diversity in response is achieved by the intracellular adapters and signaling proteins targeted by each TLR.

Toll-Like Receptor 5

Toll-like receptor 5 was discovered in 1998 and in 2001 was shown to recognize both Gram-positive and Gram-negative bacterial flagellin, and to robustly induce IL-6 production *in vivo* in a MyD88-dependent manner [49]. TLR5 engagement leads to MAPK and NF-κB activation and the eventual downstream activation of 500 genes including chemokines, stress response genes and anti-apoptotic genes [50]. The receptor is expressed on dendritic cells, monocytes and epithelial cells, and is likely involved not only in classic response to pathogens, but also in keeping proper gut homeostasis [51, 52].

TLR5 binds most bacterial flagellin. In the *Salmonella* FliC protein, the specific recognition site has been isolated to a 13 amino acid sequence [53]. This sequence is required for flagellin filament polymerization and therefore bacterial motility, demonstrating the precision of the host innate immunity response [53]. Further, previous studies have demonstrated that flagellin is the major proinflammatory determinant of *Salmonella* in some cases and that flagellin exposure elicits a strong activation of cytokine release by host cells [50].

TLR5 activity is robustly pro-inflammatory, and therefore multiple mechanisms exist to keep activity in check. The cell is capable of down-regulating TLR5 signaling thru PI3K (phosphoinositide 3-kinase), which prevents over-expression of proinflammatory genes by regulating MAPK signaling [54]. There is also evidence that the host protein Muc1 can interact with flagellin and dampen downstream TLR5 signaling [55]. The location of TLR5 also contributes to its control. *In vivo*, TLR5 expression is limited to the basolateral membrane of the colon, thereby preventing overactive signaling due to flagellated commensal microbes in the intestinal lumen [56]. Flagellin must therefore breach the gastrointestinal barrier to induce signaling in normal cells. Still, TLR5 is readily able to be activated by flagellin of commensals as well as pathogens, indicating that the accessibility of flagellin, and not the pathogenicity of the species, is the main factor in TLR5 activation [57].

As an integral activator of inflammatory signaling, TLR5 loss or dysfunction has very serious consequences in the host. A TLR5-deficient mouse model has been developed that fails to activate any proinflammatory pathways in response to flagellin, providing a valuable and informative system to study the importance of TLR5 *in vivo*. The mice develop a severe metabolic syndrome marked by obesity and insulin resistance in addition to a tendency to develop spontaneous colitis [58, 59]. These phenotypes may be a result of changes in the composition of the microbiota, identifying a role for TLR5 in maintenance of proper gut homeostasis [58, 59].

TLR5 loss has differing effects on *Salmonella* pathogenesis, depending on the route of infection. TLR5 knockout mice develop more severe gastroenteritis in an antibiotic pretreatment mouse model of *Salmonella* intestinal infection [60]. However, the mice are

resistant to *Salmonella* infection in a typhoid-mouse model, and this resistance is not specific to flagellated *Salmonella* [60]. Finally, TLR5 knockout mice demonstrate higher levels of basal expression of certain innate immunity genes and of IgG and IgA, indicating constitutively active immune responses may protect mice in the typhoid model [60]. The complicated role of TLR5 uncovered by the TLR5-deficient mouse demonstrates the need to further characterize the exact downstream signaling pathways to understand how *Salmonella* interacts with its host.

TLR signaling may also promote *Salmonella* infection. In one study utilizing a mouse model of gastroenteritis, *Salmonella* relied on induction of host pro-inflammatory responses to target host normal microbial flora to optimally colonize the host [61]. This may reduce competition for *Salmonella*, allowing the bacteria to gain better access to host cells and promote invasion. In another study, while the researchers did not look individually at TLR5, they showed signaling by other TLRs induced vacuolar acidification and consequently, provided a cue to induce bacterial virulence factor expression and secretion by intracellular *Salmonella* [62]. Clearly, TLR5 signaling may lead to varied host responses to *Salmonella* infection, depending on the route and site of inoculation, highlighting the need for a more thorough understanding of *Salmonella*-induced signaling pathways.

NF-κB Signaling

One of the major transcriptional nodes activated downstream of all TLR signaling is NF-κB. NF-κB was originally discovered as a transcription factor utilized during B

lymphocyte development, but was later recognized as a broad transcriptional activator used in numerous situations**.** NF-κB now refers to a family of multiple transcription factors that act as master regulators and integrators of host innate immunity and as promoters of inflammation as well as general cellular responses to stress and cellular differentiation and development. Specific receptors including TLRs, Tumor Necrosis Factor Receptor (TNFR), and Interleukin-1Receptor (IL-1R) signal through NF-κB to activate target genes involved in cytokine production, cell adhesion, immunoreceptors, and additional transcription factors [63]. NF-κB signaling pathways can generally be divided into two types: canonical and non-canonical signaling [64]. Canonical NF-κB signaling includes the typical inflammatory-associated NF-κB signaling and occurs on a much shorter timescale than non-canonical signaling [64].

The NF-κB family consists of 5 proteins with a Rel homology domain (RHD): RelA, RelB, cRel, p50 and p52 [63]. These monomers are capable of associating via their RHDs into 15 potential homodimers and heterodimers [63]. The primarily used NF-κB dimer in the canonical pathway is the RelA-p50 heterodimer, where RelA contains the transactivating domain [63]. In a resting state, the NF-κB heterodimer is held in the cell cytoplasm by one of three classical IκB proteins, IκBα, IκBβ, or IκBε, which bind NF-κB through their ankyrin repeats domain (ARD) [63]. When an upstream receptor, such as a TLR, is activated, signal transduction pathways lead to activation of IKK kinase complexes containing IKKγ , IKKα and IKKβ [63]. Activated IKK phosphorylates IκBα, which induces recruitment of an E3 ubiquitin ligase [63]. IκBα is ubiquitinated and subsequently degraded by the proteasome, leaving the nuclear localization signal (NLS) of the NF-κB dimer unmasked [63]. NF-κB translocates to the host nucleus, where it

activates host genes involved in management of stress response and inflammation as well as its own negative regulator IκBα, making this a classic negative feedback loop [63].

Because NF-κB is such a crucial regulator in host innate immunity, *Salmonella* has evolved multiple mechanisms to evade host detection and activation of NF-κB. First, the organization of flagellin itself is such that the immunogenic portion is predominantly hidden in the polymerized protein [53]. It seems *Salmonella* has evolved a way to mask the majority of flagellin's immunostimulatory activity as it is polymerized on the bacterial surface. *Salmonella* also secretes multiple effectors capable of down-regulating NF-κB signaling. One of these, SspH1, translocates to the host nucleus, where it inhibits NF-κB transcriptional activation [65]. Another *Salmonella* effector protein, AvrA, is also injected into the host cell cytoplasm by the SPI-1 TTSS and seems to play an important role in reducing host proinflammatory signaling [66, 67]. Although its exact mechanisms are not fully understood, it blocks NF-κB activity, perhaps by acetyltransferase activity on downstream players in the NF-κB pathway [66, 67]. NF-κB represents a potential block to a productive *Salmonella* infection, and to compensate, the pathogen positions considerable resources into the development of an anti-NF-κB response.

1.4 Salmonella Interactions with Neoplastic Host Cells

The Inflammation-Cancer Axis

Overactive NF-κB signaling can have dire consequences for the host, indicated by the multiple mechanisms in place that keep its activity in check. Perhaps the most important tactic used by the host to control NF-κB signaling is NF-κB's direct transcriptional activation of its own negative regulator. Activated NF-κB induces transcription of IκBα, which, after translation in the cytoplasm, is thought to translocate to the nucleus, bind

NF-κB, and export the transcription factor [68]. The RelA subunit of NF-κB has also been demonstrated to interact with histone deacetylasese (HDACs), which are known to negatively regulate transcription [69]. Further, once activated, the NF-κB signaling pathway resists further stimulation [70]. In one study, NF-κB activation was measured after a TNFα preconditioning step [70]. Following a 30-second exposure to TNFα, IKK-mediated NF-κB activation was severely compromised for up to 120 minutes, indicating that cells can be desensitized to NF-κB stimulatory activity, thus preventing over-response [70].

However, even with mechanisms in place to prevent over-stimulation of NF-κB, cells exposed to excessive amounts of proinflammatory stimuli may experience deleterious effects. Chronic and overactive inflammation has long been suspected as a contributing factor to cancer development, and recently, more information on how infection and inflammation may lead to carcinogenesis has emerged. Collectively, infections and inflammation may be at least part of the underlying cause of up to 20% of all cancer deaths [71]. There are several known clinical associations between infection or inflammation and cancers including Hepatitis viruses HBV and HCV in liver cancers, *Helicobacter pylori* in gastric cancers and the link between inflammatory bowel diseases (IBDs) and colorectal cancers, as well as leukemia and other cancers caused by human T-lymphotropic virus (HTLV) [72-74]. Additionally, there is evidence of genetic polymorphisms within the TLR and IL-1β promoters that positively associate with prostate and gastric cancers, respectively [75].

Because carcinogenesis is a lengthy and undefined process, it is difficult to effectively study the cancer-inflammation linkage in the laboratory. However, several studies have

produced convincing examples of how misregulated NF-κB signaling can directly contribute to tumor formation. In a colitis-associated cancer (CAC) model in mice, the chemical dextran-sulfate sodium salt (DSS) contributes to tumor formation by damaging the mucosal barrier and exposing underlying cells to resident normal flora bacteria. Inactivation of IKK-β in enterocytes of this model reduced tumor number by 80%, clearly indicating a role for the NF-κB pathway in tumor induction in this system [76]. In another model system, the *mdr2* knockout mouse, the lack of an *mdr2* transporter causes accumulation of lipids and bile acids within hepatic cells, which results in spontaneous tumor formation within 8-10 months [77, 78]. However, when the IκB super repressor blocks signaling, tumor formation was blocked as well, indicating cellular stress mediates tumor development through NF-κB signaling [77]. In another study, Oguma *et al* link the TNF secreted by macrophages, presumably a result of macrophage NF-κB signaling activation when recruited to the site of a gastric infection, with increased Wnt/β catenin signaling and gastric tumor formation [79]. Finally, the protein HIF-1α links bacteria, NF-κB and cancer as well. HIF-1α is a transcription factor that is stabilized and activated in conditions of low oxygen [80]. Researchers have recently shown that following detection of bacteria and subsequent host activation of innate immunity pathways, NF-κB activates HIF-1α transcription, likely in response to the hypoxic conditions replicating bacteria induce in their host [80]. Coincidentally, tumors produce low oxygen environments as well, indicating that activation of this transcription factor in response to bacteria also better equips the host for fitness in a pro-tumor environment. Between epidemiological associations and the new data being uncovered in the laboratory, the link between inflammation, infection and cancer is growing.

Bacteria as a Cancer Therapeutic: A Historical Perspective

Interestingly, in addition to being a hypothesized contributor to cancer formation, *Salmonella* has recently received consideration as a potential theraputic for cancer. Although the typical route of *Salmonella* infection is gastrointestinal, which may lead to chronic carriage or a systemic infection, *Salmonella* infections of the host are also capable of another unique consequence [4]. *Salmonella* are capable of colonizing a host animal at the site of a tumor *in vivo* [81]. Notably, a correlation between cancer remission and coincident bacterial infection was observed as early as the 14th century [81]. In the 1800's, the first intentional use of bacteria to treat cancer has been attributed to Dr. W. Busch, who exposed a tumor patient to the bed linens previously used by a patient with a *Streptococcus* infection [82]. Despite rapid tumor shrinkage, the woman contracted a severe bacterial infection and died soon thereafter [82]. In later work, Dr. William Coley pioneered the use of "Coley's toxin", a treatment composed of inactivated bacteria including *Streptococci* and *Serratia marcesens* [82]. Dr. Coley reported tumor regression, perhaps via host systemic responses involving induction of tumor necrosis factor [81, 82]. Still, intentional infection with bacteria, especially before the advent of antibiotic use, was generally unpredictable and difficult to control [81, 82]. The toxic side effects and lack of reproducibility of such treatments eventually led to discontinuation of their use [82].

Salmonella: *Localization to Tumors*

Recently, anaerobic and facultatively anaerobic bacteria, among other organisms, have been shown to selectively localize to and replicate within malignant tumors. *Clostridium, Bifidobacteria, Escherichia coli, Listeria, Streptococcus pyogenes* and *Salmonella* have

each been used in contemporary studies exploring bacterial-based tumor treatment [82]. *Salmonella* appears to affect a diverse set of neoplastic cells or tumors, including: melanomas, gliomas and neuroblastomas, renal carcinomas, and cancers of the prostate, breast, bladder and colon [82-88]. Using noninvasive bioluminescent imaging to track *Salmonella* expressing plasmid encoded *luxCDABE*, Yu *et al* showed that *Salmonella* could report malignant tumor locations in living mice. *Salmonella* are impressively tumor adaptable. They have been shown to localize in tumors with tumor:tissue ratios up to 9,000 times that of normal tissue, to localize to tumors in both immunocompetent and immunocompromised mice, and to detect and replicate within metastases as well [88, 89]. In independent work, electron micrographs of excised melanoma tumors detect *Salmonella* within the cytosol of melanoma tumor cells, suggesting bacteria not only localize to, but may actually invade, malignant tumor cells [82]. However, it remains to be definitively shown how *Salmonella* behave in the tumor environment. For instance, it is not fully understood whether *Salmonella* are capable of invading cancer cells or what types of cancer cells *Salmonella* will enter. Also, it is unclear to what extent the molecular mechanisms of *Salmonella* virulence and the specific gene regulation events during interactions with cancer cells recapitulate those utilized during a classical *Salmonella* infection.

Salmonella *as a Potential Cancer Therapeutic*

Cancer is predicted to kill more than 500,000 people in the United States in 2011 [90]. In this same year, more than 1.5 million Americans will be newly diagnosed with cancer [90]. Unfortunately, despite some notable advances, many patients with cancer still must contend with remarkably poor diagnosis and treatment options [91-93]. Diagnosis often

occurs far too late in disease progression, after metastases decrease the odds of survival. In general, chemotherapy and radiation therapy regimens have significant associated systemic side effects. One way to improve the therapeutic index (overall efficacy vs. toxicity) of cancer treatments may be to more specifically localize treatment effects to malignant tissues.

Given its localization to malignant tumors, appropriately engineered *Salmonella* might serve well as an anti-tumor agent. To date, some such efforts have exploited *Salmonella*'s ability to carry tumor antigens. Others have aimed to activate the immune response to attack tumor cells, independent of the bacteria localization to the tumor site. Immunotherapy-based strategies are often restricted by limited knowledge of tumor markers and their immunogenicity. *Salmonella* flagellin has been directly injected into tumors in an attempt to slow their growth, a strategy that exploits flagellin as a more general immune stimulus [87]. However, this treatment failed to effect growth of a weakly immunogenic tumor. Attenuated *Salmonella* expressing human IL-2 can also retard tumor growth in mice [94]. Yet, while *Salmonella*-based immunotherapy has enjoyed moderate success, utilizing it to treat neoplastic tumors seems contradictory, given that such tumors are a noted site of immunosuppression. It is likely that further progress in understanding – and perhaps exploiting – the interactions between bacteria and tumors can be made by investigating the mechanisms behind *Salmonella* interaction with host tumors.

Salmonella *Behavior in the Tumor Environment*

Two nonexclusive hypotheses have been proposed to explain *Salmonella*'s preference for survival in malignant tumors. First, the anaerobic, necrotic, or highly vascular

environments in and around tumors may provide bacteria with an advantageous niche for growth [95]. Second, the bacteria may selectively replicate in tumors due to immune protection. However, very little is known about whether the bacteria themselves behave differently in response to cancer cells. In particular, it has not been determined how neoplastic host cells, in contrast to normal (i.e., non-neoplastic) host cells, might specifically trigger *Salmonella* gene expression. Neoplastic cells often exhibit notable phenotypes, including alterations in cell cytoskeleton, signaling pathways, replication patterns, or expression of surface or secreted proteins [96]. In theory, any of these host cell factors might modify bacterial gene expression. Recent findings support the premise that neoplastic tumors may well alter *Salmonella*'s behavior. For example, in an *in vitro* tumor model system, *Salmonella* migrate toward and collect in cylindrical aggregates of tumor cells [97, 98]. These findings raise the prospect that tumor cells release compounds *Salmonella* can sense and travel toward. In another study, *Salmonella* recovered from tumors *in vivo* were more efficient at subsequently attaching to, invading, and replicating within colon adenocarcinoma cells *in vitro* than the parent strain [84]. The fact that *in vivo* passage through a mouse tumor produced a *Salmonella* strain with an enhanced tumor-targeting phenotype suggests that *Salmonella* can indeed be modified by interactions with tumors. Perhaps these phenotypic changes reflect *Salmonella* gene expression events involved in tumor localization, attachment and persistence.

The seemingly conflicting ideas of *Salmonella* as both pro-cancer and anti-cancer agent leave the state of the field unclear. Work must be done to clarify how *Salmonella* immunostimulatory activity may lead to cancer-causing environments and what effect colonization of the tumor has on bacterial activity. The dynamic interplay between

Salmonella and the host will inform development of future tumor and *Salmonella* therapeutics.

1.5 Bioluminescence Imaging as Tool to Study Prokaryotes and Eukaryotes

The points addressed above rely on gaining more information on *Salmonella* interactions with its host on a global level. One powerful, emerging technique, bioluminescence imaging (BLI), provides the reliability and throughput necessary to study *Salmonella* behavior much more dynamically than ever before. BLI is based on the use of eukaryotic or prokaryotic encoded luciferase enzymes that catalyze a reaction utilizing ATP, oxygen, and a luciferin substrate to produce light. In eukaryotic systems, firefly luciferase from *Photinus pyralis* is most commonly used [99]. Bioluminescently-tagged tumor xenografts have provided a convenient and reliable way to monitor tumor progression during therapeutic studies [99]. Also, eukaryotic luciferase can be coupled to proteins of interest, and used in studies of signaling pathways, protein stability, and gene transcriptional activity [99].

Several bacterial luciferases are also available, originally from the organisms *Vibrio harveyyi, Vibrio fischeri* or *Photorhabdus luminescens* [100]. Unlike eukaryotic luciferases, which generally require the addition of exogenous substrate for imaging, the biosynthetic pathways for the bacterial luciferin substrate are relatively simple and a single five gene operon is responsible for both the luciferase enzyme and substrate production [100]. Studies of microorganisms *in vivo* are uniquely suited to BLI and bacterial-based imaging strategies encompass *in vivo*, *in vitro* and *in cellulo* reporter studies. This is evident especially when imaging bacterial infection models, since use of

a bacterial *lux* operon allows for BLI in real time, without requiring administration of exogenous substrate. Furthermore, traditional *in vivo* infection models have required host sacrifice and enumeration of microorganisms from individual host organs to determine the extent and kinetics of dissemination during infection. BLI provides a unique opportunity to serially monitor infection in a single host over time, often resulting in identification of new sites of replication and persistence within an infected animal [99]. Finally, in the investigation of bacteria as a potential diagnostic and treatment tool for cancer, BLI has become a particularly popular technique. In such cases, bacterial luciferase has allowed for imaging the localization of bacteria to a tumor in a mouse in real time [99].

1.6 Conclusion of the Introduction

Salmonella Typhimurium is a well-studied human pathogen. Emerging from the wealth of knowledge on *Salmonella* and its genetic tractability is the desire to use the pathogen in new ways – namely, as a cancer diagnostic and therapeutic tool. However, *Salmonella* is still a pathogen, and therefore may still produce dangerous consequences within hosts, especially one that may be immunocompromised, such as cancer patients. The answer to this challenge is not to abandon *Salmonella*-based treatment altogether, but to search for a deeper understanding of *Salmonella*-host interactions. *Salmonella* may prove to be a simple, cost-effective and robust tumor treatment technique, but will require further study of how *Salmonella* and the host co-exist to better inform future options.

1.7 Figures

Figure 1-1

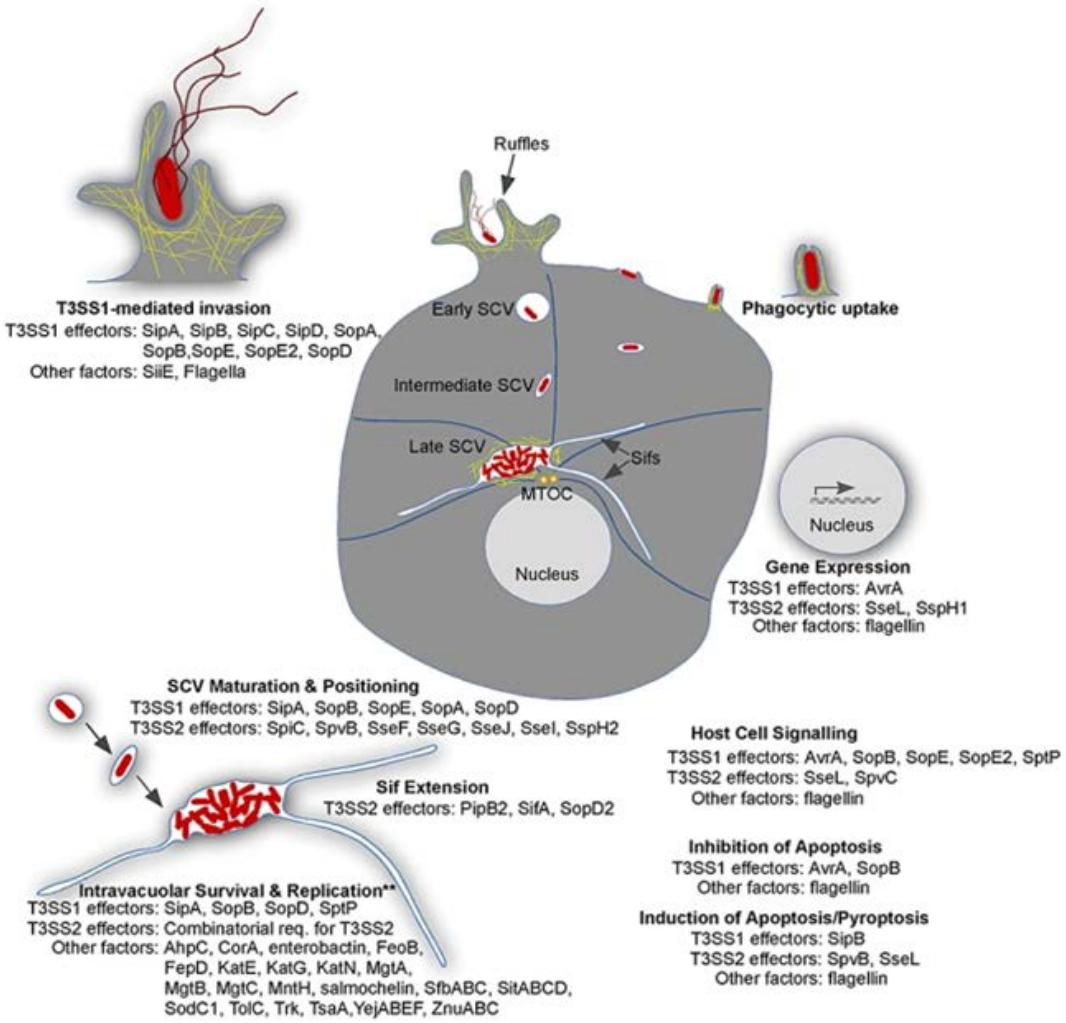

Figure 1-1: The Pathogenesis of *Salmonella* Typhimurium

Salmonella Typhimurium utilizes two separate Type Three Secretion Systems (TTSS) during invasion and pathogenesis of host cells. Initially, the SPI-1 TTSS induces host actin filamentation, resulting in bacterial uptake. Intracellularly, the SPI-2 TTSS

promotes bacterial survival and replication through futher host actin cytoskeletal remodeling and SCV maintenance.

Adapted from: Ibarra J. A., Steele-Mortimer O. (2009). *Salmonella*-the ultimate insider. *Salmonella* virulence factors that modulate intracellular survival. *Cell Microbiol.* 11, 1579–1586.

Figure 1-2

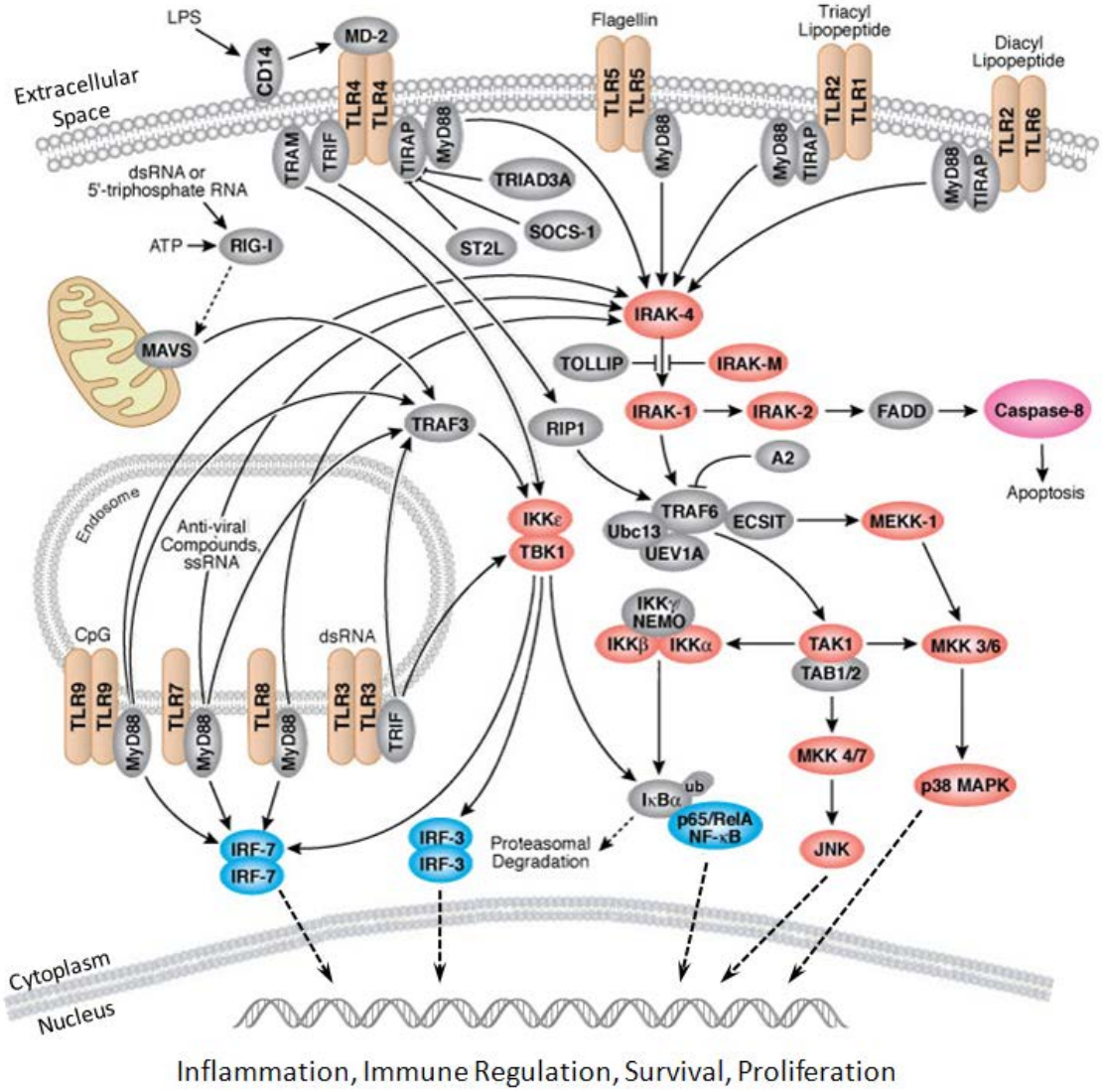

Figure 1-2: Toll-Like Receptor Signaling

Eukaryotic Toll-like receptors respond to extracellular and intracellular foreign antigens, resulting in signaling pathway activation and nuclear activation of pro-inflammatory transcriptional programming.

Adapted from: http://www.cellsignal.com/reference/pathway/pdfs/Toll_Like.pdf

1.8 References

1. Brenner, F.W., et al., *Salmonella nomenclature.* J Clin Microbiol, 2000. **38**(7): p. 2465-7.

2. Liebana, E., *Molecular tools for epidemiological investigations of S. enterica subspecies enterica infections.* Res Vet Sci, 2002. **72**(3): p. 169-75.

3. Voetsch, A.C., et al., *FoodNet estimate of the burden of illness caused by nontyphoidal Salmonella infections in the United States.* Clin Infect Dis, 2004. **38 Suppl 3**: p. S127-34.

4. Giannella, R.A., *Salmonella.* 1996.

5. Ernst, R.K., D.M. Dombroski, and J.M. Merrick, *Anaerobiosis, type 1 fimbriae, and growth phase are factors that affect invasion of HEp-2 cells by Salmonella typhimurium.* Infect Immun, 1990. **58**(6): p. 2014-6.

6. Jones, B.D., N. Ghori, and S. Falkow, *Salmonella typhimurium initiates murine infection by penetrating and destroying the specialized epithelial M cells of the Peyer's patches.* J Exp Med, 1994. **180**(1): p. 15-23.

7. Altier, C., *Genetic and environmental control of salmonella invasion.* J Microbiol, 2005. **43 Spec No**: p. 85-92.

8. Eichelberg, K., C.C. Ginocchio, and J.E. Galan, *Molecular and functional characterization of the Salmonella typhimurium invasion genes invB and invC: homology of InvC to the F0F1 ATPase family of proteins.* J Bacteriol, 1994. **176**(15): p. 4501-10.

9. Galan, J.E. and C. Ginocchio, *The molecular genetic bases of Salmonella entry into mammalian cells.* Biochem Soc Trans, 1994. **22**(2): p. 301-6.

10. Ginocchio, C.C., et al., *Contact with epithelial cells induces the formation of surface appendages on Salmonella typhimurium.* Cell, 1994. **76**(4): p. 717-24.

11. Ginocchio, C., J. Pace, and J.E. Galan, *Identification and molecular characterization of a Salmonella typhimurium gene involved in triggering the internalization of salmonellae into cultured epithelial cells.* Proc Natl Acad Sci U S A, 1992. **89**(13): p. 5976-80.

12. Galan, J.E., C. Ginocchio, and P. Costeas, *Molecular and functional characterization of the Salmonella invasion gene invA: homology of InvA to members of a new protein family.* J Bacteriol, 1992. **174**(13): p. 4338-49.

13. Zierler, M.K. and J.E. Galan, *Contact with cultured epithelial cells stimulates secretion of Salmonella typhimurium invasion protein InvJ.* Infect Immun, 1995. **63**(10): p. 4024-8.

14. Galan, J.E., *Molecular genetic bases of Salmonella entry into host cells.* Mol Microbiol, 1996. **20**(2): p. 263-71.

15. Kubori, T., et al., *Molecular characterization and assembly of the needle complex of the Salmonella typhimurium type III protein secretion system.* Proc Natl Acad Sci U S A, 2000. **97**(18): p. 10225-30.

16. Kubori, T., et al., *Supramolecular structure of the Salmonella typhimurium type III protein secretion system.* Science, 1998. **280**(5363): p. 602-5.

17. Scherer, C.A., E. Cooper, and S.I. Miller, *The Salmonella type III secretion translocon protein SspC is inserted into the epithelial cell plasma membrane upon infection.* Mol Microbiol, 2000. **37**(5): p. 1133-45.

18. Hayward, R.D. and V. Koronakis, *Direct nucleation and bundling of actin by the SipC protein of invasive Salmonella.* Embo J, 1999. **18**(18): p. 4926-34.

19. Zhou, D., M.S. Mooseker, and J.E. Galan, *Role of the S. typhimurium actin-binding protein SipA in bacterial internalization.* Science, 1999. **283**(5410): p. 2092-5.

20. Hardt, W.D., et al., *S. typhimurium encodes an activator of Rho GTPases that induces membrane ruffling and nuclear responses in host cells.* Cell, 1998. **93**(5): p. 815-26.

21. Stender, S., et al., *Identification of SopE2 from Salmonella typhimurium, a conserved guanine nucleotide exchange factor for Cdc42 of the host cell.* Mol Microbiol, 2000. **36**(6): p. 1206-21.

22. Friebel, A., et al., *SopE and SopE2 from Salmonella typhimurium activate different sets of RhoGTPases of the host cell.* J Biol Chem, 2001. **276**(36): p. 34035-40.

23. Fu, Y. and J.E. Galan, *A salmonella protein antagonizes Rac-1 and Cdc42 to mediate host-cell recovery after bacterial invasion.* Nature, 1999. **401**(6750): p. 293-7.

24. Kubori, T. and J.E. Galan, *Temporal regulation of salmonella virulence effector function by proteasome-dependent protein degradation.* Cell, 2003. **115**(3): p. 333-42.

25. Steele-Mortimer, O., *The Salmonella-containing vacuole: moving with the times.* Curr Opin Microbiol, 2008. **11**(1): p. 38-45.

26. Steele-Mortimer, O., et al., *Biogenesis of Salmonella typhimurium-containing vacuoles in epithelial cells involves interactions with the early endocytic pathway.* Cell Microbiol, 1999. **1**(1): p. 33-49.

27. Rathman, M., M.D. Sjaastad, and S. Falkow, *Acidification of phagosomes containing Salmonella typhimurium in murine macrophages.* Infect Immun, 1996. **64**(7): p. 2765-73.

28. Salcedo, S.P. and D.W. Holden, *SseG, a virulence protein that targets Salmonella to the Golgi network.* Embo J, 2003. **22**(19): p. 5003-14.

29. Drecktrah, D., et al., *The mechanism of Salmonella entry determines the vacuolar environment and intracellular gene expression.* Traffic, 2006. **7**(1): p. 39-51.

30. Lober, S., et al., *Regulation of Salmonella pathogenicity island 2 genes by independent environmental signals.* Int J Med Microbiol, 2006. **296**(7): p. 435-47.

31. Hensel, M., et al., *Simultaneous identification of bacterial virulence genes by negative selection.* Science, 1995. **269**(5222): p. 400-3.

32. Abrahams, G.L. and M. Hensel, *Manipulating cellular transport and immune responses: dynamic interactions between intracellular Salmonella enterica and its host cells.* Cell Microbiol, 2006. **8**(5): p. 728-37.

33. Brumell, J.H., D.L. Goosney, and B.B. Finlay, *SifA, a type III secreted effector of Salmonella typhimurium, directs Salmonella-induced filament (Sif) formation along microtubules.* Traffic, 2002. **3**(6): p. 407-15.

34. Brumell, J.H., et al., *Characterization of Salmonella-induced filaments (Sifs) reveals a delayed interaction between Salmonella-containing vacuoles and late endocytic compartments.* Traffic, 2001. **2**(9): p. 643-53.

35. Brown, J., et al., *TLR-signaling networks: an integration of adaptor molecules, kinases, and cross-talk.* J Dent Res. **90**(4): p. 417-27.

36. Slack, J.L., et al., *Identification of two major sites in the type I interleukin-1 receptor cytoplasmic region responsible for coupling to pro-inflammatory signaling pathways.* J Biol Chem, 2000. **275**(7): p. 4670-8.

37. Gorden, K.K., et al., *Oligodeoxynucleotides differentially modulate activation of TLR7 and TLR8 by imidazoquinolines.* J Immunol, 2006. **177**(11): p. 8164-70.

38. Hasan, U., et al., *Human TLR10 is a functional receptor, expressed by B cells and plasmacytoid dendritic cells, which activates gene transcription through MyD88.* J Immunol, 2005. **174**(5): p. 2942-50.

39. Yamamoto, M., et al., *Essential role for TIRAP in activation of the signalling cascade shared by TLR2 and TLR4.* Nature, 2002. **420**(6913): p. 324-9.

40. Yamamoto, M., et al., *Role of adaptor TRIF in the MyD88-independent toll-like receptor signaling pathway.* Science, 2003. **301**(5633): p. 640-3.

41. Akira, S. and K. Takeda, *Toll-like receptor signalling.* Nat Rev Immunol, 2004. **4**(7): p. 499-511.

42. Sato, S., et al., *Toll/IL-1 receptor domain-containing adaptor inducing IFN-beta (TRIF) associates with TNF receptor-associated factor 6 and TANK-binding kinase 1, and activates two distinct transcription factors, NF-kappa B and IFN-regulatory factor-3, in the Toll-like receptor signaling.* J Immunol, 2003. **171**(8): p. 4304-10.

43. Adhikari, A., M. Xu, and Z.J. Chen, *Ubiquitin-mediated activation of TAK1 and IKK.* Oncogene, 2007. **26**(22): p. 3214-26.

44. Wang, C., et al., *TAK1 is a ubiquitin-dependent kinase of MKK and IKK.* Nature, 2001. **412**(6844): p. 346-51.

45. Yamamoto, M., et al., *TRAM is specifically involved in the Toll-like receptor 4-mediated MyD88-independent signaling pathway.* Nat Immunol, 2003. **4**(11): p. 1144-50.

46. Kawai, T., et al., *Unresponsiveness of MyD88-deficient mice to endotoxin.* Immunity, 1999. **11**(1): p. 115-22.

47. Kawai, T. and S. Akira, *Signaling to NF-kappaB by Toll-like receptors.* Trends Mol Med, 2007. **13**(11): p. 460-9.

48. Oganesyan, G., et al., *Critical role of TRAF3 in the Toll-like receptor-dependent and -independent antiviral response.* Nature, 2006. **439**(7073): p. 208-11.

49. Hayashi, F., et al., *The innate immune response to bacterial flagellin is mediated by Toll-like receptor 5.* Nature, 2001. **410**(6832): p. 1099-103.

50. Zeng, H., et al., *Flagellin is the major proinflammatory determinant of enteropathogenic Salmonella.* J Immunol, 2003. **171**(7): p. 3668-74.

51. Muzio, M., et al., *Differential expression and regulation of toll-like receptors (TLR) in human leukocytes: selective expression of TLR3 in dendritic cells.* J Immunol, 2000. **164**(11): p. 5998-6004.

52. Cario, E. and D.K. Podolsky, *Differential alteration in intestinal epithelial cell expression of toll-like receptor 3 (TLR3) and TLR4 in inflammatory bowel disease.* Infect Immun, 2000. **68**(12): p. 7010-7.

53. Smith, K.D., et al., *Toll-like receptor 5 recognizes a conserved site on flagellin required for protofilament formation and bacterial motility.* Nat Immunol, 2003. **4**(12): p. 1247-53.

54. Yu, Y., et al., *TLR5-mediated phosphoinositide 3-kinase activation negatively regulates flagellin-induced proinflammatory gene expression.* J Immunol, 2006. **176**(10): p. 6194-201.

55. Lu, W., et al., *Cutting edge: enhanced pulmonary clearance of Pseudomonas aeruginosa by Muc1 knockout mice.* J Immunol, 2006. **176**(7): p. 3890-4.

56. Gewirtz, A.T., et al., *Cutting edge: bacterial flagellin activates basolaterally expressed TLR5 to induce epithelial proinflammatory gene expression.* J Immunol, 2001. **167**(4): p. 1882-5.

57. Bambou, J.C., et al., *In vitro and ex vivo activation of the TLR5 signaling pathway in intestinal epithelial cells by a commensal Escherichia coli strain.* J Biol Chem, 2004. **279**(41): p. 42984-92.

58. Vijay-Kumar, M., et al., *Deletion of TLR5 results in spontaneous colitis in mice.* J Clin Invest, 2007. **117**(12): p. 3909-21.

59. Vijay-Kumar, M., et al., *Metabolic syndrome and altered gut microbiota in mice lacking Toll-like receptor 5.* Science. **328**(5975): p. 228-31.

60. Vijay-Kumar, M., et al., *Toll-like receptor 5-deficient mice have dysregulated intestinal gene expression and nonspecific resistance to Salmonella-induced typhoid-like disease.* Infect Immun, 2008. **76**(3): p. 1276-81.

61. Stecher, B., et al., *Salmonella enterica serovar typhimurium exploits inflammation to compete with the intestinal microbiota.* PLoS Biol, 2007. **5**(10): p. 2177-89.

62. Arpaia, N., et al., *TLR signaling is required for Salmonella typhimurium virulence.* Cell. **144**(5): p. 675-88.

63. Hacker, H. and M. Karin, *Regulation and function of IKK and IKK-related kinases.* Sci STKE, 2006. **2006**(357): p. re13.

64. Shih, V.F., et al., *A single NFkappaB system for both canonical and non-canonical signaling.* Cell Res. **21**(1): p. 86-102.

65. Haraga, A. and S.I. Miller, *A Salmonella enterica serovar typhimurium translocated leucine-rich repeat effector protein inhibits NF-kappa B-dependent gene expression.* Infect Immun, 2003. **71**(7): p. 4052-8.

66. Collier-Hyams, L.S., et al., *Cutting edge: Salmonella AvrA effector inhibits the key proinflammatory, anti-apoptotic NF-kappa B pathway.* J Immunol, 2002. **169**(6): p. 2846-50.

67. Jones, R.M., et al., *Salmonella AvrA Coordinates Suppression of Host Immune and Apoptotic Defenses via JNK Pathway Blockade.* Cell Host Microbe, 2008. **3**(4): p. 233-44.

68. Ghosh, S. and M. Karin, *Missing pieces in the NF-kappaB puzzle.* Cell, 2002. **109 Suppl**: p. S81-96.

69. Chen, L., et al., *Duration of nuclear NF-kappaB action regulated by reversible acetylation.* Science, 2001. **293**(5535): p. 1653-7.

70. Moss, B.L., et al., *Identification of a ligand-induced transient refractory period in nuclear factor-kappaB signaling.* J Biol Chem, 2008. **283**(13): p. 8687-8698.

71. Kuper, H., H.O. Adami, and D. Trichopoulos, *Infections as a major preventable cause of human cancer.* J Intern Med, 2000. **248**(3): p. 171-83.

72. Karin, M., *The IkappaB kinase - a bridge between inflammation and cancer.* Cell Res, 2008. **18**(3): p. 334-42.

73. Mitra-Kaushik, S., et al., *Enhanced tumorigenesis in HTLV-1 Tax transgenic mice deficient in interferon gamma.* Blood, 2004. **In press**.

74. Gao, L., et al., *HTLV-1 Tax transgenic mice develop spontaneous osteolytic bone metastases prevented by osteoclast inhibition.* Blood, 2005. **106**(13): p. 4294-302.

75. Zeng, Z.R., et al., *Association of interleukin 1B gene polymorphism and gastric cancers in high and low prevalence regions in China.* Gut, 2003. **52**(12): p. 1684-9.

76. Chen, L.W., et al., *The two faces of IKK and NF-kappaB inhibition: prevention of systemic inflammation but increased local injury following intestinal ischemia-reperfusion.* Nat Med, 2003. **9**(5): p. 575-81.

77. Pikarsky, E., et al., *NF-kappaB functions as a tumour promoter in inflammation-associated cancer.* Nature, 2004. **431**(7007): p. 461-6.

78. Smit, J., et al., *Mice which are deficient in mdr2 have severe liver disease caused by greatly reduced excretion of phosphatidylcholine and cholesterol into bile.* Cell, 1993. **75**: p. 451-462.

79. Oguma, K., et al., *Activated macrophages promote Wnt signalling through tumour necrosis factor-alpha in gastric tumour cells.* Embo J, 2008. **27**(12): p. 1671-81.

80. Rius, J., et al., *NF-kappaB links innate immunity to the hypoxic response through transcriptional regulation of HIF-1alpha.* Nature, 2008. **453**(7196): p. 807-11.

81. Hoption Cann, S.A., J.P. van Netten, and C. van Netten, *Dr William Coley and tumour regression: a place in history or in the future.* Postgrad Med J, 2003. **79**(938): p. 672-680.

82. Pawelek, J.M., K.B. Low, and D. Bermudes, *Bacteria as tumour-targeting vectors.* Lancet Oncol, 2003. **4**(9): p. 548-56.

83. Yu, Y.A., et al., *Visualization of tumors and metastases in live animals with bacteria and vaccinia virus encoding light-emitting proteins.* Nat Biotechnol, 2004. **22**(3): p. 313-20.

84. Zhao, M., et al., *Targeted therapy with a Salmonella typhimurium leucine-arginine auxotroph cures orthotopic human breast tumors in nude mice.* Cancer Res, 2006. **66**(15): p. 7647-52.

85. Low, K.B., et al., *Lipid A mutant Salmonella with suppressed virulence and TNFalpha induction retain tumor-targeting in vivo.* Nat Biotechnol, 1999. **17**(1): p. 37-41.

86. Pawelek, J.M., K.B. Low, and D. Bermudes, *Tumor-targeted Salmonella as a novel anticancer vector.* Cancer Res, 1997. **57**(20): p. 4537-44.

87. Sfondrini, L., et al., *Antitumor activity of the TLR-5 ligand flagellin in mouse models of cancer.* J Immunol, 2006. **176**(11): p. 6624-30.

88. Forbes, N.S., *Engineering the perfect (bacterial) cancer therapy.* Nat Rev Cancer, 2010. **10**(11): p. 785-94.

89. Forbes, N.S., et al., *Sparse initial entrapment of systemically injected Salmonella typhimurium leads to heterogeneous accumulation within tumors.* Cancer Res, 2003. **63**(17): p. 5188-93.

90. *Cancer Facts and Figures 2006*. 2006, American Cancer Society: Atlanta.

91. Pickhardt, P.J., et al., *Location of adenomas missed by optical colonoscopy.* Ann Intern Med, 2004. **141**(5): p. 352-9.

92. Wils, J., *Adjuvant therapy for colon cancer: the European experience.* Tumori, 2001. **87**(1 Suppl 1): p. S85.

93. Gutmann, D.H., K. Hunter-Schaedle, and K.M. Shannon, *Harnessing preclinical mouse models to inform human clinical cancer trials.* J Clin Invest, 2006. **116**(4): p. 847-52.

94. al-Ramadi, B.K., et al., *Potent anti-tumor activity of systemically-administered IL2-expressing Salmonella correlates with decreased angiogenesis and enhanced tumor apoptosis.* Clin Immunol, 2009. **130**(1): p. 89-97.

95. Ryan, R.M., J. Green, and C.E. Lewis, *Use of bacteria in anti-cancer therapies.* Bioessays, 2006. **28**(1): p. 84-94.

96. Robbins, S.L., R.S. Cotran, and V. Kumar *Pathologic Basis of Disease.* 3rd ed. 1984, Philidephia: W. B. Saunders Company.

97. Kasinskas, R.W. and N.S. Forbes, *Salmonella typhimurium specifically chemotax and proliferate in heterogeneous tumor tissue in vitro.* Biotechnol Bioeng, 2006. **94**(4): p. 710-21.

98. Kasinskas, R.W. and N.S. Forbes, *Salmonella typhimurium lacking ribose chemoreceptors localize in tumor quiescence and induce apoptosis.* Cancer Res, 2007. **67**(7): p. 3201-9.

99. Dothager, R., et al., *Advances in bioluminescence imaging of live animal models.* Curr Opin Biotechnol, 2009. **20**: p. 45-53.

100. Meighen, E.A., *Bacterial bioluminescence: organization, regulation, and application of the lux genes.* Faseb J, 1993. **7**(11): p. 1016-22.

CHAPTER 2

Stably Integrated *luxCDABE* for Assessment of *Salmonellae* Invasion Kinetics

2.1 Abstract

Salmonella Typhimurium is a common cause of gastroenteritis in humans, and also localizes to neoplastic tumors in animals. Invasion of specific eukaryotic cells is a key mechanism of *Salmonella* interactions with host tissues. Early stages of gastrointestinal cell invasion are mediated by a *Salmonella* type-three secretion system, powered by the ATPase *invC*. The aim of this work was to characterize the *invC*-dependence of invasion kinetics into disparate eukaryotic cells traditionally used as models of gut epithelium or neoplasms. Thus, a nondestructive real-time assay was developed to report eukaryotic cell invasion kinetics, using *lux+ Salmonellae* that contain chromosomally integrated *luxCDABE* genes. Bioluminescence-based invasion assays using *lux+ Salmonellae* exhibited inoculum dose-response correlation, distinguished invasion-competent from invasion-incompetent *Salmonellae*, and discriminated relative *Salmonellae* invasiveness in accordance with environmental conditions that induce invasion gene expression. In standard gentamicin protection assays, bioluminescence from *lux+ Salmonellae* correlated with recovery of colony forming units of internalized bacteria, and could be visualized by bioluminescence microscopy. Furthermore, this assay distinguished invasion-competent from invasion-incompetent bacteria independent of gentamicin treatment in real time. Bioluminescence reported *Salmonellae* invasion of disparate eukaryotic cell lines, including neoplastic melanoma, colon adenocarcinoma, and glioma

cell lines used in animal models of malignancy. In each case, *Salmonella* invasion of eukaryotic cells was *invC* dependent.

2.2 Introduction

Eukaryotic cell invasion is utilized by *Salmonellae* during initial steps of pathogenesis (1), and leads to enteric symptoms and disseminated infection. *Salmonellae* also localize to, and sometimes invade, cancerous tumors in mice (2). One basic tool for dissecting the mechanisms of these bacterial-eukaryotic cell interactions is the *in vitro* cell invasion assay.

The standard technique to assess *Salmonella* invasion into cultured cells is the gentamicin protection assay (3), which exploits the poor penetration of this antibiotic into eukaryotic cells (4). Specifically, gentamicin is postulated to kill susceptible extracellular bacteria, but not "protected" bacteria that have invaded. Presumably, such selective killing permits the preferential recovery of intracellular bacteria on subsequent culture of lysed cells. Gentamicin protection assays have been used to illuminate genetic and cellular mechanisms of cell invasion by *Salmonellae* (5). For example, the *invC* gene in *Salmonella* encodes an ATPase that powers a type-three secretion system, triggering eukaryotic actin reorganization and *Salmonella* invasion of some eukaryotic cell lines (6, 7).

Despite their widespread use, standard gentamicin protection assays are technically and conceptually limited, because they attempt to quantify the invasiveness of individual bacterial strains via direct enumeration of bacterial colony forming units recovered from lysed eukaryotic cells. The lysis and colony forming unit (CFU) determination steps

consume time, materials and labor. Colonies are not necessarily correlated with bacterial numbers, so agglomerated organisms might be under-enumerated. Additionally, because eukaryotic cells must be destroyed to release invaded bacteria, serial evaluations of bacterial invasion in a single temporal assay are precluded. Furthermore, by definition, current gentamicin-protection, CFU-based assays of invasion require that extracellular bacteria of interest are killed by gentamicin, which is a condition not always met.

To attempt to address such limitations, we have modified current gentamicin protection assays of bacterial invasion into eukaryotic cells, including neoplastic lines, by using bioluminescence to report bacterial invasion. Contag *et al*. originally pioneered the use of bacteria expressing luciferase to monitor *in vitro* and *in vivo* pathogenesis with organisms containing plasmid-encoded luciferase (8). Here, we employ constitutively bioluminescent *Salmonellae*, which contain chromosomally integrated *luxCDABE* genes from *Photorhabdus luminescens* (9), and imaging systems that sensitively and specifically detect bioluminescent *Salmonellae* (10). This nondestructive assay requires neither eukaryotic cell lysis, nor gentamicin. Rather, we use bioluminescence to track the invasion of *lux+ Salmonellae* into various eukaryotic cells in tissue culture. These eukaryotic cells include those traditionally used for models of gastroenteritis, as well as cells previously used in whole mouse models of metastatic cancers. To determine the *invC* dependence of invasion kinetics in these different systems, we compare the invasiveness of *lux+ Salmonellae* that are isogenic except for *invC*.

2.3 Methods

Bacterial Strains and Eukaryotic Cell Lines: The bacterial strains and eukaryotic cell lines used in this study are listed in **Table 2-1**.

Construction of Salmonellae *Strains with Stably Integrated*: luxCDABE Conjugative mating was performed between donor strain *E. coli* S17-1 (containing the transfer plasmid pUT mini-Tn5 *lux Km2*; gift of Michael Winson), and recipient *Salmonella enterica* serovar Typhimurium strain SB300A1 (11). Mating was performed as described (12) in Luria-Bertani (LB) broth, then plated onto LB agar, and incubated at 37^{o}C overnight. Mated colonies were scraped from the LB agar, and onto kanamycin (50 µg/mL) MacConkey agar to discriminate *Salmonellae* from *E. coli*. The isolated candidate *Salmonellae* were grown at dilutions of 10^{-5}, 10^{-6}, and 10^{-7} on these agar plates for 48 hours. Replating on LB/kanamycin plates documented the kanamycin resistance of the recipients of pUT mini-Tn5 lux Km2. PCR confirmed the gross presence of each gene of *luxCDABE* in the new strains, but not in the parent *Salmonella* SB300A1.

Identification of Site of luxCDABE *Integration into the* Salmonella *Genome*: First, the general location of *luxCDABE* integration was determined from sequences of amplicons produced using touchdown PCR (13) of the genomic DNA of our new *lux+ Salmonella* strain. Touchdown PCR used high fidelity *Taq* DNA polymerase (Invitrogen), and thermal cycling conditions (95^{o}C for 5 minutes; then 25 cycles of 95^{o}C for 45 seconds, annealing at variable temperature for 45 seconds (60^{o}C in the first cycle and, at each of the 24 cycles, decreased by 0.5^{o}C per cycle down to 47.5^{o}C), and extension at 72^{o}C for 2 minutes). This was followed by 25 cycles of 95^{o}C for 45 seconds, 50^{o}C for 45 seconds, and 72^{o}C for 2 minutes. Primer pairs included a degenerate primer

CCGAATTCCGGATNGAYKSNGGNTC (where N=A, C, G, or T; Y=C or T; K=G or T; and S=C or G), in combination with either an outward facing *luxC* or *luxE* primer (outward *luxC*: CCATCTTTGCCCTACCGTATAGAG and outward *luxE*: TGAGGATGAAATGCAGCGTA). Sequence data from the resulting amplicons suggested *luxCDABE* integration between *Salmonella* chromosomal genes *acrB* and *hha*.

The precise integration site of *luxCDABE* was then identified. PCR amplification from the genomic DNA of our new *lux+ Salmonella* strain was performed using two sets of primers. One reaction, which produced an amplicon of approximately 2.5kb, used *luxE* (TGAGGATGAAATGCAGCGTA) and *hha* (GCCAGAACGAGGAGGCAGATAACA) primers, and PCR conditions of 94^{o}C for 3 minutes; 30 cycles of 94^{o}C for 30 seconds, 51^{o}C for 30 seconds, 72^{o}C for 3 minutes; and 72^{o}C for 7 minutes. The second reaction produced an amplicon of approximately 3kb, with *luxC* (ATCCAATTGGCCTCTAGCTTAGCC) and *acrB* (ACCTCAACGGATGAGTTTGG) primers, and PCR conditions directly above. These amplicons above were sequenced by the Protein and Nucleic Acid Chemistry Laboratory at Washington University in St. Louis. Sequences were aligned with the *Salmonella enterica* serovar Typhimurium strain LT2 complete genome sequence (14).

Growth Curves in Liquid Culture: Otherwise isogenic *Salmonellae* with and without chromosomal *luxCDABE* were grown in overnight liquid cultures then diluted 1:10 into fresh liquid media for growth curve analysis. Growth was assessed via serial optical transmission measurements. For growth curve analyses, growth media was Luria-Bertani (LB) broth, and incubation was at 37^{o}C in a shaker incubator at 200-250 rpm.

Construction of an In-frame invC *Deletion Mutant of* luxCDABE+ Salmonella: An in-frame excision of *invC* nucleotides between 506 and 590 was performed using the pCVD442 suicide vector, engineered as previously described (15), for gene allele exchange (16). Here, 5' and 3' segments of *invC* were amplified from wild-type *invC*+ *Salmonella* SB300A1 (11) by PCR using the respective primer pairs 5′GGAGCGAGCTCACTGCAATATCTGGCCTACCCACA3′ with 5′GGAGCAAGCTTATCAGCATGGTCTTACCGCATCCT3′; and 5′GGAGCAAGCTTGGATATGTTGCGCGCTTCGCATAA3′ with 5′GCTATCTCGAGTTTCGCCAGGACGATATTCTCCCA3′. These four primers contain *SacI*, *HindIII*, *HindIII*, and *XhoI* sites, respectively, and nucleotides (underlined, above) of the published *Salmonella* LT2 genomic sequence for *invC* (14). The resulting PCR products were digested with *SacI* and *HindIII*, or with *HindIII* and *XhoI*, respectively; then individually cloned into pBSIISK+. Following digestion of these two plasmids with *SacI* and *HindIII*, or with *HindIII* and *XhoI*, respectively, the small fragments were cloned in tandem into *SacI* and *XhoI* digested pBSIISK+, producing pBSIISK+(invCΔ506-590). Finally, the *SacI* delimited insert of pBSIISK+(*invC*Δ506-590) was ligated into *SacI* linearized suicide plasmid pCVD442 (16). The resulting pCVD442(*invC*Δ506-590) was transformed into *E. coli* SM10(λpir) (17). Mating was performed between the donor SM10(λpir) strain and the bioluminescent chromosomal *luxCDABE+ Salmonella* strain SB300A1FL6 on LB agar. The cells were then scraped from the LB plates and serial dilutions (to 10^{-7}) were made in LB. 100 µL of the dilutions were spread on MacConkey agar containing ampicillin (100 µg/mL) and kanamycin (50

µg/mL) to select merodiploids. Of 30 merodiploid candidates, five were picked and grown overnight in LB media without salt. These cultures were then plated on 5% sucrose plates and incubated overnight at 30^{o}C to select for *sacB* removal. Presumptive *sacB* deficient colonies on sucrose plates were further screened on LB ampicillin (100 µg/mL) plates for a phenotype consistent with concomitant excision of the *bla* gene. One such ampicillin susceptible clone was analyzed by PCR amplification using *invC* flanking primers. The resulting amplicon was sequenced, to confirm the anticipated 84 nucleotides deletion from the 1296 nucleotide long *invC*, between *invC* nucleotides 506 and 590. The *invC* mutant also includes a six nucleotide HindIII site introduced as a byproduct of subcloning steps above (i.e., TGCTGATAAGCTTGGATAT, with *invC* nucleotides 506T and 590G underlined). Accordingly, the predicted InvC protein encoded by our *invC* mutation is missing intact InvC amino acids 169 to 197, and has an isoleucine-serine-leucine insert encoded by the TAA/GCT/TGG sequence created by the HindIII site insert. This *invC* mutant does not create a frame shift; so should not have polar effects on adjacent genes**.**

Invasion Assays: Standard gentamicin-protection assays were performed as described (18). *Salmonellae* grown overnight in LB broth (37^{o}C) were diluted 1:100 or 1:10 and grown to an OD_{600} of between 0.45 and 0.7, with OD_{600} matched across samples for a given experiment. Incubations were not shaken, except where noted, and as previously described (19). These bacteria were diluted 1:10 in DMEM, or to a multiplicity of infection of 100 where noted.

Diluted bacterial suspensions were added to tissue culture plates, at 500 µL to each well in 24 well plates, or 100 µL to each well in 96 well plates. For 60 minutes, the bacteria were coincubated with adherent tissue culture monolayers at 60 to100% confluence. Wells were then washed with DMEM and treated with media containing gentamicin at a final concentration of 100 µg/mL. The antibiotic-containing media was replaced with phenol-red free media after 90 minutes of treatment and bioluminescence was measured three and a half hours later (five hours after the initiation of gentamicin treatment), unless otherwise noted. Gentamicin-free conditions represented use of phenol-red free DMEM lacking gentamicin after the wash step; imaging occurred three hours after washing.

In the CFU recovery assay, following bioluminescence imaging, bacteria were quantified by CFU recovery after immediate lysis of tissue culture cells with detergent lysis as described (McKinney *et al*., 2004).

Measurement of Bioluminescence: Bioluminescence measurements were performed as published (20-22). Images were captured with a cooled CCD camera (IVIS 100, Caliper, Hopkinton, MA). Acquisition parameters were: exposure time, 30s; binning, 8; no filter; f/stop, 1; FOV, 15 cm. Signals were measured as the radiance (photons/second/cm^2/sr). To calculate the bioluminescence from a given well, total photon flux (photons/second) was determined from a region-of-interest (ROI) positioned over the given well and an empty well, which was subtracted to correct for background machine noise using Living Image (Xenogen) and Igor Pro (WaveMetrics) Software. Bioluminescence was presented as mean ± standard deviation of the mean of the total photon flux for replicate well assays.

Bioluminescence Microscopy: Henle cell monolayers cultured on glass bottom 35 mm dishes, with or without *luxCDABE+ Salmonellae,* were treated as described for gentamicin protection invasion assays. Two to three hours after *Salmonellae* inoculation, these plates were examined on an inverted microscope (Nikon TE 2000-S) housed in a light tight microscope incubator (In Vivo Scientific) with temperature maintained at 36ºC. Bioluminescence was recorded with a cooled intensified CCD camera (XR/MEGA10-AW, Stanford Photonics) controlled by Piper Imaging software version 1.3.6 (Agile Automation). Due to high amplification of the signal (gain set at 400,000), camera noise was reduced during image acquisition by setting a minimum threshold for the signal that was kept constant for all cultures. Fifteen image sequence frames were obtained per second and integrated later in 40 min stacks to obtain a single image. Integration, pseudo-color processing and color merge were performed with ImageJ (National Institutes of Health, USA) and Photoshop CS2 (Adobe) software.

2.4 Results

Chromosomal Integration of *luxCDABE* To create a *Salmonella* strain that constitutively produced bioluminescence, a Tn5 transfer plasmid was used to engineer a strain with chromosomal integration of the *luxCDABE* operon without disrupting essential genes in this process. Independent PCR assays, followed by amplicon DNA sequencing, defined the *luxCDABE* integration site in the *Salmonella* chromosome (**Figure 2-1**). According to *Salmonella* strain LT2 complete genomic sequence annotation convention (14), *luxCDABE* in our *Salmonella* integrated at nucleotide 528,771, twenty nucleotides 5' to the start codon of *ybaJ*.

Despite some preference for insertion at G/C pairs (23), Tn5 is considered to mediate near-random integration into bacterial genomes (24). Interestingly, in bioluminescent *Salmonellae* produced by another laboratory using the same suicide vector system, the transposon is reported to have integrated at *hha* (25). Given that *hha* is immediately 3' to *ybaJ* in the *Salmonella* genome, perhaps there is preferential integration of the Tn5 *luxCDABE* element into the *Salmonella* genome near *ybaJ* / *hha*.

Alterations in *hha* gene expression, secondary to *luxCDABE* integration, in principle could alter pathogenesis, because Hha negatively regulates *hilA* (26), and *hilA* regulates the invasive phenotype of *Salmonellae* (27). However, our new *luxCDABE+ Salmonella* does not exhibit decreased *hha* mRNA levels, assessed by RT-PCR, compared to its parent (data not shown).

Fitness and bioluminescence of *luxCDABE+ Salmonellae* The growth curves of otherwise isogenic *Salmonellae* with and without *luxCDABE* were identical in LB broth (data not shown). As predicted, the *Km2* kanamycin selection marker integrated with *luxCDABE* did not bestow resistance to gentamicin at concentrations of 100 µg/mL (data not shown). Furthermore, the kanamycin resistance and bioluminescence phenotypes of our *luxCDABE+ Salmonellae* were stably maintained without kanamycin selection, both in long term *in vitro* cultures and in mouse infections (data not shown).

Invasion Competence of *luxCDABE+ Salmonellae* To determine the impact of integrated *luxCDABE* on *Salmonella* invasiveness, we performed parallel standard gentamicin protection assays with equal inoculations of otherwise isogenic *Salmonellae*, differing only in the presence or absence of chromosomally integrated *luxCDABE*. Based

on numbers of bacterial colony forming units from lysed eukaryotic cells, there was no defect in *Salmonella* invasion because of *luxCDABE* integration (data not shown).

Bioluminescence as a Reporter of Invasion by *luxCDABE+ Salmonellae* As determinates of host cell invasion, we compared *Salmonellae* bioluminescence assays and colony forming units (CFU) from standard gentamicin invasion assays in tissue culture wells. Following measurement of bioluminescence signals from invasion assay tissue culture wells, we processed the tissue culture wells to obtain CFU data from the same assay wells that had been imaged for bioluminescence. We lysed the eukaryotic cells and used plate counts to recover and enumerate *Salmonellae* CFU. There was concordance between bioluminescence output and CFU recovery in gentamicin protection assays (**Figure 2-2**). Furthermore, bioluminescence readily discriminated between invasion-competent and invasion-incompetent *luxCDABE+ Salmonellae* strains. The protein encoded by *invC* is an ATPase that powers a type-three secretion system, triggering eukaryotic actin reorganization and *Salmonella* invasion (6, 7). Bioluminescence distinguished between otherwise isogenic chromosomal *luxCDABE+ Salmonellae* strains that had an *invC* gene that was either intact (*invC+*), or ablated by an in-frame deletion (*invC-*) (**Figure 2-2**). Our *invC-* strain is more than 200-fold less invasive compared with isogenic *invC+ Salmonella* concordantly assessed by standard gentamicin protection assay (6, 7, 18).

Salmonella invasiveness can also be modified by varying environmental conditions. For example, entry into eukaryotic cells can be significantly enhanced when invasion competent *Salmonellae* are prepared using standing rather than shaken cultures (19).

Using a bioluminescence-based gentamicin protection assay, we could discriminate these invasion phenotype differences for *invC+ Salmonellae* that differ only in culture conditions prior to exposure to eukaryotic cells (**Figure 2-3**). By contrast, the otherwise isogenic *invC- Salmonella* remained minimally invasive when prepared in either standing or shaken cultures (**Figure 2-3**).

We reproducibly observed bioluminescence enhancement with increasing *Salmonella* inoculum (**Figure 2-4**). In standard gentamicin protection assays, the multiplicity of infection often requires optimization (3). In the bioluminescence assay, we detected wild type *Salmonella* invasion into eukaryotic cells over a twenty-fold range in multiplicity of infection (**Figure 2-4**).

Salmonella Invasion into Diverse Eukaryotic Cells: Dependence on *invC*

Salmonellae often invade eukaryotic cells postulated to be relevant to cell-cell interactions during pathologic intestinal infections (e.g., Henle intestinal epithelial cells (3), HT29 colon carcinoma cells (28)). *Salmonellae* also localize to cancerous tumors in animals (2, 29, 30), including non-intestinal cells, such as melanoma, glioma, breast and prostate neoplastic cells. *Salmonellae* can be recovered from these tumors, and in some cases appear by electron microscopy to have invaded the neoplastic cells (2). Here, we examined the ability of *Salmonellae* to invade various cells used for models of malignancy in mice. Our wild type bioluminescent *Salmonella* invaded not only Henle (**Figure 2-2**) and HT29 colon cells, but also eukaryotic cells of diverse origins, including colon adenocarcinoma MC38, melanoma B16F10 and even, albeit to a lesser extent, glioma C6 cells. In each case, this invasion depended on *invC* (**Figure 2-5**).

Real-Time Kinetic Measurements of Bioluminescence During Invasion Assays The nondestructive nature of bioluminescence now permits serial assessments of the same invaded cells over time. We assessed the kinetics of *Salmonella* bioluminescence from single wells of C6 glioma cells during invasion assays. The bioluminescence from a given well reflects several factors, including *Salmonella* cell numbers and viability. At a given time, *Salmonella* viability is influenced by the effects of gentamicin and the protection from gentamicin killing afforded by *Salmonella* invasion into eukaryotic cells. Bioluminescence versus time is shown in **Figure 2-6**. In this experiment, the distinction between bioluminescence of *invC*+ versus *invC*- *Salmonellae* was most pronounced five hours after initial inoculation.

***Salmonella* Invasion Assay, With and Without Gentamicin Protection** Our ability to distinguish invasion-competent from invasion-incompetent *Salmonellae* at time points soon after adding gentamicin (**Figure 2-6**) raised the possibility that bioluminescence could assess invasion independent of gentamicin protection *per se*. Accordingly, rather than gentamicin treatment, we employed a washing step with three rounds of gentamicin-free media to physically deplete noninvaded *Salmonella* from the assay wells. In assays in which gentamicin was not used, *invC*-dependent invasion competence of *Salmonellae* could still be readily resolved (**Figure 2-7**). While overall assay time was shorter, the background activity was higher.

Bioluminescent *Salmonellae* Visualized by Cooled CCD Microscopy. Traditionally, bioluminescent bacteria have been most extensively exploited for imaging studies of bacterial spread within whole animals, such as for *Salmonellae* infections manifesting as

gastroenteritis or disseminated infections (8, 25), or for the targeted localization of *Salmonellae* to malignant tumors (29). By contrast, for microscopic level studies of bacterial localization (30) or gene expression (31), fluorescent rather than bioluminescent bacteria have been most widely used. Given recent advances in cooled CCD cameras and our interest in tracking *luxCDABE Salmonellae* microscopically, we attempted to visualize our *luxCDABE+ Salmonellae* using a cooled CCD bioluminescence microscope. Compared to uninfected eukaryotic cell controls, tissue cultures inoculated with *luxCDABE+ Salmonellae* with intact *invC* exhibited foci of bioluminescence, with maximal intensity foci clustered near or within eukaryotic cells (**Figure 2-8**). For *luxCDABE+ Salmonellae* lacking *invC,* the number and intensity of these foci at the single cell level were much reduced (data not shown). The ability to use microscopy to visualize invasion by our bioluminescent *Salmonellae* provides an additional advantage as bioluminescent microscopy does not require potentially cytotoxic excitation light and typically has low background signal.

2.5 Discussion

We report a new constitutively bioluminescent *Salmonella* strain (SB300A1FL6). We have subsequently deleted (in frame) specific segments of invasion competence genes in this primary *luxCDABE+ Salmonella* strain, creating a set of reagents to study the functions of specific *Salmonella* genes during bacterial-host interactions. In our *Salmonellae* clones, *luxCDABE* was apparently maintained at low fitness cost. This contrasts with other *Salmonellae* strains that have been engineered to be constitutively fluorescent via the presence of green fluorescent protein. For example, green fluorescent

proteins can significantly inhibit *Salmonella* growth in epithelial cells and macrophages (32), and increase *Salmonella* doubling time (33).

Plasmid-based *lux* constructs have been exploited as reporter systems for bacterial location *in vitro* and *in vivo* (8, 29). However, plasmid-based *lux* systems can suffer from instability. Using the pLITE *lux* expression plasmid in *Salmonella* infections of mice, loss rates of plasmid (and bioluminescence) exceeding 95% of bacterial colonies have been reported (29). We observed no loss of bioluminescence of our chromosomal *luxCDABE+ Salmonellae* strains after serial passages in bacterial cultures or after prolonged infections in mice, even in the absence of kanamycin selection to maintain the *luxCDABE* / kanamycin resistance gene insert.

One motivation for constructing and characterizing these *luxCDABE+ Salmonellae* strains was to use bioluminescence to assess *Salmonellae* invasion kinetics into eukaryotic cells. Herein, we described a robust and versatile eukaryotic cell invasion assay using chromosomal *luxCDABE+ Salmonellae.* The new assay correlated well with the standard detection methodology over a broad inoculum range. The bioluminescence assay readily discriminated the invasion competencies of *invC+* and *invC- Salmonella*. Indeed, the resolution between *invC+* and *invC-* organisms was reliable across a twenty-fold range of bacterial inoculated dose and multiplicities of infection. By contrast, CFU-based assays are notably non-linear with respect to the number of inoculated bacteria (3). Bioluminescence-based invasion assays also resolved invasion differences among *lux+ Salmonellae* as regulated by environmental stimuli (19).

Bioluminescence-based tracking of *lux+ Salmonellae* during eukaryotic cell invasion permits invasion assays to be performed independent of the stringent requirements of gentamicin protection assays. For example, bioluminescence assays need not depend on the use of gentamicin to kill extracellular bacteria, or eukaryotic cell lysis to report intracellular "gentamicin-protected" bacteria. This allows studies on bacteria intrinsically resistant to gentamicin or enables analysis in growth conditions that compromise gentamicin activity (e.g., acidic pH or divalent cation concentrations (34)), as while also allowing assays in which gentamicin-mediated effects on eukaryotic phenotypes are a concern (35, 36).

Our assay had similarities to other techniques for assessing bacterial invasion, such as direct observation of internalized bacteria following Giemsa staining (37), or direct observation of *gfp* labeled bacteria within eukaryotic cells via fluorescent microscopy (30) or FACS analysis (31). However, *luxCDABE* encoded bioluminescence provided potential advantages to detect intracellular bacteria. For example, in contrast to Giemsa staining of inanimate features of bacterial cell walls, or to *gfp* based fluorescence, *lux* bioluminescence only reported bacteria that were alive and biochemically active (38). This direct detection of living bacteria removed the lag time and intermediate maneuvers imposed by experiments that rely on bacterial staining or recovery of bacterial CFUs for data. The real-time and non-destructive nature of *lux*-based tracking of *Salmonellae* in eukaryotic cells also allowed serial measurements from the same well over time. Hence, it was well-suited to kinetic studies of bacterial invasion and intracellular survival. From a technical perspective, bioluminescence-based detection of *lux+ Salmonellae* should

readily allow high throughput experimental scaling in multiwell plate assays, with readout times within minutes.

Furthermore, the components of the experimental system described here for studying bacterial invasion into eukaryotic cells in tissue cultures can also be used to noninvasively detect and localize *luxCDABE+ Salmonellae* during infections in living mice (data not shown). Thus, bioluminescence-based detection of *lux+ Salmonellae* presents opportunities to more directly correlate *in vitro* and *in vivo* models of bacterial-host interactions. This can be used to detect *Salmonellae* in experimental mouse models of infection and malignancy. Intriguingly, our bioluminescent *Salmonellae* invade a disparate range of malignant eukaryotic cells *in vitro*, each in an *invC*-dependent manner. This suggests that *Salmonellae* interactions with eukaryotic neoplastic cells may recapitulate features of *Salmonellae* interactions with eukaryotic epithelial cells in the host intestinal tract.

2.7 Tables

Table 2-1: Strains and eukaryotic cell lines used in the study

Strain or Cell Line	Description	Source or reference
Salmonella SB300A1	Parent Strain, not bioluminescent. Contains *araC*-P_{BAD} regulated T7 RNA polymerase.	Reference (11)
Salmonella SB300A1FL6	SB300A1, modified by chromosomal integration of *luxCDABE* to be constitutively bioluminescent	This study
Salmonella SB300A1FL6AM1	SB300A1FL6, modified by in-frame excision of *invC* nucleotides between 506 and 590	This study
E. coli S17-1	Donor strain in conjugation with SB300A1, for delivery of pUT mini-Tn5 *lux Km2*	Reference (12)
E. coli SM10(λpir)	Donor strain in conjugation with SB300A1FL6, for delivery of plasmid pCVD442(*invC*□506-590)	Reference (17)
Henle 407	Human epithelial cell line	ATCC: CCL-6
B16F10	Murine melanoma cell line	ATCC: CRL-6475
HT29	Human colon carcinoma cell line	ATCC: HTB-38
C6	Rat glioma cell line	ATCC: CCL-107
MC38	Murine colon adenocarcinoma cell line	Gift: N.O. Davidson

2.8 Figures

Figure 2-1

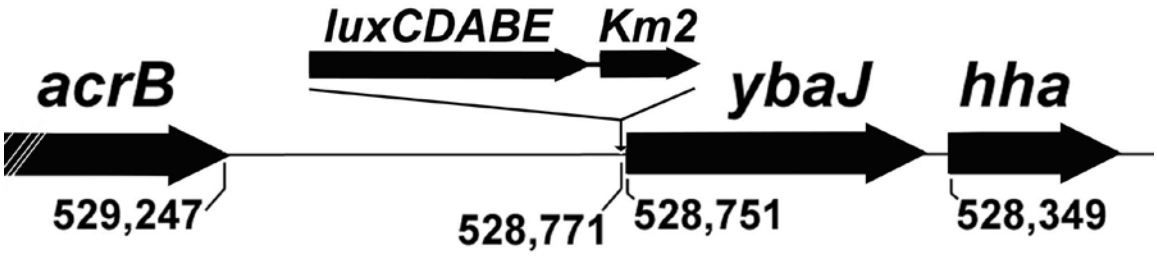

Figure 2-1: Foreign DNA integration site into *Salmonella* genome, at nucleotide 528,771. Nearby loci are *acrB*, *ybaJ*, and *hha*, flanking the insert site of *luxCDABE* and *Km2* as shown. The following DNA sequence from the chromosome of our bioluminescent *Salmonella* identifies the junction between *Salmonella* genomic DNA (non-italics, corresponding to *Salmonella* LT2 genome nucleotides 529,230 to 528,771) and foreign DNA (italics, with *luxC* coding nucleotides 1-163 in underlined italics):

AAGGCCGCGCAAGCGGCCTTTTTTACGCAAAAATCATAAAATACGCTTAT
TGTTAGATTGATTATTTTTTGCCATATTAATAAAAGGTATAATCCTTACTG
CGTTAAAGGCTTTTCTTAGGAAAGTTGGCCATTTCTTAATTCAGCCATTA
ATTAAGAAATATTAAGAATATTCCTGGCTATTTTCTCCTGTCAGAGTCTA
TTGTTTTAGCCTGAAAAGCTAAAAAACGTTAACCCAATGATTACACAAAC
AATAAAACTGGTTCCTTTTTAGGCGACCGACGATCACTGTTAAAATTCGA
AAAAGTATGGCAACACGCGGCTTTCACGCAATTGTAATTTTTAGTAATAT
GACGATGAAAAGTTTTTTAGAGTAGATTATAGTTAAATCATAAGGTGACG
TGGGAAGTACCAGGTTAGTTAGTTGTATCCATCCCGAAGGTGTTCGGTT

AGTTTAAGCC*CTGACTCTTATACACAAGTGCGGCCGCGTTTAAACCCATGGACGT*

GTTGACAATTAATCATCGGCATAGTATATCGGCATAGTATAATACGACTCAGGGCC

CACTAGTGGTACCCGGGGATCCTCTAGAGTCGACCTGCAGGTCGACGGATCCGG

GGAATTCAGGCTTGGAGGATACGT<u>ATGACTAAAAAAATTTCATTCATTATTAACGGC</u>

<u>CAGGTTGAAATCTTTCCCGAAGGTGATGATTTAGTGCAATCCATTAATTTTGGTGAT</u>

<u>AATAGTGTTTACCTGCCAATATTGAATGACTCTCATGTAAAAAACCATTATTGATTGT</u>

<u>AATGGAAATAACGAA</u>

Figure 2-2

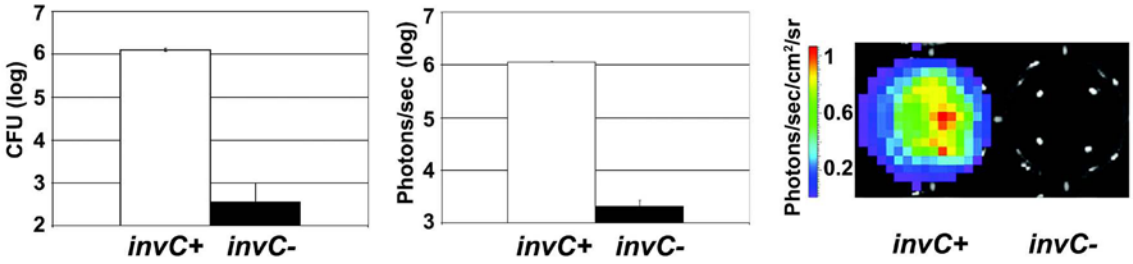

Figure 2-2: Comparison of colony forming unit (CFU) recovery and bioluminescence (photon flux, in photons/second) from gentamicin protection assays using bioluminescent *Salmonellae* that vary only by *invC* gene status. Data from a representative gentamicin protection assay performed in triplicate wells are shown. Here, invasion of Henle epithelial eukaryotic cells was assessed by bioluminescent *Salmonellae* either with *invC* (wild type, *invC+*) or without *invC (invC-)*. In each case the multiplicity of infection was 100. CFUs report *Salmonellae* grown from lysates, per single wells in a 24 well plate. Photon flux is in units of photons/second, also per single wells in a 24 well plate. CFU and photon flux results are shown as means (+/- SD). A representative pair of wells from the bioluminescence-based assay is shown with adjacent wells containing either *invC+* (left well) or *invC-* (right well) *luxCDABE+ Salmonellae*; the pseudo-color scale denotes photon intensity radiance. Similar results were obtained in experiments using HT29, rather than Henle eukaryotic cells (Figure 2-5 and data not shown).

Figure 2-3

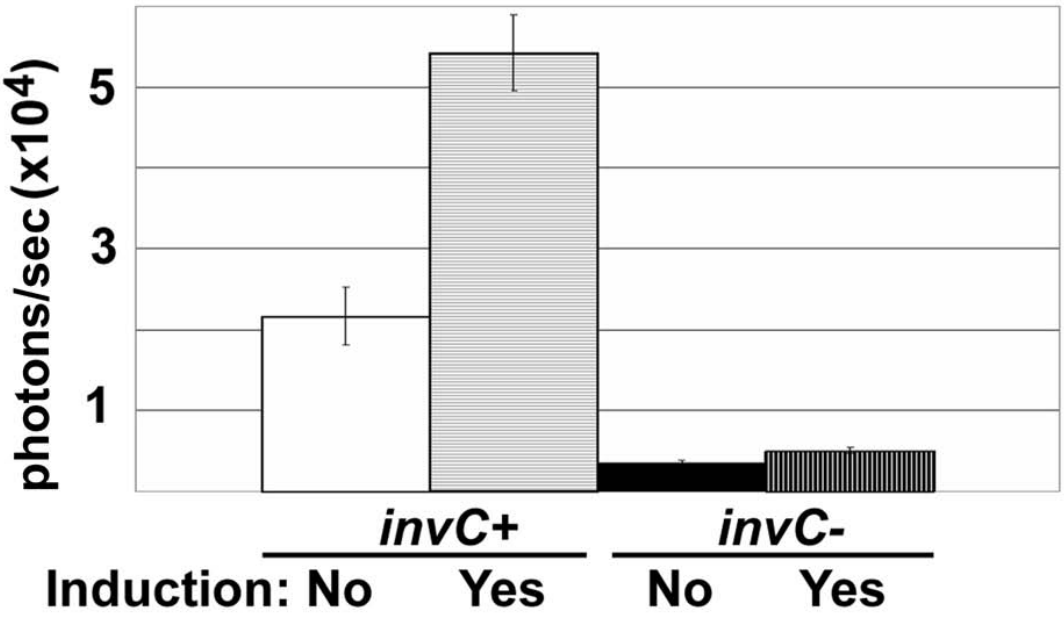

Figure 2-3. Bioluminescence and gentamicin protection following differing *Salmonella* growth conditions known to induce enhanced *Salmonella* invasiveness. The bar graph compares bioluminescence data obtained from a bacterial invasion assay of HT29 eukaryotic cells by bacteria previously grown in cultures that were either shaken or standing. Standing cultures are known to induce enhanced *Salmonella* invasiveness in cell culture, as compared with shaken culture conditions (19). Induction state is as indicated. Photon flux data are shown as means (+/- SD), in units of photons/second, and were obtained 90 minutes after adding gentamicin.

Figure 2-4

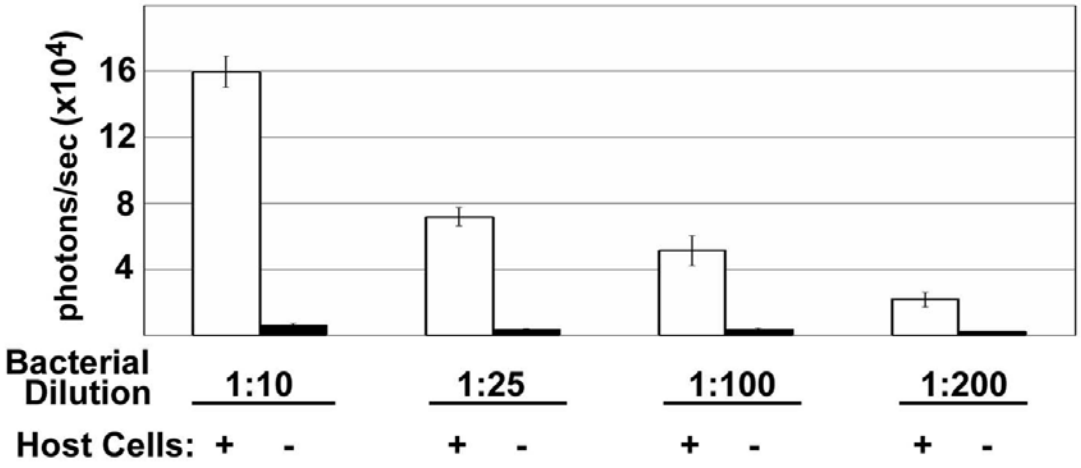

Figure 2-4. Bioluminescence signal intensity correlated with *Salmonella* inoculum dose. Photon flux signals from invasion assays of HT29 cells across a 20-fold dilution range of invasion competent (*invC*+) bioluminescent *Salmonella*. Because eukaryotic cell numbers per well were constant, this also corresponds to 20-fold range of multiplicity of infection. In wells lacking eukaryotic cells, photon flux signals approach ambient background. Results are from quadruplicate samples, with photon flux data (in units of photons/second) shown as means (+/- SD).

Figure 2-5

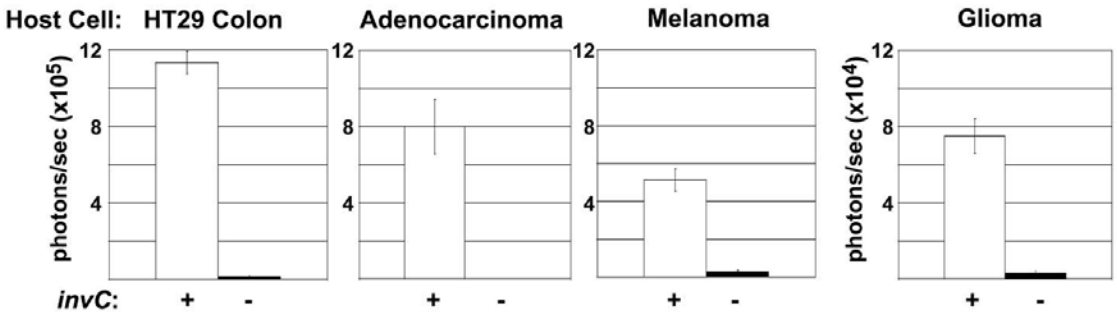

Figure 2-5. Invasion of bioluminescent *Salmonellae* into eukaryotic cell lines of diverse origins. Photon flux data represent invasion of wild type *invC*+ and *invC*- *Salmonellae* into human intestinal HT29, mouse colon adenocarcinoma MC38, mouse melanoma B16F10 or rat glioma C6 cell lines. For *invC*+ bioluminescent *Salmonellae*, the photon signal following exposure to glioma eukaryotic cells was approximately one-tenth that seen with adenocarcinoma cells (note different y-axis scale for glioma cells). Data are from triplicate wells, shown as means (+/- SD), in photons/second.

Figure 2-6

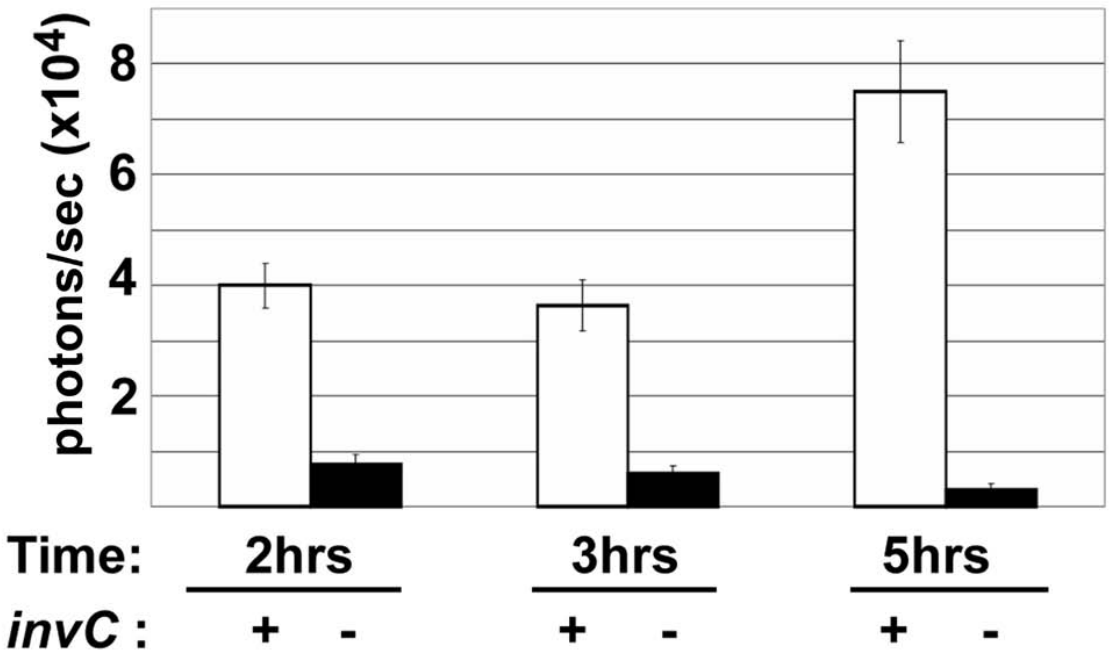

Figure 2-6. Kinetics of bioluminescence during *Salmonellae* infection. Photon flux data of bacteria serially measured from the same invasion assay wells. The times indicated hours after initiation of a 90 minute gentamicin treatment followed by replacement with media. *Salmonellae invC+* and *invC-* strains, and C6 glioma eukaryotic cells, are as described above. Data are from triplicate wells, shown as means (+/- SD), in units of photons/second.

Figure 2-7

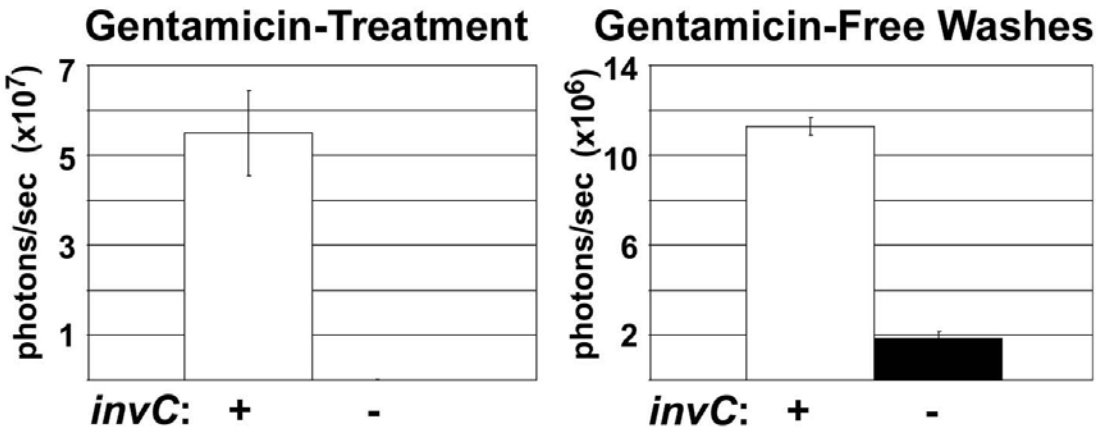

Figure 2-7. Bioluminescence monitoring of *Salmonella* interactions with eukaryotic cells, using gentamicin-containing and gentamicin-free media. Photon output from *invC*+ and *invC*- *Salmonellae* invasion of Henle cells, from quadruplicate samples, with photon flux data shown in units of photons/second, expressed as means (+/- SD). Gentamicin-treatment conditions represented 90 minutes of gentamicin incubation, following replacement with phenol-red free DMEM media, and imaging at 5 hours after initiating gentamicin addition. Gentamicin-free conditions represented use of phenol-red free DMEM media lacking gentamicin throughout, followed by three washes; imaging occurred three hours after washing.

Figure 2-8

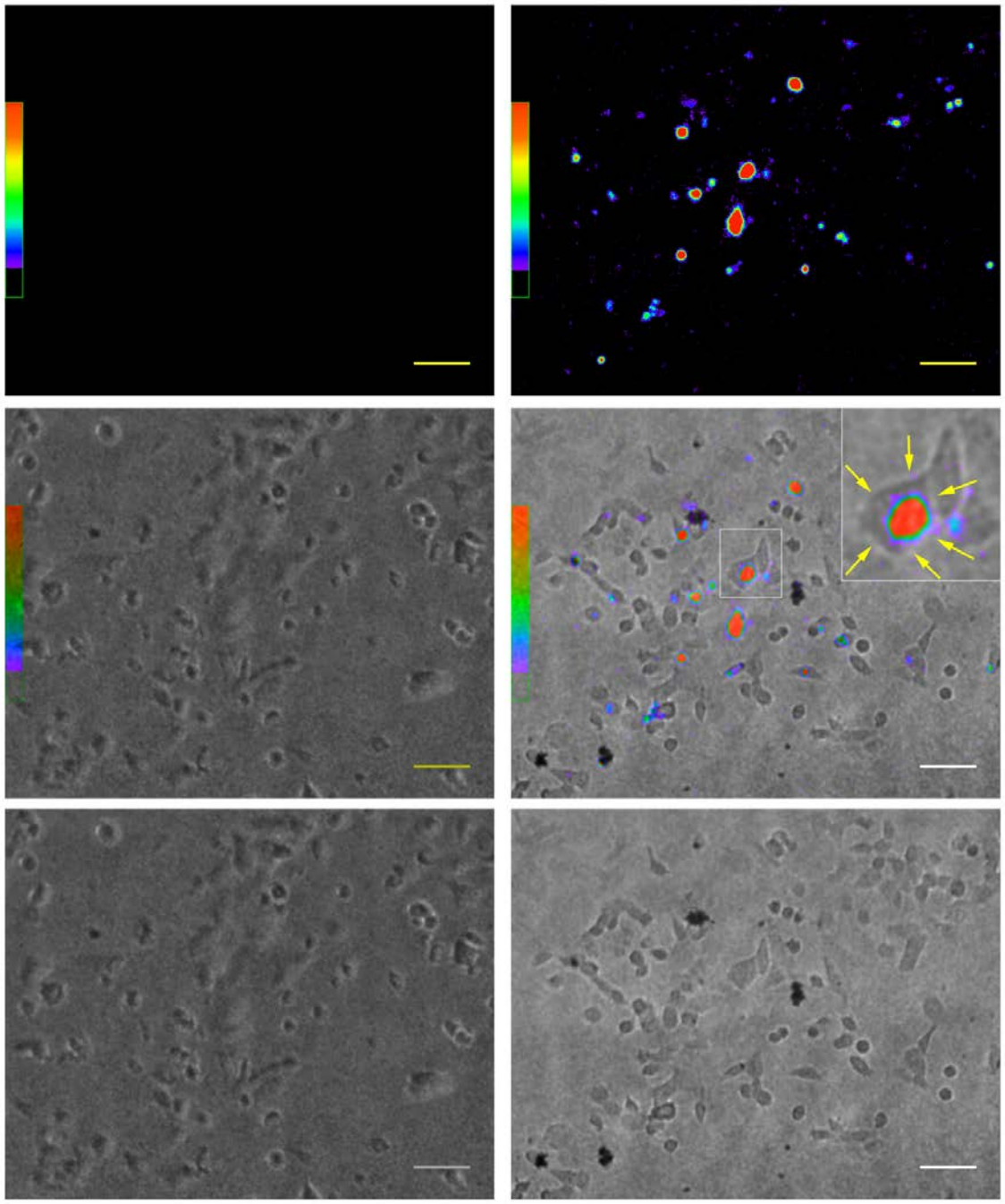

Figure 2-8. Microscopic detection of bioluminescence from *luxCDABE+ Salmonella* in eukaryotic cell cultures. Henle cell monolayers are shown either alone (left panels)

or following inoculation with *luxCDABE invC+ Salmonella* (right panels). For each sample, images show the bioluminescence signal alone (top), the phase contrast (bottom), and a merged image of bioluminescence and phase contrast (middle). Within the merged image of the Henle cells inoculated with *luxCDABE Salmonella*, a box demarcates the image area enlarged in the upper right corner (*inset*). Yellow arrows outline a Henle cell; maximal intensity foci occur near or within eukaryotic cells. Spectral scales denote pseudo-color representation of bioluminescence signal intensity in relative light units (RLU), ranging from 1 to 50 RLU for samples without *Salmonella*, and 1 to 100 RLU for samples with *Salmonella*. Processing of these samples followed the same methods as gentamicin protection assays described in the text; images were obtained two to three hours after inoculation of *Salmonella*. Bar = 50µM.

2.8 References

1. Ohl, M. E. and Miller, S. I. Salmonella: a model for bacterial pathogenesis. Annu Rev Med 2001; 52:259-274.

2. Pawelek, J. M., Low, K. B., and Bermudes, D. Bacteria as tumour-targeting vectors. Lancet Oncol 2003; 4:548-556.

3. Elsinghorst, E. A. Measurement of invasion by gentamicin resistance. Methods Enzymol 1994; 236:405-420.

4. Vaudaux, P. and Waldvogel, F. A. Gentamicin antibacterial activity in the presence of human polymorphonuclear leukocytes. Antimicrob Agents Chemother 1979; 16:743-749.

5. Galan, J. E. and Curtiss, R., 3rd. Cloning and molecular characterization of genes whose products allow Salmonella typhimurium to penetrate tissue culture cells. Proc Natl Acad Sci U S A 1989; 86:6383-6387.

6. Eichelberg, K., Ginocchio, C. C., and Galan, J. E. Molecular and functional characterization of the Salmonella typhimurium invasion genes invB and invC: homology of InvC to the F0F1 ATPase family of proteins. J Bacteriol 1994; 176:4501-4510.

7. Akeda, Y. and Galan, J. E. Genetic analysis of the Salmonella enterica type III secretion-associated ATPase InvC defines discrete functional domains. J Bacteriol 2004; 186:2402-2412.

8. Contag, C. H., Contag, P. R., Mullins, J. I., Spilman, S. D., Stevenson, D. K., and Benaron, D. A. Photonic detection of bacterial pathogens in living hosts. Mol Microbiol 1995; 18:593-603.

9. Duchaud, E., Rusniok, C., Frangeul, L., Buchrieser, C., Givaudan, A., Taourit, S., Bocs, S., Boursaux-Eude, C., Chandler, M., Charles, J. F., Dassa, E., Derose, R., Derzelle, S., Freyssinet, G., Gaudriault, S., Medigue, C., Lanois, A., Powell, K., Siguier, P., Vincent, R., Wingate, V., Zouine, M., Glaser, P., Boemare, N., Danchin, A., and Kunst, F. The genome sequence of the entomopathogenic bacterium Photorhabdus luminescens. Nat Biotechnol 2003; 21:1307-1313.

10. Doyle, T. C., Burns, S. M., and Contag, C. H. In vivo bioluminescence imaging for integrated studies of infection. Cell Microbiol 2004; 6:303-317.

11. McKinney, J., Guerrier-Takada, C., Galan, J., and Altman, S. Tightly regulated gene expression system in Salmonella enterica serovar Typhimurium. J Bacteriol 2002; 184:6056-6059.

12. Winson, M. K., Swift, S., Hill, P. J., Sims, C. M., Griesmayr, G., Bycroft, B. W., Williams, P., and Stewart, G. S. A. B. Engineering the luxCDABE genes from Photorhabdus luminescens to provide a bioluminescent reporter for constitutive and promoter probe plasmids and mini-Tn5 constructs. FEMS Microbiology Letters 1998; 163:193-202.

13. Levano-Garcia, J., Verjovski-Almeida, S., and da Silva, A. C. Mapping transposon insertion sites by touchdown PCR and hybrid degenerate primers. Biotechniques 2005; 38:225-229.

14. McClelland, M., Sanderson, K. E., Spieth, J., Clifton, S. W., Latreille, P., Courtney, L., Porwollik, S., Ali, J., Dante, M., Du, F., Hou, S., Layman, D., Leonard, S., Nguyen, C., Scott, K., Holmes, A., Grewal, N., Mulvaney, E., Ryan, E., Sun, H., Florea, L., Miller, W., Stoneking, T., Nhan, M., Waterston, R., and Wilson, R. K. Complete genome sequence of Salmonella enterica serovar Typhimurium LT2. Nature 2001; 413:852-856.

15. Tarr, P. I., Bilge, S. S., Vary, J. C., Jr., Jelacic, S., Habeeb, R. L., Ward, T. R., Baylor, M. R., and Besser, T. E. Iha: a novel Escherichia coli O157:H7 adherence-conferring molecule encoded on a recently acquired chromosomal island of conserved structure. Infect Immun 2000; 68:1400-1407.

16. Donnenberg, M. S. and Kaper, J. B. Construction of an eae deletion mutant of enteropathogenic Escherichia coli by using a positive-selection suicide vector. Infect Immun 1991; 59:4310-4317.

17. Simon, R., Priefer, U., and Puhler, A. A broad host range mobilization system for in vivo genetic engineering: transposon mutagenesis in gram negative bacteria. Bio/Technology 1983; 1:784-791.

18. McKinney, J. S., Zhang, H., Kubori, T., Galan, J. E., and Altman, S. Disruption of type III secretion in Salmonella enterica serovar Typhimurium by external guide sequences. Nucleic Acids Res 2004; 32:848-854.

19. Lee, C. A. and Falkow, S. The ability of Salmonella to enter mammalian cells is affected by bacterial growth state. Proc Natl Acad Sci U S A 1990; 87:4304-4308.

20. Gross, S., Piwnica-Worms, D. Monitoring proteasome activity in cellulo and in living animals by bioluminescent imaging: technical considerations for design and use of genetically encoded reporters. Methods Enzymology 2005; 399:512-530.

21. Leevy, W. M., Gammon, S. T., Levchenko, T., Daranciang, D. D., Murillo, O., Torchilin, V., Piwnica-Worms, D., Huettner, J. E., and Gokel, G. W. Structure-activity relationships, kinetics, selectivity, and mechanistic studies of synthetic hydraphile channels in bacterial and mammalian cells. Org Biomol Chem 2005; 3:3544-3550.

22. Beyer, W. and Bohm, R. Labeling Salmonella live vaccine strains with the lux operon from Vibrio fischeri improves their detection and discrimination from wild type. Microbiol Res 1996; 151:407-419.

23. Lodge, J. K., Weston-Hafer, K., and Berg, D. E. Transposon Tn5 target specificity: preference for insertion at G/C pairs. Genetics 1988; 120:645-650.

24. Hayes, F. Transposon-based strategies for microbial functional genomics and proteomics. Annu Rev Genet 2003; 37:3-29.

25. Burns-Guydish, S. M., Olomu, I. N., Zhao, H., Wong, R. J., Stevenson, D. K., and Contag, C. H. Monitoring age-related susceptibility of young mice to oral Salmonella enterica serovar Typhimurium infection using an in vivo murine model. Pediatr Res 2005; 58:153-158.

26. Fahlen, T. F., Wilson, R. L., Boddicker, J. D., and Jones, B. D. Hha is a negative modulator of transcription of hilA, the Salmonella enterica serovar Typhimurium invasion gene transcriptional activator. J Bacteriol 2001; 183:6620-6629.

27. Bajaj, V., Lucas, R. L., Hwang, C., and Lee, C. A. Co-ordinate regulation of Salmonella typhimurium invasion genes by environmental and regulatory factors is mediated by control of hilA expression. Mol Microbiol 1996; 22:703-714.

28. Raffatellu, M., Wilson, R. P., Chessa, D., Andrews-Polymenis, H., Tran, Q. T., Lawhon, S., Khare, S., Adams, L. G., and Baumler, A. J. SipA, SopA, SopB, SopD, and SopE2 contribute to Salmonella enterica serotype typhimurium invasion of epithelial cells. Infect Immun 2005; 73:146-154.

29. Yu, Y. A., Shabahang, S., Timiryasova, T. M., Zhang, Q., Beltz, R., Gentschev, I., Goebel, W., and Szalay, A. A. Visualization of tumors and metastases in live animals with bacteria and vaccinia virus encoding light-emitting proteins. Nat Biotechnol 2004; 22:313-320.

30. Zhao, M., Yang, M., Li, X. M., Jiang, P., Baranov, E., Li, S., Xu, M., Penman, S., and Hoffman, R. M. Tumor-targeting bacterial therapy with amino acid auxotrophs of GFP-expressing Salmonella typhimurium. Proc Natl Acad Sci U S A 2005; 102:755-760.

31. Bumann, D. Examination of Salmonella gene expression in an infected mammalian host using the green fluorescent protein and two-colour flow cytometry. Mol Microbiol 2002; 43:1269-1283.

32. Knodler, L. A., Bestor, A., Ma, C., Hansen-Wester, I., Hensel, M., Vallance, B. A., and Steele-Mortimer, O. Cloning vectors and fluorescent proteins can significantly inhibit Salmonella enterica virulence in both epithelial cells and macrophages: implications for bacterial pathogenesis studies. Infect Immun 2005; 73:7027-7031.

33. Rang, C., Galen, J. E., Kaper, J. B., and Chao, L. Fitness cost of the green fluorescent protein in gastrointestinal bacteria. Can J Microbiol 2003; 49:531-537.

34. Fass, R. J. and Barnishan, J. Effect of divalent cation concentrations on the antibiotic susceptibilities of nonfermenters other than Pseudomonas aeruginosa. Antimicrob Agents Chemother 1979; 16:434-438.

35. Keeling, K. M. and Bedwell, D. M. Clinically relevant aminoglycosides can suppress disease-associated premature stop mutations in the IDUA and P53 cDNAs in a mammalian translation system. J Mol Med 2002; 80:367-376.

36. Lai, C. H., Chun, H. H., Nahas, S. A., Mitui, M., Gamo, K. M., Du, L., and Gatti, R. A. Correction of ATM gene function by aminoglycoside-induced read-through of premature termination codons. Proc Natl Acad Sci U S A 2004; 101:15676-15681.

37. Yabuuchi, E., Ikedo, M., and Ezaki, T. Invasiveness of Salmonella typhi strains in HeLa S3 monolayer cells. Microbiol Immunol 1986; 30:1213-1224.

38. Meighen, E. A. Molecular biology of bacterial bioluminescence. Microbiol Rev 1991; 55:123-142.

CHAPTER 3

Cancer Cell–Induced Transcriptional Response of *Salmonella* Typhimurium Visualized with a Bioluminescent Transposon Reporter-Trap

3.1 Abstract

Salmonella specifically localize to malignant tumors *in vivo*, a trait potentially exploitable as a cancer drug delivery system. To characterize mechanisms and genetic responses of *Salmonella* during interaction with living neoplastic cells, we custom designed a promoterless transposon reporter containing bacterial luciferase. Analysis of 7,400 independent *Salmonella* transposon insertion mutants in co-culture with melanoma or colon carcinoma cells identified five bacterial genes specifically activated by cancer cells, *adiY*, *yohJ*, *STM1787*, *STM1791*, and *STM1793*. Further experiments identified acidic pH, a common characteristic of the tumor microenvironment, to be a strong, specific and reversible stimulus for *Salmonella* gene activation *in vivo* and *in vitro*. Finally, a *Salmonella* reporter strain expressing a plasmid encoding the luciferase transgene driven by the *STM1787*-inducible promoter showed tumor-mediated transgene activation *in vivo*, demonstrating the potential for a new bacterial-based cancer therapeutic. *Salmonella*, which often encounter acidic environments during classical host infection, may co-opt evolutionarily conserved pathways for tumor colonization in response to the acidic tumor microenvironment. Therefore, specific promoter sequences may provide a platform for *Salmonella*-based tumor therapy with two inherent levels of target specificity *in vivo*.

3.2 Introduction

Salmonella Typhimurium is a Gram-negative bacterium and a common human gastrointestinal pathogen. In human hosts, the organism is typically acquired by ingestion of bacteria causing a gastroenteritis that may progress to a systemic infection. *Salmonella* Typhimurium, characterized by its ability to invade host cells, utilizes genes from two chromosomally-encoded pathogenicity islands, SPI-1 and SPI-2, which contain genes encoding two separate type-three secretion apparatuses, as well as suites of effector genes and various transcription regulators. Research has uncovered important functions during both cell invasion and disease pathogenesis for many of these virulence genes.

Recently, new research has indicated that *Salmonella,* in addition to its ability to cause gastrointestinal disease, may be utilized as a potential diagnostic or therapeutic reagent for malignant tumors. Using bioluminescent and fluorescent bacteria, previous research has shown that intravenously delivered *Salmonella* are remarkably capable of localizing to and persisting within xenograft tumor models *in vivo* [1]. The ability of *Salmonella* to localize to tumors is impressive, as it has been shown that *Salmonella* bacteria are capable of colonizing and persisting in tumors at rates 10,000 times greater than colonization of other organs [2]. *Salmonella* localize both to metastases and tumors, and show specific replication in tumors for weeks *in* vivo [1, 3]. Studies have also utilized the genetic tractability of the organism to design strains that cause little widespread damage to their hosts while retaining the ability to target and persist within tumors [3, 4].

At least two popular hypotheses are proposed to describe the *Salmonella* tumor-targeting phenotype. The first assumes tumors are a relatively immunoprotected site within a host animal, and bacteria may survive specifically in the privileged microenvironment of the

tumor, whereas in other normal tissues are cleared by the host's immune system. The second hypothesis proposes that bacteria are attracted by chemotactic factors to a necrotic environment wherein the availability of excess nutrients in the tumor facilitates replication within this site. To this end, Kasinskas, et al., has shown that bacteria tend to accumulate in specific regions of an *in vitro* tumor model and this behavior is based on nutrient sensors and the chemotaxis machinery [5, 6].

Compared to investigations of the *Salmonella* pathogenic cycle, few experiments have investigated the specific genetic responses of *Salmonella* to eukaryotic tumor cells and bacterial mechanisms regulating this unusual and interesting detour from the typical disease route. In the present work, we engineered a bioluminescent transposon reporter-trap to screen a *Salmonella* Typhimurium library for genes specifically regulated by co-culture with malignant cells *in vitro*. Five genes were identified by the screen and their promoter sequences were found to be specifically activated by the acidic microenvironment associated with cancer cells *in vitro* and tumors *in vivo*. Finally, we utilized one of the activated promoter sequences to demonstrate proof-of-principle studies of *Salmonella*-based tumor therapy with two inherent levels of target specificity *in vivo*.

3.3 Methods

Bacterial strains and culture conditions: The *Salmonella* typhimurium strains SB300A1 [7], SB300A1FL6 (*luxCDABE)* [8], luxAB and AM3 (*luxCDABE msbB*-) were grown in LB broth with appropriate antibiotics. SB300A1FL6 is modified by chromosomal integration of *luxCDABE* and is constitutively bioluminescent. The luxAB strain consists of SB300A1FL6 with the integrated *luxE* gene disrupted. This strain does not

bioluminesce without addition of exogenous decanal substrate. The AM3 strain has the SB300A1FL6 background, but also has an *msbB* gene disruption, giving it a less immunogenic LPS structure. The Tn:27.8 strain, specifically identified from the screen as a non-inducible mutant, phenocopies luxAB with constitutive bioluminescence that requires exogenous decanal.

Tissue culture cell lines and culture conditions: B16F10 murine melanoma cells were obtained from ATCC and cultured according to ATCC directions. HCT116 human colon carcinoma cells were a gift from Bert Vogelstein and were cultured according to ATCC methods.

Plasmids: The plasmid pMAAC001 contains the full bacterial luciferase operon *luxCDABE* driven by a T7 promoter and an ampicillin resistance cassette. The plasmid pLuxCDE consists of the pMAAC001 backbone amplified using the forward primer cccgggattggggaggttggtatgtaa and the reverse primer cccgggtgaatgatttgatgagccaaa (*XmaI* sites underlined). This product was then *XmaI* digested and re-ligated to exclude the majority of the *luxA* and *luxB* genes. pLux and pPROMOTERLux plasmids were constructed by inserting the full bacterial luciferase operon between the *KpnI* and *BamHI* restriction sites in the vector puc19. The pPROMOTERLux plasmid additionally had a 500 base pair promoter region (*STM1787*) from the *Salmonella* genome inserted upstream of the luciferase operon between the *SacI* and *KpnI* restriction enzyme sites. The 500 base pair sequence was amplified from the *Salmonella* genome using the forward primer aaagagctcatttgtcgagagctgggatg and the reverse primer aaaggtacccaggaaacggcattggtaat (*SacI* and *KpnI* sites underlined).

Construction of a Salmonella *Typhimurium reporter-trap library: Salmonella* strain SB300A1 was used to construct a bacterial library comprising approximately 7400 clones of unique chromosomal integrations of our reporter transposon [7]. The custom *Tn5*-based transposon was designed with the EZ-Tn5 system (Epicentre, Madison, WI) using the pMOD4 transposon construction vector. A kanamycin-resistance cassette and promoter from EZ-Tn5<KAN-2> was amplified using the forward primer acgacaaagcttggacgcgatggatatgttct and the reverse primer agcttttctagaggtggaccagttggtgattt (*HindIII* and *XbaI* restriction sites underlined) and inserted into the *HindIII* and *XbaI* restriction sites of pMOD4. The luciferase enzyme genes *luxAB* from *Photorhabdus luminescens* were amplified with the forward primer acagtcgaattccgccgaatgagaattgagat and the reverse primer aagctgggtacctgttggctgctttcactcac (*EcoRI* and *KpnI* sites underlined) and inserted between the *EcoRI* and *KpnI* sites in pMOD4 [8]. The plasmid contained an R6Kγ origin of replication and therefore was amplified in *E. coli* DH5α λpir, purified, digested with Pvu II, and the transposon fragment recovered by gel purification. The purified transposon was combined with transposase (Epicentre). After bench top incubation for 30 minutes, followed by 48 hours at 4°C, the transposon DNA was electroporated into bacteria as per the vendor's instructions. Bacteria were plated on LB kanamycin plates to select for transformants containing the chromosomally-integrated transposon. Each clone was expanded and stored in 60% glycerol in 96-well plates at -80°C.

Screening the library: To screen for gene activation events occurring in the context of malignant cells, *Salmonella* library clones were cultured under three different conditions: co-culture with B16F10 mouse melanoma cells, co-culture with HCT116 human colon

carcinoma cells and culture in media alone. Each of the two tumor cell lines were seeded into 96-well white plates at approximately 70-80% confluency in DMEM with 10% FBS. In the plate containing media alone, each well contained 100 µl of DMEM with 10% FBS only. Plates were incubated overnight to allow tumor cell adhesion to the 96-well white plates. Independently, bacterial clones were grown overnight in LB broth with kanamycin in 96-well plates and subcultured the following day 1:10 into LB broth. Five to six hours after subculturing, 30 µl of bacterial culture were added to three replicate plates, each corresponding to a separate culture condition. Bacteria were allowed to co-incubate with the malignant cells or media alone for 2 hours. Subsequently, bacteria were imaged by adding 30 µl of decanal solution, waiting 10 minutes, and imaging with an IVIS 100 imaging system (Caliper; acquisition time, 60 sec; binning, 4; filter, < 510; f stop, 1; FOV, 23 cm) [9]. Because white plates were used to maximize signal intensity, images were aquired utilizing a <510 filter to reduce phosphorescence from the plates. Three control wells were included on every plate comprising: *luxCDABE Salmonella* (SB300A1FL6), which contain the full luciferase operon inserted into the chromosome; *luxAB* strain, which contains the luciferase enzyme genes only and therefore requires addition of exogenous substrate to image reporter activity in the assay; and a blank well, which contained media, but was not inoculated with bacteria, to serve as a control for background luminescence. Imaged plates were analyzed with Living Image (Caliper) and Igor (Wavemetric) analysis software packages as described[10]. Data were normalized by dividing the photon flux of experimental wells by media alone wells and presented as the $\log_2$ of the normalized photon flux data.

Identification of hits: Library screening data representing photon flux from each well of a library plate were analyzed with Image J software [11]. To identify statistically significant hits from the primary screens, we utilized a set of statistical requirements. First, a threshold was set to identify active clones. Clones that did not produce photon signals greater than three standard deviations above the signal in the un-inoculated, media alone wells were not further analyzed. A quartile method of statistical analysis was then applied to the remaining clonal data [12]. For quartile analysis, plates of clones were grouped by assay date into sets for data analysis. For each set, we normalized data by calculating the $\log_2$ of the fold-change of photon flux signal between the condition of interest (co-culture with B16F10 or HCT116 cells) and media alone. From this data, we calculated the median (Q2), first (Q1), and third (Q3) quartile values. The boundary for hit selection was calculated as Q3 + c(ICQ), where ICQ=Q3-Q1 and c = 1.7239, corresponding to a high stringency targeted error rate of $\alpha = 0.0027$ [12].

Verification of primary screen hits: To verify hits identified by the primary screen, clones were tested again in a similar manner, in quadruplicate. The assay followed the same steps as those in the primary screen, except each clone was tested in 4 wells under each of three conditions across a 12-well row in a black 96-well plate. Imaging was done with an IVIS 100 imaging system (acquisition time, 60 sec; binning, 4; filter, open; f stop, 1; FOV, 23 cm).

Identification of transposon insertion site: To map sites of transposon integration in the chromosome of clones of interest, an inverse touchdown PCR strategy was used [13]. Genomic DNA was isolated from bacteria using DNAzol (Molecular Research Center,

Cincinatti, Ohio). PCR was performed using bacterial chromosomal DNA, 20 pmols of a primer specific to the 5' end of the transposon (atggctcataacacccttg), and 100 pmols of a degenerate primer (cggaatccggatngayksnggntc). Reactions were initiated with a 95°C preparation step for 5 minutes, followed by 25 cycles comprising denaturation at 95°C for 45 seconds, annealing at various temperatures for 45 seconds and extension at 72°C for 2 minutes. The annealing temperature started at 60°C and decreased 0.5°C per cycle for the subsequent 24 cycles. Then PCR proceeded with 25 cycles of 95°C for 45 seconds, 50°C for 45 seconds and 72°C for 2 minutes. PCR reaction products were fractionated on a 1% agarose gel, and the most prominent bands in each lane were excised and gel purified (Qiagen kit). For some reactions, PCR products were purified (Qiagen) and the resulting purified PCR product was used as a template for a second round of PCR using a different transposon-specific primer (aacatcagagattttgagacacc) before gel purification of products. The cycling conditions and degenerate primer used in the second round of PCR were the same as round one.

Semi-quantitative RTPCR: *Salmonella* strain SB300A1 was subcultured from a stationary phase culture 1:10 and grown for 6 hours. Bacteria were then diluted 1:20 and added to 96-well plates containing tissue culture media alone or B16F10 melanoma cells, seeded 24 hours previously at 100,000 cells/well. After three and a half hours of co-culture, extracellular media containing bacteria were removed from the 96-well plates and triplicates pooled. Media were centrifuged to pellet bacteria and pellets were frozen at -80°C. After thawing, pellets were resuspended in 200 µl water with 5 mg/ml lysozyme and incubated at room temperature for 5 minutes. Then, 700 µl of RLT buffer was added and bacterial RNA was purified using the Qiagen RNeasy kit (Qiagen Inc, Valencia, CA).

Samples were then treated with DNase I at room temperature for 15 minutes, after which EDTA was added and samples were incubated for 10 minutes at 65°C to inactivate the DNase. Samples were then ethanol precipitated and resuspended in 30 μl water. For reverse transcriptase PCR, 1 μg of total RNA was used as a template and reverse transcribed using Superscript II Reverse Transcriptase and 300 ng random primers as per the manufacturer's instructions (Invitrogen, Carlsbad, CA). Following RTPCR, samples were treated with RNase H for 25 minutes at 37°C. To perform semi-quantitative PCR, samples were amplified using primers specific to each gene target or to ribosomal RNA: STM1787 (forward: tcggtagatcgcatgatgtc, reverse: ggttggtcataagcctgtcg), STM1791 (forward: acacgggaacatccagattc, reverse: cggcaaaggacaaatctcat), STM1793(forward: ttcggcaacctgtttttagg, reverse: acgcctccttgcataatcac), *adiY* (forward: ccttattgaccgccaactgt, reverse: gtggtcaagaaagcgggata), *yohJ* (forward: caggcatttttcttgcatca, reverse: cgccatataacgaatcagca), *rrsH* (forward: cagccacactggaactgaga, reverse: gttagccggtgcttcttctg). PCR cycling conditions were: 95°C for 5 minutes, 30 cycles (or 20 cycles for *rrsH* reactions) of denaturation at 95°C for 45 seconds, annealing at 50°C for 45 seconds and extension at 72°C for 1 minute. PCR products were fractionated on a 1% agarose gel.

Construction of deletion mutants: Mutant strains deficient for the identified target genes were constructed in *Salmonella* strain *luxCDABE msbB*- (AM3), which contains a constitutively active, chromosomally-encoded bacterial luciferase operon as well as a mutation in *msbB* to create a less immunogenic LPS structure. Mutants were constructed using a lambda red recombinase strategy [14]. First, primers were designed to amplify the chloramphenicol-resistance cassette in pKD3 with tails flanking the targeted locus of the

Salmonella genome to be deleted. Primer sequences specifically targetting the genome for each mutant were used (*adi* forward targetting primer: atgaaagtattaattgttgaaagtgagtttctgcatcaggacacctgggtgtgtaggctggag-ctgcttc, *adi* reverse targetting primer: atcctgtttaaccggcgcatccagcggatacgggtttttgtgaatgc-ggtcatatgaatatcctccttag; *yohJ* forward targetting primer: agtaagtcactgaatattatctg-gcaatatatacgcgcttgtgtaggctggagctgcttc, *yohJ* reverse targetting primer: ttttttcgttcc-cttctgcccaaccactttacgctcaccgcatatgaatatcctccttag; STM1789-1793 forward targetting primer: atgaatgcgcaacgcgtagtggtgatggggttaggaaaccgtgtaggctggagctgcttc, STM1789-1793 reverse targetting primer: ctaataaagttcatgatcgttgcggcggagggtccccaggcatatgaa-tatcctccttag). PCR fragments were then electroporated into AM3 bacteria expressing plasmid-encoded red recombinase. Following electroporation, growth on chloramphenicol plates at 37°C selected for strains that had lost the temperature-sensitive recombinase plasmid and inserted the chloramphenicol-resistance cassette into the targeted genomic loci. Deletion of the genes was confirmed by PCR.

Dose-response to tumor cells: To test the dose-response of hits from the screen to tumor cell co-culture, the assay was performed as described, except that either B16F10 or HCT116 cells were plated at $1x10^5$; $2 x10^5$; or $3 x10^5$ cells per well 24 hours before co-culture with bacteria. Stationary phase bacteria were diluted 1:50 and incubated for 6 hours before identical aliquots were allowed to co-culture with the malignant cells. Imaging was done with an IVIS 100 imaging system (acquisition time, 10 sec; binning, 8; filter, open; f stop, 1; FOV, 20 cm). Imaged plates were analyzed with Living Image (Caliper) and Igor (Wavemetrics) analysis software packages as described [10].

Assaying promoter activation in different pH media: Stationary phase bacteria were subcultured 1:100 into LB broth. Five to six hrs after subculturing, 10 µl of bacterial culture were added to 190 µl pre-warmed HEPES-buffered media in black 96-well plates adjusted to different pH values, and allowed to incubate for three and a half hours. Bacteria were then imaged with an IVIS 100 imaging system (acquisition time, 60 sec; binning, 8; filter, open; f stop, 1; FOV, 20 cm).

Mouse imaging studies: To generate tumor xenografts, 6-week old *nu*/*nu* mice (Taconic) were injected subcutaneously in the right flank with 1 $x10^6$ B16F10 cells or 2.5 $x10^6$ HCT116 cells in 100 µl PBS. Tumors were allowed to grow for two (B16F10) or three (HCT116) weeks before bacterial challenge. Saturated cultures of strain AM3 and deletion mutant bacteria were subcultured 1:100 into LB and grown for 3 hours. Bacteria were then diluted to 1 $x10^6$ bacteria/ml and 100 µl were injected via tail vein. Mice were imaged as indicated using an IVIS 100 imaging system (acquisition time, 60 sec; binning, 8; filter, open; f stop, 1; FOV, 20 cm). Photon flux data were calculated by utilizing user-determined regions of interest (ROIs) around bioluminescent tumors with Living Image software.

For *in vivo* promoter inducibility experiments, 6-week old *nu*/*nu* mice (Taconic) were injected subcutaneously in the right and left flanks with 1 $x10^7$ HCT116 cells in 100 µl PBS. Tumors were allowed to grow for one week. Saturated cultures of *Salmonella* strain SB300A1 containing plasmids pMAAC001, pPROMOTERLux, or pLux were subcultured 1:100 into LB and grown for 3 hours. Twenty microliters of bacterial culture were injected intratumorally. Mice were imaged as indicated using an IVIS 100 imaging

system (acquisition time, 180 or 60 sec; binning, 8; filter, open; f stop, 1; FOV, 25 cm). Photon flux data were calculated by utilizing software-determined regions of interest (ROIs) around bioluminescent tumors with Living Image software.

Tumor ex vivo *imaging*: 6-week old *nu*/*nu* mice (Taconic) were injected subcutaneously in the right flank with 1 $x10^5$ B16F10 cells and tumors allowed to grow for two and a half weeks. Saturated cultures of bacteria were diluted and 5 $x10^5$ bacteria were injected intratumorally. At 24 and 48 hours following bacterial injections, mice were sacrificed, and tumors excised and dissected into 4 sections each. The bacterial-colonized tumor sections were incubated in HEPES/Tris-buffered media at the indicated pH values and imaged using an IVIS 100 imaging system at the indicated times (acquisition time, 180 sec; binning, 8; filter, open; f stop, 1; FOV, 12 cm).

Statistics: Error bars represent the standard error of the linearly regressed data or the standard error of the mean where noted.

3.4 Results

To conduct a large-scale, unbiased screen for genes up-regulated by contact with malignant cells, we used a Tn5-based transposon as the backbone of a LuxAB reporter construct. We chose to use the bacterial luciferase enzyme genes (*luxAB)* only, in contrast to the full bacterial luciferase operon (*luxCDABE*), because the size of the transposon containing the full operon prohibited efficient chromosomal integration, while using only the *luxAB* genes allowed for efficient genomic insertion of the transposon. The transposon was designed to restrict reporter gene expression to only those chromosomal integration sites downstream of an active promoter. A kanamycin resistance cassette with

a constitutive promoter was also included to select for integration into the chromosome (**Figure 3-1a**). After construction, the purified transposon was electroporated into *Salmonella* Typhimurium strain SB300A1 for random chromosomal integration, producing a 7,400 clone bacterial library[7].

Initially, the entire *Salmonella* library was subjected to a primary screen in the context of three conditions: tissue culture media alone, B16F10 melanoma cells and HCT116 colon carcinoma cells, both of the latter in monolayer co-culture with the *Salmonella* reporter library. The eukaryotic tumor cells were grown in 96-well plate format overnight and then bacterial clones added to wells corresponding to each of the two co-culture conditions and media alone. After a two-hour incubation, bioluminescence imaging of plates enabled identification of clones specifically up-regulating genes in the context of exposure to melanoma and/or colon carcinoma cells (**Figure 3-1a**). Results of the screen from co-culture with melanoma and colon carcinoma cells are shown in **Figures 3-1b** and **3-1c**, respectively. In each case, data are shown as a rank-ordered S-plot of the $\log_2$ of the normalized signal for each clone of the library, where normalized signal was the ratio of the signal in the condition of interest to the signal in media alone. The majority of data points clustered around zero, indicating that most mutants interrogated in the assay did not show tumor-specific gene regulation. However, quartile analysis with a boundary for hit selection corresponding to a high stringency targeted error rate ($\alpha = 0.0027$) identified five candidate mutants wherein the transposon reporter was specifically up-regulated during co-culture with malignant cells.

Following the primary screen, we utilized inverse touchdown PCR to map the specific location of each transposon in the *Salmonella* genome [13]. **Table 3-1** documents the site of chromosomal integration for the transposon and candidate gene up-regulated in each isolate. All genes were novel in that they have not been previously reported to be involved in *Salmonella*-host interactions, nor involved in *Salmonella* colonization of neoplasia. Interestingly, the genomic insertion sites of the transposon in three of the clones inserted in a cluster in the chromosomal sequence. Mapped to three different, but closely linked genes (*STM1787*, *STM1791* and *STM1793*, respectively), two are known hydrogenases, and all three genes are likely co-regulated and involved in the same *Salmonella* function. Although three integrations in the same putative operon may seem to indicate a transposon insertion bias, this is not likely. Because the transposon insertion library contained more than 7400 individual mutants, the average distance between two different transposon integration sites was therefore approximately 650 base pairs throughout the entire *Salmonella* genome. In the case of the three transposon insertions discussed above, integration sites were located 2843 base pairs (*STM1787* and *STM1791*) and 2185 base pairs (*STM1791* and *STM1793*) apart, indicating random integration by the Tn5-based system could easily have produced this result. Sequencing showed that in one high stringency hit, the transposon had inserted into *adiY*, a *Salmonella* gene known to be involved in an acid tolerance response [15]. The transposon in the fifth clone was identified to have landed in *yohJ*, a putative membrane protein [16].

To validate cancer cell co-culture-specific gene activation events identified in the primary screen, we first repeated the co-culture assay in quadruplicate in at least three independent experiments for each clone. **Figure 3-2a** shows the data from one

representative experiment for clones verified by this assay. Again, all five clones showed statistically significant enhancement of bioluminescence in the presence of tumor cells, with a trend toward greater gene up-regulation when co-cultured with B16F10 melanoma cells. Then, to further characterize tumor cell-induced response of *Salmonella*, we utilized the tumor cells in a dose-response assay (**Figures 3-2b, c**). Additionally, to verify that the reporter activation seen in the *Salmonella* reporter-trap clones was not an effect of differing substrate permeability due to mutations in bacterial genes, the bacteria used in this assay contained the original chromosomal *luxAB* insertion as well as a plasmid constitutively expressing *luxCDE*, the biosynthetic genes for the long-chain aldehydes that act as the optical substrates of the bacterial luciferase operon. Therefore, for this assay, it was not necessary to add decanal to the media. Identical innoculations of bacteria showed greater up-regulation of the reporter when exposed to greater numbers of tumor cells in co-culture conditions, indicating that the stimuli from tumor cells instigated a graded response from the bacteria. Because expression of the *lux* operon genes fully complemented the use of exogenous decanal in the system, the data confirmed that the effect was not an artifact of exogenous decanal permeability in the primary screen.

Finally, to verify that the reporters in fact reflected mRNA transcriptional regulation in wild-type *Salmonella* during co-culture with tumor cells, we utilized semi-quantitative PCR. Following a three-hour co-culture of wild-type (SB3001A1) bacteria with B16F10 cells or in tissue culture media alone, isolated RNA was reverse transcribed to cDNA. Semi-quantitative PCR of the cDNA showed co-culture with B16F10 melanoma cells

enhanced the intensity of target gene transcripts, but not of the control ribosomal RNA transcripts (*rrsH*) (**Figure 3-2d**).

Notably, of the genes identified in this screen, at least one, *adiY*, has previously been reported to be up-regulated in acidic pH conditions [15]. One characteristic of tumor microenvironments *in vivo* is an abnormally acidic pH [17]. For these reasons, the *Salmonella* transposon insertion mutants were further investigated for reporter signal activation in acidic conditions. **Figure 3-3** shows that reporter signals increased in acidic pH media compared to neutral media. Each of the clones up-regulated the reporter gene at pH 6.0 compared to the physiological pH of normal body tissue (pH 7.5), suggesting that the stimulus *Salmonella* responded to in the context of neoplastic cells was microenvironment acidification.

To determine whether the activated genes were required for localization to tumors or required for colonization and growth within tumors *in vivo*, *Salmonella* strains mutant for genes identified in the screen were constructed. Selected genes were deleted using a lambda red recombinase insertional deletion strategy, which inserted a chloramphenicol resistance cassette into the targeted genes. The deletion mutants were created from a parental *Salmonella* strain (*luxCDABE msbB*-) containing a chromosomally-integrated and constitutively-expressed bacterial luciferase operon for imaging bacterial localtization *in vivo* in real time. The stain also contained a *msbB* gene deletion, which causes a less immunogenic LPS structure and minimizes septic shock effects when the strain is administered intravenously [3]. Based on the analysis that the identified *STM1787*, *STM1791* and *STM1793* genes were contained in a single operon, we targeted

a large region of this operon for deletion in a single mutant strain, 1789-1793⁻. The gene *adiY* also appeared to be a part of a larger operon of co-regulated genes and was therefore targeted along with the adjacent genes *adi* and *yjdE*. The gene *yohJ* was targeted individually. In a B16F10 melanoma tumor xenograft model, all bacterial strains were injected via mouse tail vein and deletion mutants compared to the parental strain for localization to and persistence within the tumor using bioluminescence imaging (**Figure 3-4**). All mutant strains and the parent strain were capable of tumor localization and persistence, indicating that the identified genes were not essential for bacterial *colonization* of the tumor. The experiment was also performed in an HCT116 colon carcinoma xenograft model with similar results. **Table 3-2** details the numbers of mice with colonized tumors on or before day 10 in each experiment.

We next sought to demonstrate the specificity of selected promoter activation in the tumor microenvironment *in vivo*. Here, we used the constitutively bioluminescent *Salmonella* strain Tn:27.8+p*luxCDE* or the conditionally bioluminescent strain Tn:1787+p*luxCDE*, each of which constitutively express plasmid-encoded *luxCDE,* but the latter strain will only bioluminesce upon activation of the chromosomally-encoded *luxAB* reporter. In a B16F10 melanoma tumor xenograft model, bacteria were injected via mouse tail vein or intratumorally and allowed two days to localize and adapt to tumors *in vivo*. Tumors were then excised, incubated in solutions of various pH values and imaged periodically for six hours. Initially, all tumors showed bioluminescent bacteria *ex vivo*. Over time, constitutive Tn:27.8 *Salmonella* showed an increase in signal consistent with bacterial growth in the tumor explants. This behavior was also observed in the Tn:1787 *Salmonella*-infected tumor suspension in low pH media. By contrast, when the Tn:1787

Salmonella-infected tumor was maintained in basic media conditions throughout, the signal initially increased, but then plateaued around 4 hours and decreased in comparison to the constitutively bioluminescent Tn:27.8 strain (**Figure 3-5**). This finding indicated that bacterial gene expression was initially engaged by the low pH conditions of the *in vivo* tumor microenvironment, but after exposure to a higher pH environment *ex vivo*, the promoter driving the reporter was repressed and signal declined. Further, this *ex vivo* effect was reversible. When the medium on the Tn:1787 *Salmonella*-infected tumor suspension was changed from pH 6.0 to pH 7.5, the bioluminescent signal decreased. Conversely, when the media was changed from pH 7.5 to pH 6.0, the signal increased (**Figure 3-5b**). These effects were not seen with the constitutive Tn:27.8 *Salmonella*-infected tumor explants, and provided further evidence in support of the specificity of the trapped *Salmonella* promoter in the Tn:1787 transposon mutant for the tumor microenvironment.

Because the identified *Salmonella* genes were dispensable for tumor localization, but their respective promoters were activated in the tumor microenvironment, these strains provided a unique opportunity to design tumor-targeting bacterial vectors subject to various levels of controlled specificity. Thus, we sought to determine if the acidic pH of the tumor microenvironment could be exploited to specifically activate a target transgene during tumor localization. As proof of principle, we constructed *Salmonella* reporter strains expressing plasmids encoding the bacterial luciferase operon driven by either constitutive promoters or an inducible promoter to demonstrate tumor-mediated transgene activation *in vivo*. The plasmids p*MAAC001* and p*Lux* both encoded constitutively-expressed luciferase operons, while the p*PROMOTERLux* plasmid was

engineered to contain the luciferase operon driven by the *Salmonella* candidate promoter (*STM1787*) comprising 500 base pairs upstream of the putative transcription start site of tumor-activated genes *STM1787*, *STM1793* and *STM1791* (which we will now refer to as the *STM1787* promoter). Bacteria expressing these plasmids were identically injected into mice bearing HCT116 tumor xenografts on each flank (**Figure 3-6**). We chose to utilize intratumoral injection to directly compare reporter gene activation from two different bacterial strains, one inducible and the other constitutive, over time in the same mouse. Although reporter signals from p*PROMOTERLux*-expressing bacteria were low immediately after injection into the tumor, the bacteria quickly induced a 90-fold enhanced expression of the reporter after an 8 hr exposure to the tumor microenvironment (**Figure 3-6a**). Concurrently, bacteria constitutively expressing p*Lux*- or p*MAAC001*-luciferase showed <20-fold or no reporter activation, respectively, after exposure to the tumor microenvironment (**Figures 3-6a and 3-6b**). These data directly demonstrated tumor-specific induction of a transgene from the *Salmonella STM1787* promoter in an *in vivo* system. Therefore, the *STM1787* promoter could be used as a platform to design tumor-targeting *Salmonella* strains capable of specifically delivering a therapeutic gene or toxin to the site of a tumor *in vivo*.

3.5 Discussion

Salmonella Typhimurium bacteria are typically classified as human gastrointestinal pathogens and a common cause of modern food-borne illness. However, another noted characteristic of *Salmonella* is the bacterium's coincident colonization of tumor tissue. In fact, in the 1800's, some physicians began to intentionally use bacteria as tumor therapeutics. Yet, due to significant toxicity and lack of consistent, reliable results, these

practices were abandoned. However, more recent studies using longitudinal imaging demonstrate *Salmonella* colonization of tumors in real time and have sparked a renewed interest in this concept using *Salmonella* [1, 18] as well as various other tumor-localizing microbes as an option for cancer treatment [19-25].

A number of these studies capitalize on utilizing bacteria as treatments *per se* or as drug delivery vehicles, by exploiting their potentially low toxicity and high tractability [23, 26-30]. Various attenuated *Salmonella* strains have been developed for use in tumor-targeting studies, including specific amino acid auxotrophs and LPS mutants [3, 31]. However, the greatly reduced toxicity of *Salmonella* LPS mutants (*msbB*-) observed in swine models has not been observed in mouse models [32, 33]. In more than one instance, attenuated *Salmonella* have even been used in a clinical trial to treat cancer in humans [33-35]. However, trials so far show relatively low rates of tumor colonization in human hosts, which may be due to excessive attenuation of bacteria [32, 36]. Additionally, one study indicates that induction of TNFα by bacteria is necessary for optimal colonization of tumors [37]. Nonetheless, few studies have investigated the phenotypic and gene expression patterns of these tumor-targeting bacteria following exposure to tumor cells.

Tumor-targeting bacteria present a challenge: how to produce a bacterial strain sufficiently attenuated to limit side effects, but not so attenuated that tumor colonization is unlikely. One approach to this problem is to increase the tumor specificity of the treatment strategy. By using bacterial strains containing therapeutic gene products for which expression is specifically activated in the tumor microenvironment, it may be

possible to reduce the dose of potentially toxic bacteria. However, the ideal location for this transgene in the *Salmonella* genome must demonstrate two critical properties. First, the location must be highly up-regulated in the tumor microenvironment. Second, the insertion of a gene at this site must not disrupt the ability of the *Salmonella* to target and colonize tumor tissues. Candidate genes that meet the above criteria may serve as ideal target sites for inserting therapeutic transgenes.

In this study, we utilized an engineered transposon to interrogate the *Salmonella* genome for genes activated during exposure to cancer cells. Toward this objective, we generated a library of greater than 7,400 independent transposon insertions, which, assuming random integration, would predict genomic coverage of approximately 1.5X. From this library, we identified five *Salmonella* genes specifically up-regulated during co-culture with cancer cells, *STM1787*, *STM1791*, *STM1793*, *adiY* and *yohJ*. Following identification of these tumor cell-activated genes, verification in secondary assays and confirmation in wild-type *Salmonella*, we determined that the common stimulus for up-regulation of target gene expression was acidic pH. In another study aimed at identifying *Salmonella* promoters involved in tumor colonization *in vivo*, *Salmonella* genomic DNA was digested and ligated randomly upstream of a GFP reporter. In this study, the major stimulus identified in reporter activation was hypoxia, but no pH-regulated promoters were identified [38]. While pH and hypoxia are physiologically linked, the five genes identified herein show no overlap with the promoters identified by Arrach et. al. [38]. The lack of concordance may reflect the different strategies for gene identification or the inherent enhanced sensitivity of bioluminescence readouts (due to the lack of background signals) compared with fluorescence. Nonetheless, hydrogenase genes are noted in some

cases to be up-regulated in low oxygen conditions, indicating that hypoxia may serve as a further stimulus for the pH-induced promoters identified in the present study [39]. However, in pilot studies using an incubation pouch system used for growing anaerobic bacteria, we did not observe any significant changes in transposon reporter activity (KF, unpublished data). While these data don't necessarily rule out entirely oxygen-independence, pH appeared to be the dominant signal inducing responses in the promoters identified by our bioluminescent transposon reporter-trap screen.

In view of the usual pathophysiology of *Salmonella*, it is not surprising that *Salmonella* strains have gained the ability to precisely regulate genes in response to different pH environments. *Salmonella* encounter low pH conditions regularly during human infection, for example, during transit through the stomach, and later during intracellular trafficking through the phagosome [40, 41]. Interestingly, the acidic pH of the tumor environment *in vivo* has long been noted as an important microenvironmental condition when designing effective tumor treatment techniques [17, 42]. Additionally, the low pH environment of the tumor inhibits host defense. Cytotoxic immune cell activity and cytokine secretion has been shown to be impaired by a low extracellular pH [43, 44]. In contrast, with a bacterial-driven tumor therapeutic, low pH may become an exploitable advantage, by adding another level of selectivity to bacterial gene activation. In this case, a bacterial-based system may succeed, while both conventional therapeutics and host defenses fail.

When using bacteria as a vector for drug delivery studies, tumor-specific expression is a major concern. The genes identified herein are highly expressed in an acidic pH tumor

environment, but are not required for bacterial tumor targeting. Therefore, the promoters regulating these genes may be ideal candidates for utilization in therapeutic gene, pro-drug or toxin delivery studies. We have identified the *STM1787* promoter as an ideal bacterial sequence capable of driving tumor-specific expression of a transgene, and demonstrated this *in vivo* using bioluminescent imaging. By adapting the *STM1787* promoter in *Salmonella* to drive expression of an appropriate therapeutic transgene, the resulting bacterial vector would provide two independent mechanisms for specifically targeting tumors. First, *Salmonella* specifically localize to and accumulate in tumors *in vivo*. Second, the *STM1787* promoter is preferentially activated in the acidic tumor microenvironment. The combined effect of these two levels of specificity provides a potential option to design more successful bacterial therapeutics in the future.

3.6 Tables

Table 3-1. Transposon chromosomal insertion locations in *Salmonella* reporter mutants.

Strain Name	**Transposon Insertion Location**	**Base pairs Downstream of Start Codon**	**Function (Putative) [16]**
Tn:1787	*STM1787*	1,189	Hydrogenase
Tn:1791	*STM1791*	505	Hydrogenase
Tn:1793	*STM1793*	661	Cytochrome oxidase
Tn:adiY	*adiY*	439	araC-like transcriptional activator; arginine-dependent acid tolerance
Tn:yohJ	*yohJ*	205	Hypothetical membrane protein

Table 3-2. Tumor localization of constitutively bioluminescent *Salmonella* mutants.

Mutant	**Number of Mice with Bioluminescent, Colonized Tumors/Total Mice Injected (HCT116 Colon Carcinoma)**	**Number of Mice with Bioluminescent, Colonized Tumors/Total Mice Injected (B16F10 Melanoma)**	**Totals**
luxCDABE	2/3	3/4	5/7
STM1789-1793	2/3	2/5	4/8
adi	1/2	4/5	5/7
yohJ	3/3	3/5	6/8

3.7 Figures

Figure 3-1

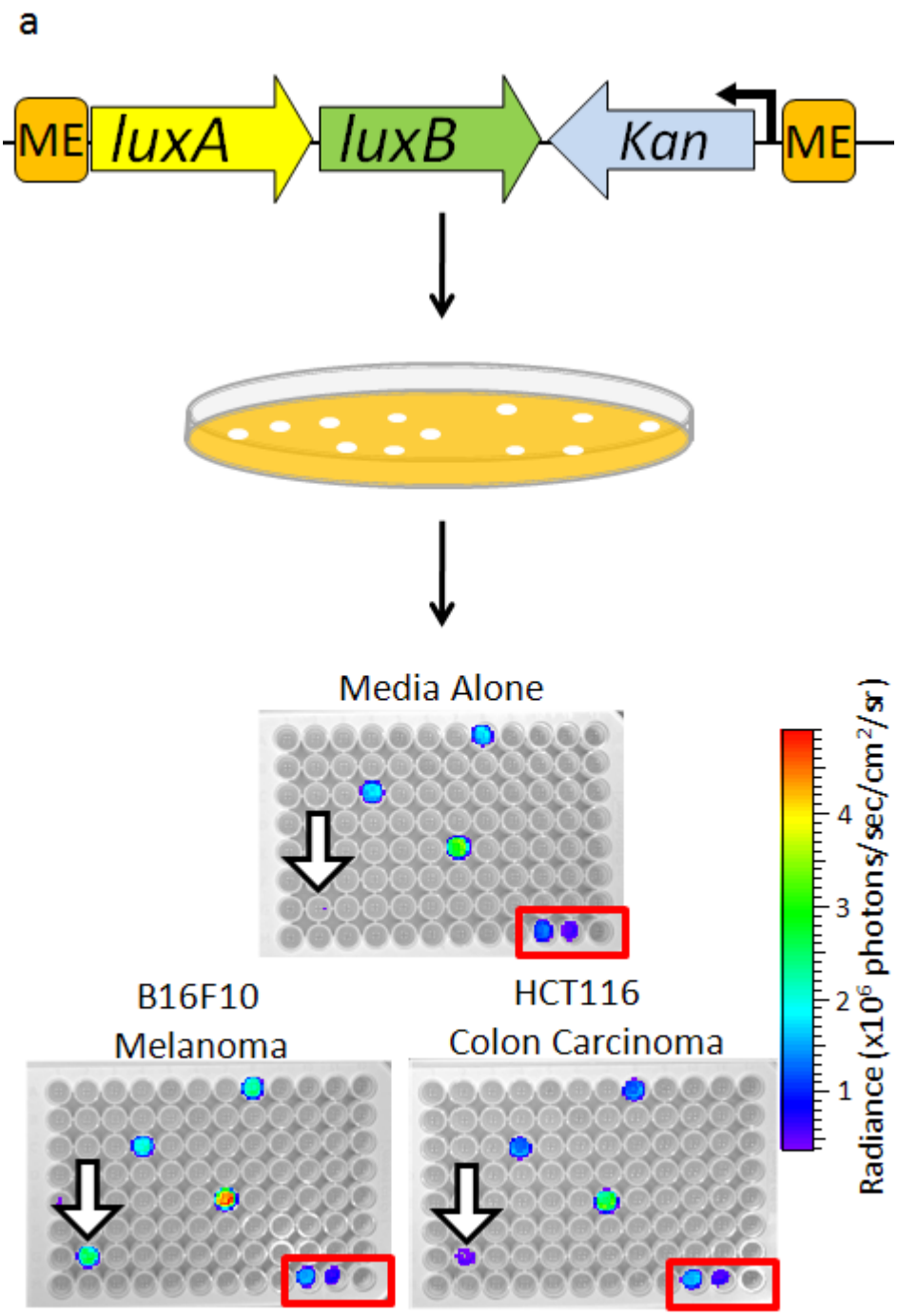

b

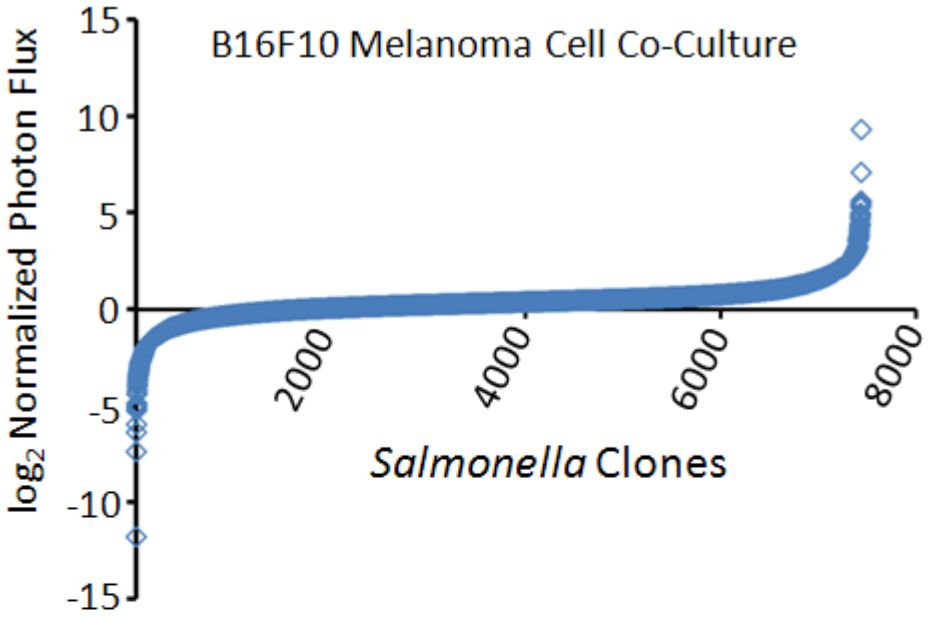
B16F10 Melanoma Cell Co-Culture
log2 Normalized Photon Flux
15
10
5
0
-5
-10
-15
2000
4000
6000
8000
Salmonella Clones

c

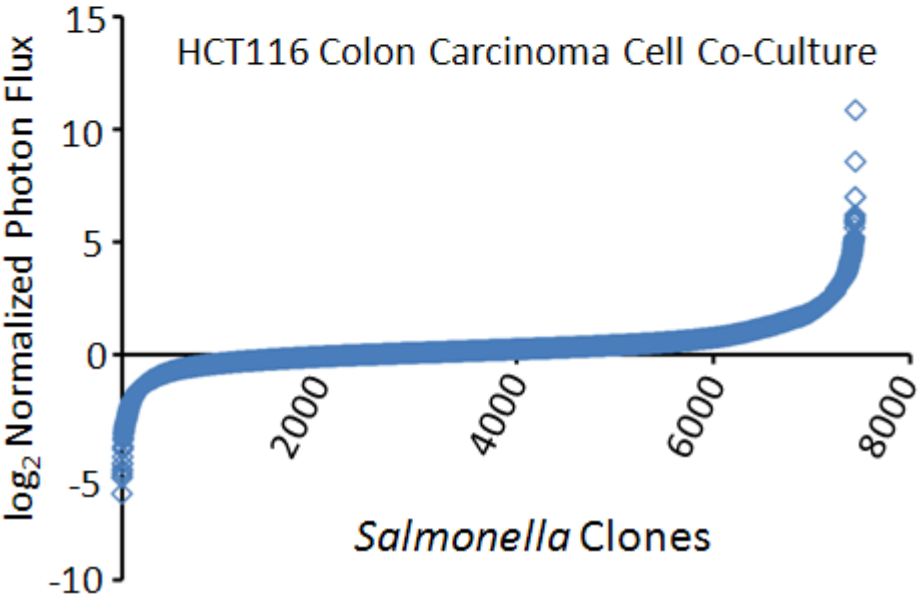
HCT116 Colon Carcinoma Cell Co-Culture
log2 Normalized Photon Flux
15
10
5
0
-5
-10
2000
4000
6000
8000
Salmonella Clones

Figure 3-1. **Design and utilization of a high throughput screen to identify tumor cell-induced gene activation events in *Salmonella*.** (a) A schematic of the promoter trap system using Tn5-based *luxAB* chromosomal integration. Expression of the promoterless *luxAB* reporter vector, and resulting *Salmonella* bioluminescence, is dependent on "trapping" an active promoter upstream of the chromosomal integration site. The transposon was randomly integrated into SB300A1, and kanamycin-resistant colonies were selected and arrayed into 96-well plates for library screening. Representative primary screening plates in triplicate show responses of *Salmonella* library strains to three separate co-culture conditions: media alone (top), B16F10 melanoma cells (bottom left), HCT116 colon carcinoma cells (bottom right). Hit 47.74, showing selective activation in co-culture with cancer cells, is indicated by the black open arrowhead, while the signals in the upper and central wells represent non-selective activation of clones. In each plate, wells H10, H11, and H12 (red box) contain media and bacteria constitutively expressing *luxCDABE*, bacteria constitutively expressing *luxAB*, and no bacteria, respectively, as controls. Primary library screening data from *Salmonella* promoter trap clones co-cultured with B16F10 melanoma cells (b) or HCT116 colon carcinoma cells (c). Data are reported as the $\log_2$ of the normalized signal for each library clone, where normalized signal was the ratio of the signal in the condition of interest to the signal in media alone.

Figure 3-2

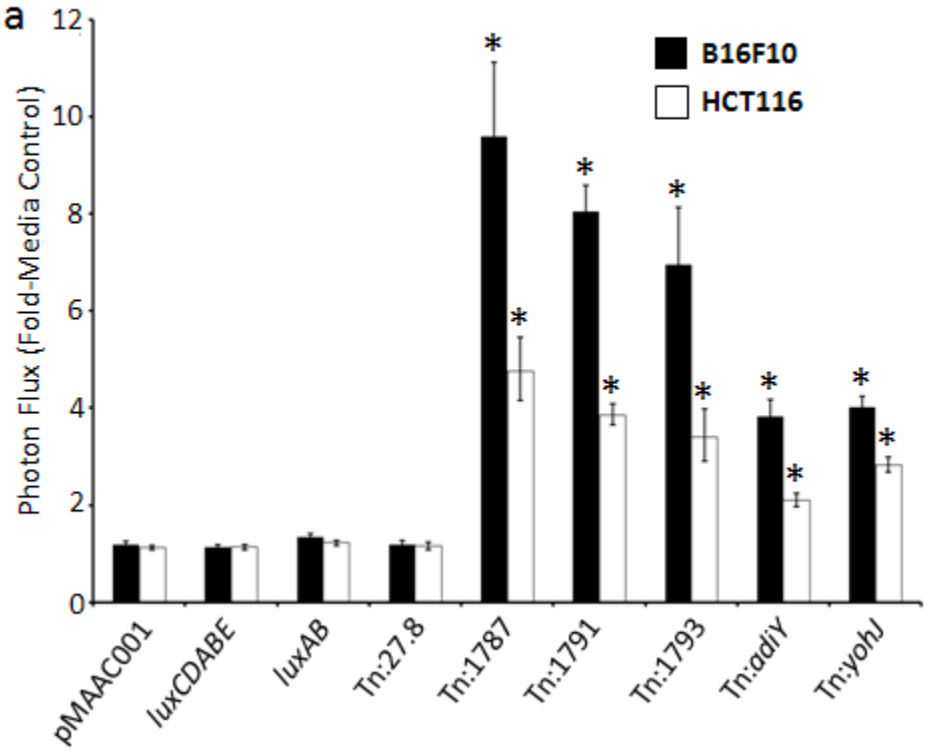
a
Photon Flux (Fold-Media Control)
12
10
8
6
4
2
0
B16F10
HCT116
*
pMAAC001
luxCDABE
luxAB
Tn:27.8
Tn:1787
Tn:1791
Tn:1793
Tn:adiY
Tn:yohJ

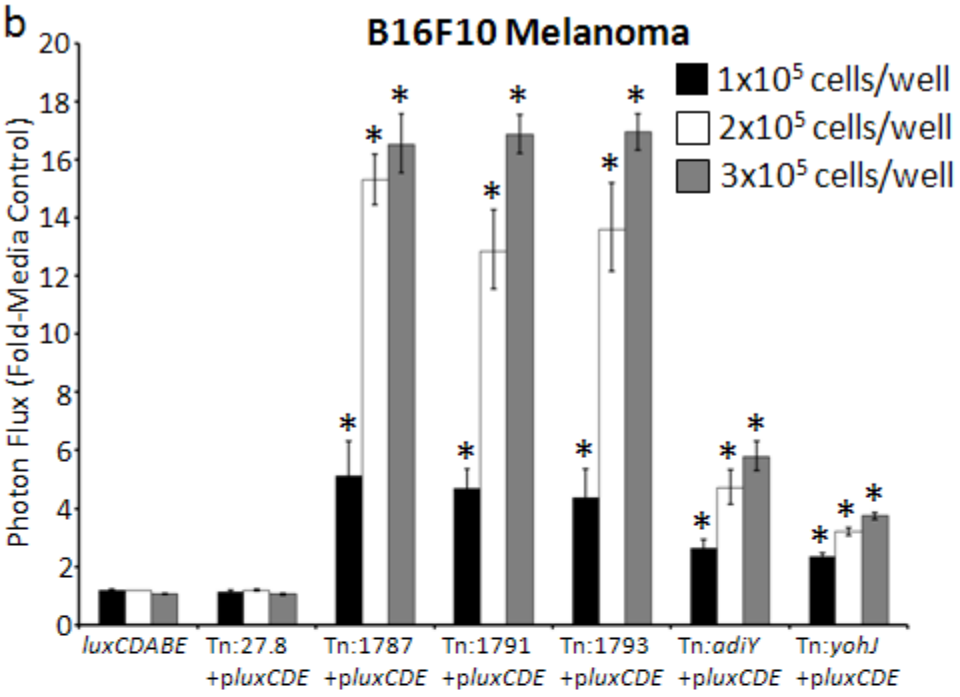
b
B16F10 Melanoma
1x10^5 cells/well
2x10^5 cells/well
3x10^5 cells/well
Photon Flux (Fold-Media Control)
0
2
4
6
8
10
12
14
16
18
20
luxCDABE
Tn:27.8 +pluxCDE
Tn:1787 +pluxCDE
Tn:1791 +pluxCDE
Tn:1793 +pluxCDE
Tn:adiY +pluxCDE
Tn:yohJ +pluxCDE

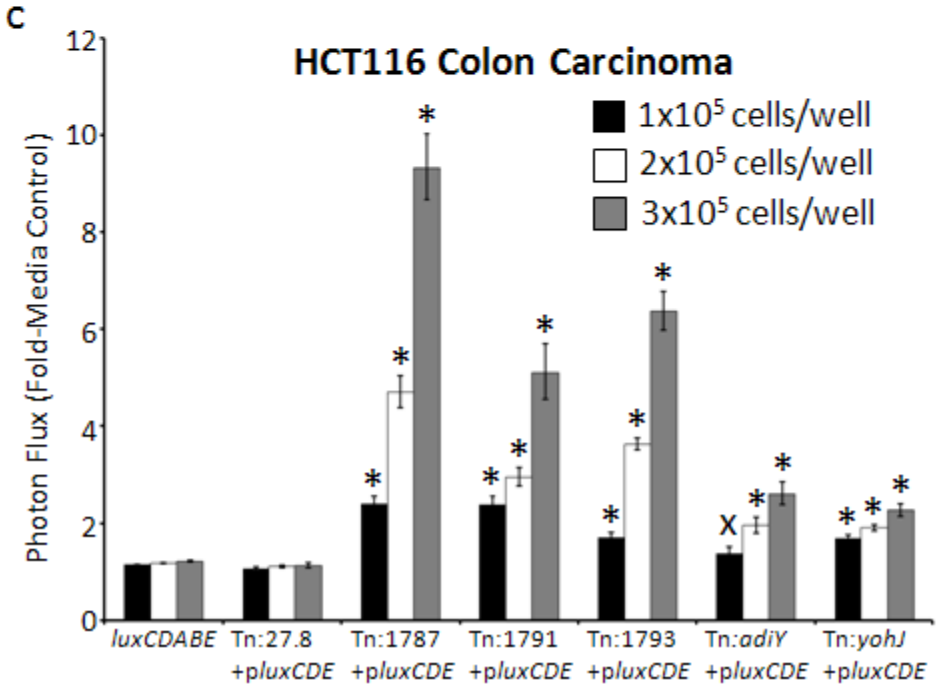
c
HCT116 Colon Carcinoma
1x10^5 cells/well
2x10^5 cells/well
3x10^5 cells/well
Photon Flux (Fold-Media Control)
0
2
4
6
8
10
12
X
luxCDABE
Tn:27.8 +pluxCDE
Tn:1787 +pluxCDE
Tn:1791 +pluxCDE
Tn:1793 +pluxCDE
Tn:adiY +pluxCDE
Tn:yohJ +pluxCDE

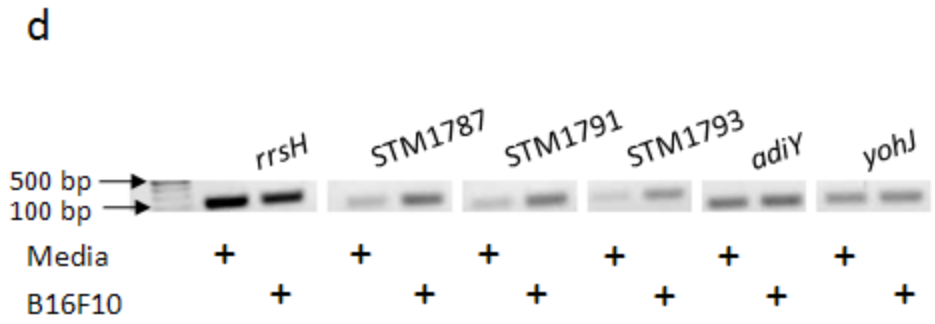

Figure 3-2. Verification of *Salmonella* gene activation events in the context of tumor cell co-culture. (a) *Salmonella* reporter clones displaying gene activation signals during co-culture with tumor cell lines (black bars, B16F10 melanoma cells; open bars, HCT116 colon carcinoma cells). *Salmonella* strains *luxAB* and Tn:27.8 contain chromosomal *luxAB* genes under constitutive promoter control; *luxCDABE Salmonella* contain the full luciferase operon inserted into the chromosome; pMAAC001 constitutively expresses plasmid-encoded *luxCDABE*. (b, c) *Salmonella* reporter clones display dose-responsive gene activation in co-culture with B16F10 and HCT116 cells. Bacteria were co-cultured with $1x10^5$, $2x10^5$, or $3x10^5$ B16F10 or HCT116 cells/well. Data were normalized as the ratio of the signal in the condition of interest to signal in media alone. Error bars correspond to SEM. All *p* value calculations are between *luxCDABE* and the group indicated by the symbol: (*), $p \leq 1x10^{-7}$; (^{x}), $p \leq 0.06$. (d) Semi-quantitative reverse transcriptase PCR with wild-type SB300A1 bacteria verifies that genes identified by the reporter transposon screen in *Salmonella* are activated during co-culture with B16F10 melanoma cells. *rrsH* = ribosomal RNA.

Figure 3-3

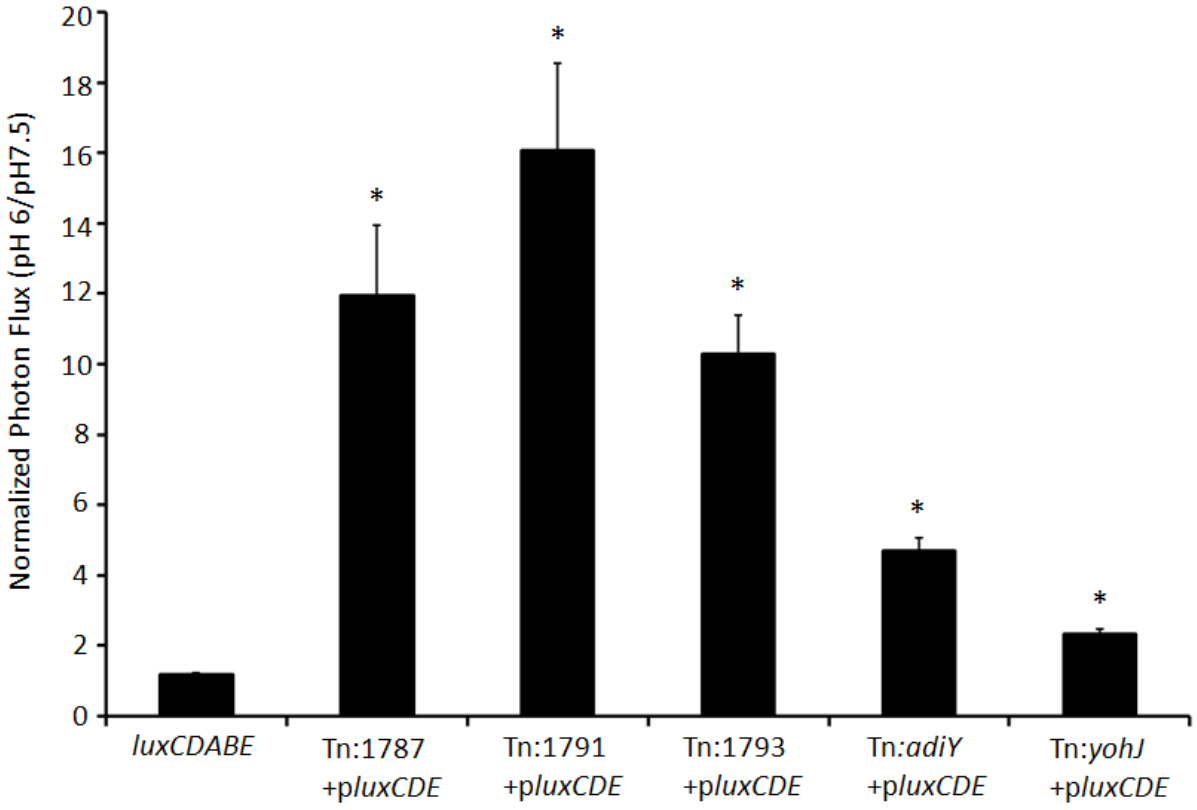

Figure 3-3. Acidic pH stimulates targeted *Salmonella* gene activation. Bacteria were cultured in media of different pH values and reporter activation by *Salmonella* library clones in low pH media (pH 6) were compared to reporter activation in normal pH (7.5). Genes identified in the tumor cell co-culture screen were activated in the context of acidic pH compared to pH 7.5. pMAAC001 and *luxCDABE* constitutively express plasmid-encoded and chromosomally-encoded *luxCDABE*, respectively. Data were normalized as the ratio of the signal in media pH 6.0 to signal in media pH 7.5. Error bars correspond to standard error. The data show one representative experiment with 4 replicates per condition tested. All *p*-value calculations are between *luxCDABE* and the group indicated by the asterisk (*), $p \leq 2\text{x}10^{-14}$.

Figure 3-4

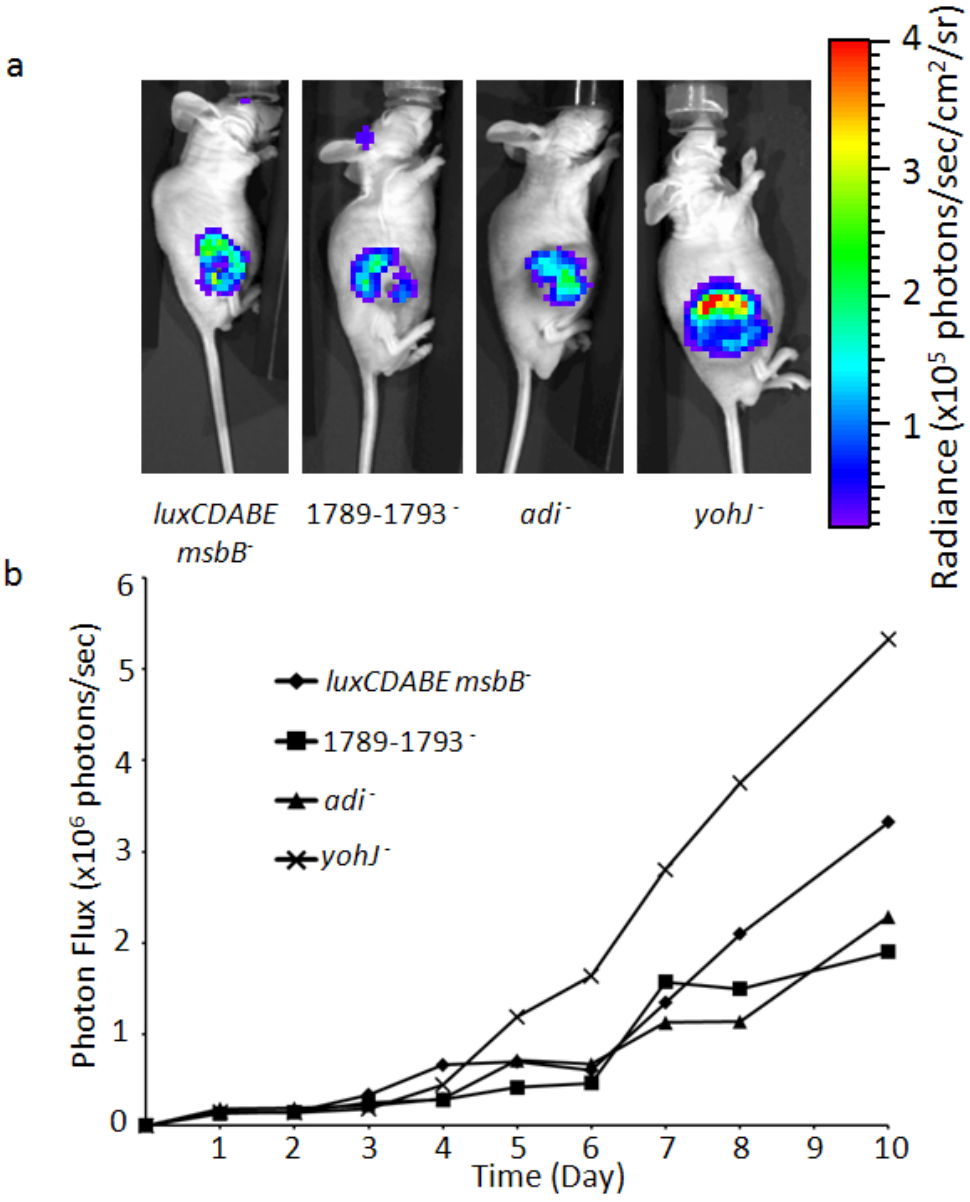

Figure 3-4. Activated genes are not essential for *Salmonella* tumor localization. Mice bearing B16F10 melanoma flank tumor xenografts were injected intravenously with constitutively bioluminescent mutant *Salmonella*. (a) Representative mice on day 10 post *Salmonella* injection. (b) Bioluminescent photon flux of the four mice depicted in (a) as a function of time following injection of bacteria.

Figure 3-5

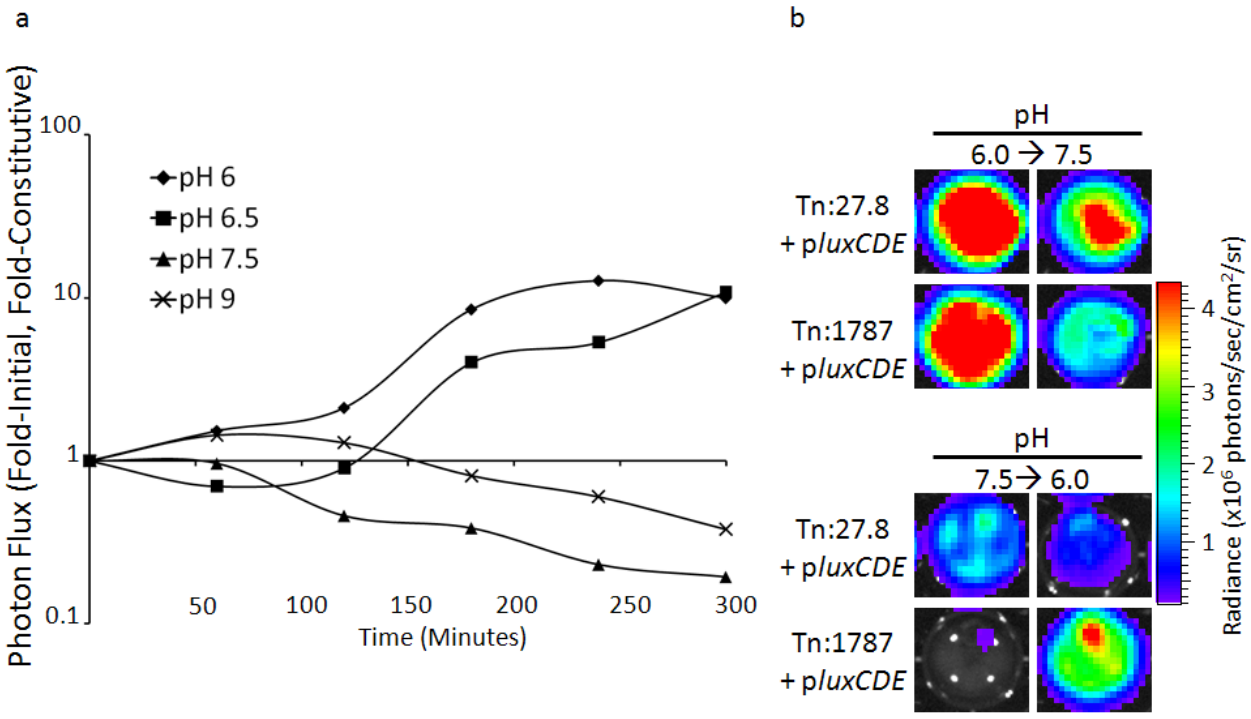

Figure 3-5. The Tn:1787 trapped promoter is specifically and reversibly activated by the pH of the tumor microenvironment. Mice bearing B16F10 melanoma flank tumor xenografts were injected intratumorally with tumor-activated (Tn:1787+p*luxCDE*) or constitutively bioluminescent (Tn:27.8+p*luxCDE*) *Salmonella*. (a) The excised tumors were imaged hourly and data are presented as the normalized signal at each time point. The normalized signal represents the ratio of the mean of the fold-initial signal of two Tn:1787+p*luxCDE*-colonized tumors to the mean of the fold-initial signal of two constitutive Tn:27.8+p*luxCDE*-colonized tumors. The data presented are from a representative experiment; the experiment was performed independently two times, each with two mice per bacterial treatment group. (b) Representative *ex vivo* tumor imaging shows reversibility of the bioluminescent signal in the tumor-activated *Salmonella*.

Images on the left show *Salmonella*-infected tumor explants after 6 hours of incubation at the indicated pH (pH 6.0, top; pH 7.5, bottom). Two hours later (8 hours total), media was removed and replaced with media of the indicated pH (pH 7.5, top; pH 6.0, bottom). Images on the right show *Salmonella*-infected tumor explants 4 hours after the pH of the media was changed.

Figure 3-6

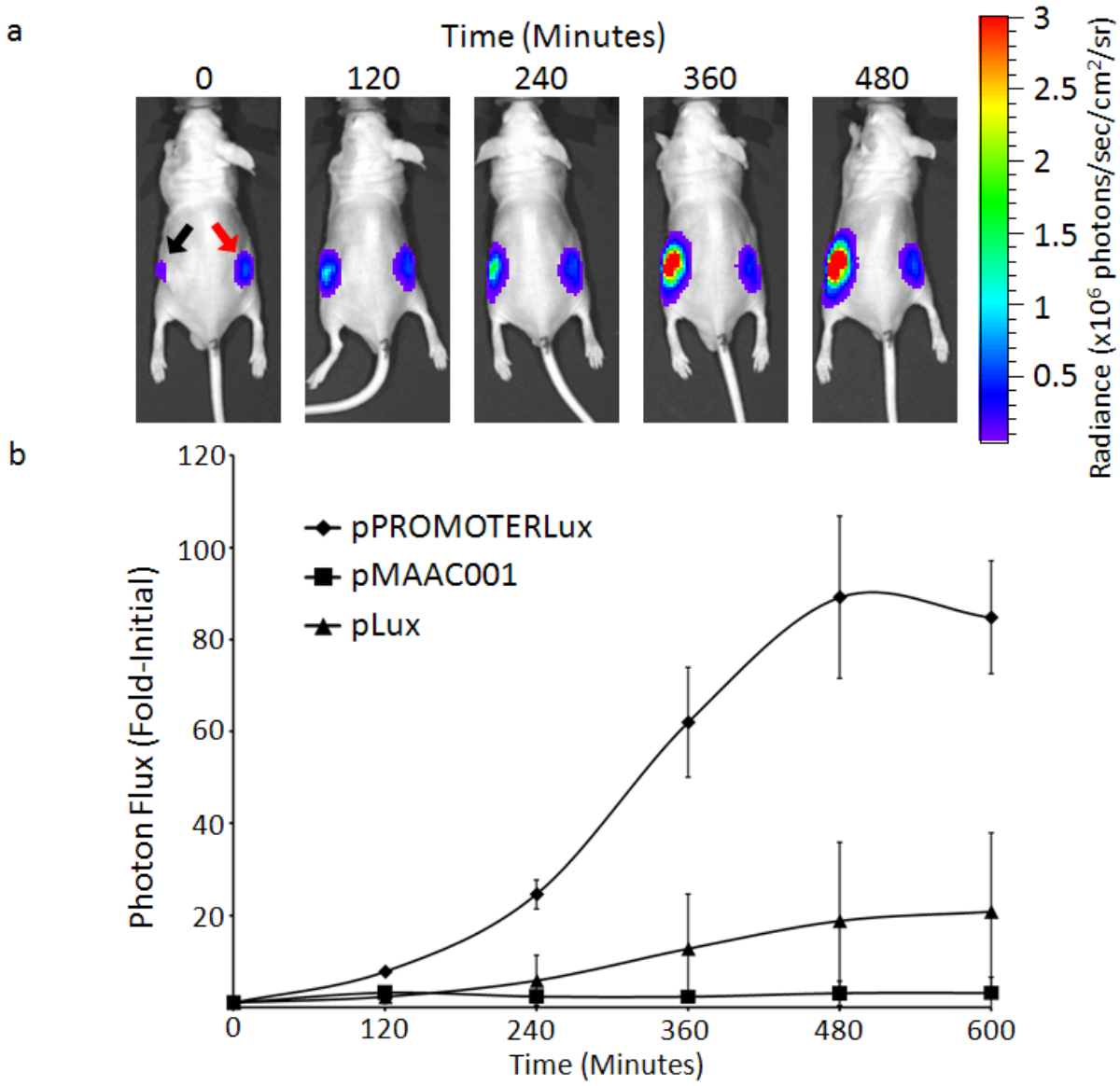

Figure 3-6. The *STM1787* promoter in *Salmonella* is rapidly activated *in vivo* by the tumor microenvironment. (a) A representative mouse with two HCT116 colon carcinoma flank tumor xenografts. The left tumor (black arrow) was injected with *STM1787* p*PROMOTERLux*-expressing *Salmonella*, while the right tumor (red arrow) was injected with constitutive p*MAAC001*-expressing *Salmonella*, and the mouse imaged

at the indicated times post-injection. (b) The mean photon flux for each set of *Salmonella*-injected tumors, normalized to the initial signal in each tumor, plotted as a function of time. Error bars represent SEM; p*PROMOTERLux* (n=6); p*Lux* (n=3); p*MAAC001* (n=3).

3.8 References

1. Yu, Y.A., et al., *Visualization of tumors and metastases in live animals with bacteria and vaccinia virus encoding light-emitting proteins.* Nat Biotechnol, 2004. **22**(3): p. 313-20.

2. Forbes, N.S., et al., *Sparse initial entrapment of systemically injected Salmonella typhimurium leads to heterogeneous accumulation within tumors.* Cancer Res, 2003. **63**(17): p. 5188-93.

3. Low, K.B., et al., *Lipid A mutant Salmonella with suppressed virulence and TNFalpha induction retain tumor-targeting in vivo.* Nat Biotechnol, 1999. **17**(1): p. 37-41.

4. Clairmont, C., et al., *Biodistribution and genetic stability of the novel antitumor agent VNP20009, a genetically modified strain of Salmonella typhimurium.* J Infect Dis, 2000. **181**(6): p. 1996-2002.

5. Kasinskas, R.W. and N.S. Forbes, *Salmonella typhimurium specifically chemotax and proliferate in heterogeneous tumor tissue in vitro.* Biotechnol Bioeng, 2006. **94**(4): p. 710-21.

6. Kasinskas, R.W. and N.S. Forbes, *Salmonella typhimurium lacking ribose chemoreceptors localize in tumor quiescence and induce apoptosis.* Cancer Res, 2007. **67**(7): p. 3201-9.

7. McKinney, J., et al., *Tightly regulated gene expression system in Salmonella enterica serovar Typhimurium.* J Bacteriol, 2002. **184**(21): p. 6056-9.

8. Flentie, K.N., et al., *Stably integrated luxCDABE for assessment of Salmonella invasion kinetics.* Mol Imaging, 2008. **7**(5): p. 222-33.

9. Pfeifer, C.G., et al., *Salmonella typhimurium virulence genes are induced upon bacterial invasion into phagocytic and nonphagocytic cells.* Infect Immun, 1999. **67**(11): p. 5690-8.

10. Gross, S. and D. Piwnica-Worms, *Real-time imaging of ligand-induced IKK activation in intact cells and in living mice.* Nat Methods, 2005. **2**: p. 607-614.

11. Rasband, W., *ImageJ*. 2005, National Institutes of Health: Bethesda, Maryland.

12. Zhang, X.D., et al., *Robust statistical methods for hit selection in RNA interference high-throughput screening experiments.* Pharmacogenomics, 2006. **7**(3): p. 299-309.

13. Levano-Garcia, J., S. Verjovski-Almeida, and A.C. da Silva, *Mapping transposon insertion sites by touchdown PCR and hybrid degenerate primers.* Biotechniques, 2005. **38**(2): p. 225-9.

14. Datsenko, K.A. and B.L. Wanner, *One-step inactivation of chromosomal genes in Escherichia coli K-12 using PCR products.* Proc Natl Acad Sci U S A, 2000. **97**(12): p. 6640-5.

15. Kieboom, J. and T. Abee, *Arginine-dependent acid resistance in Salmonella enterica serovar Typhimurium.* J Bacteriol, 2006. **188**(15): p. 5650-3.

16. *The universal protein resource (UniProt).* Nucleic Acids Res, 2008. **36**(Database issue): p. D190-5.

17. Tannock, I.F. and D. Rotin, *Acid pH in tumors and its potential for therapeutic exploitation.* Cancer Res, 1989. **49**(16): p. 4373-84.

18. Pawelek, J.M., K.B. Low, and D. Bermudes, *Tumor-targeted Salmonella as a novel anticancer vector.* Cancer Res, 1997. **57**(20): p. 4537-44.

19. Dang, L.H., et al., *Combination bacteriolytic therapy for the treatment of experimental tumors.* Proc Natl Acad Sci U S A, 2001. **98**(26): p. 15155-60.

20. Dang, L.H., et al., *Targeting vascular and avascular compartments of tumors with C. novyi-NT and anti-microtubule agents.* Cancer Biol Ther, 2004. **3**(3): p. 326-37.

21. Weibel, S., et al., *Colonization of experimental murine breast tumours by Escherichia coli K-12 significantly alters the tumour microenvironment.* Cell Microbiol, 2008. **10**(6): p. 1235-48.

22. Stritzker, J., et al., *Tumor-specific colonization, tissue distribution, and gene induction by probiotic Escherichia coli Nissle 1917 in live mice.* Int J Med Microbiol, 2007. **297**(3): p. 151-62.

23. Agrawal, N., et al., *Bacteriolytic therapy can generate a potent immune response against experimental tumors.* Proc Natl Acad Sci U S A, 2004. **101**(42): p. 15172-7.

24. Bettegowda, C., et al., *Imaging bacterial infections with radiolabeled 1-(2'-deoxy-2'-fluoro-beta-D-arabinofuranosyl)-5-iodouracil.* Proc Natl Acad Sci U S A, 2005. **102**(4): p. 1145-50.

25. Hajitou, A., et al., *A hybrid vector for ligand-directed tumor targeting and molecular imaging.* Cell, 2006. **125**(2): p. 385-98.

26. Maletzki, C., et al., *Pancreatic cancer regression by intratumoural injection of live Streptococcus pyogenes in a syngeneic mouse model.* Gut, 2008. **57**(4): p. 483-91.

27. Luo, X., et al., *Antitumor effect of VNP20009, an attenuated Salmonella, in murine tumor models.* Oncol Res, 2001. **12**(11-12): p. 501-8.

28. Jiang, S.N., et al., *Inhibition of tumor growth and metastasis by a combination of Escherichia coli-mediated cytolytic therapy and radiotherapy.* Mol Ther. **18**(3): p. 635-42.

29. Ganai, S., R.B. Arenas, and N.S. Forbes, *Tumour-targeted delivery of TRAIL using Salmonella typhimurium enhances breast cancer survival in mice.* Br J Cancer, 2009. **101**(10): p. 1683-91.

30. Loeffler, M., et al., *IL-18-producing Salmonella inhibit tumor growth.* Cancer Gene Ther, 2008. **15**(12): p. 787-94.

31. Zhao, M., et al., *Targeted therapy with a Salmonella typhimurium leucine-arginine auxotroph cures orthotopic human breast tumors in nude mice.* Cancer Res, 2006. **66**(15): p. 7647-52.

32. Leschner, S. and S. Weiss, *Salmonella-allies in the fight against cancer.* J Mol Med (Berl). **88**(8): p. 763-73.

33. Nemunaitis, J., et al., *Pilot trial of genetically modified, attenuated Salmonella expressing the E. coli cytosine deaminase gene in refractory cancer patients.* Cancer Gene Ther, 2003. **10**(10): p. 737-44.

34. Toso, J.F., et al., *Phase I study of the intravenous administration of attenuated Salmonella typhimurium to patients with metastatic melanoma.* J Clin Oncol, 2002. **20**(1): p. 142-52.

35. Heimann, D.M. and S.A. Rosenberg, *Continuous intravenous administration of live genetically modified salmonella typhimurium in patients with metastatic melanoma.* J Immunother, 2003. **26**(2): p. 179-80.

36. Forbes, N.S., *Engineering the perfect (bacterial) cancer therapy.* Nat Rev Cancer, 2010. **10**(11): p. 785-94.

37. Leschner, S., et al., *Tumor invasion of Salmonella enterica serovar Typhimurium is accompanied by strong hemorrhage promoted by TNF-alpha.* PLoS One, 2009. **4**(8): p. e6692.

38. Arrach, N., et al., *Salmonella promoters preferentially activated inside tumors.* Cancer Res, 2008. **68**(12): p. 4827-32.

39. Hayes, E.T., et al., *Oxygen limitation modulates pH regulation of catabolism and hydrogenases, multidrug transporters, and envelope composition in Escherichia coli K-12.* BMC Microbiol, 2006. **6**: p. 89.

40. Ibarra, J.A. and O. Steele-Mortimer, *Salmonella--the ultimate insider. Salmonella virulence factors that modulate intracellular survival.* Cell Microbiol, 2009. **11**(11): p. 1579-86.

41. Foster, J.W. and M.P. Spector, *How Salmonella survive against the odds.* Annu Rev Microbiol, 1995. **49**: p. 145-74.

42. Gerweck, L.E. and K. Seetharaman, *Cellular pH gradient in tumor versus normal tissue: potential exploitation for the treatment of cancer.* Cancer Res, 1996. **56**(6): p. 1194-8.

43. Fischer, B., et al., *Acidic pH inhibits non-MHC-restricted killer cell functions.* Clin Immunol, 2000. **96**(3): p. 252-63.

44. Muller, B., B. Fischer, and W. Kreutz, *An acidic microenvironment impairs the generation of non-major histocompatibility complex-restricted killer cells.* Immunology, 2000. **99**(3): p. 375-84.

CHAPTER 4

A High-Throughput siRNA Screen Identifies Nucleoside Diphosphate Kinase (NME3) as a Novel Host Regulator of NF-κB Signaling in Response to *Salmonella*-Induced Activation of TLR-5

4.1 Abstract

Salmonella is a well-known activator of the innate immune system by engaging NF-κB signaling. In this work, we now demonstrate *Salmonella*-induced IKK activation and the resulting NF-κB transcriptional activation in real time. We show that in HCT116 colon carcinoma cells, flagellin is the predominant ligand accounting for *Salmonella* induction of NF-κB. Then, an siRNA library targeting 691 known and predicted human kinases was screened in HCT116 colon carcinoma reporter cells expressing a $\kappa B_5 \rightarrow I\kappa B\alpha$-*FLuc* reporter to identify novel host kinase modulators of flagellin-induced NF-κB activation. This screen uncovered nucleoside diphosphate kinase **(**NME3) as a previously unrecognized, positive regulator of *Salmonella*-induced NF-κB signaling.

4.2 Introduction

The bacterial pathogen *Salmonella* Typhimurium commonly causes gastrointestinal illness in human hosts and is transmitted by ingestion of contaminated food and water. In the host, the bacteria invade intestinal epithelial cells, causing tissue destruction, inflammation and diarrhea. In some instances, a severe *Salmonella* infection can damage the intestinal barrier so severely that the bacteria penetrate this barrier, invade infiltrating phagocytes and progress to a systemic infection. In order to protect itself

against bacterial infections, the host employs a robust set of first line defenses collectively referred to as innate immunity. One important component of host innate immunity consists of a series of pattern recognition receptors activated by common foreign antigens, or PAMPs (pathogen associated molecular patterns). These receptors include Toll-like receptors (TLRs) and NOD receptors, both of which are involved in activation of inflammatory signaling.

Over the years, multiple TLRs have been identified, several of which are activated by *Salmonella*. *Salmonella* is capable of activating TLR2, TLR4 and TLR5 through its peptidoglycan (PG), lipopolysaccharide (LPS) and flagellin [1]. Once bound, these receptors induce downstream signaling in host cells resulting in activation of pro-inflammatory pathways, one of which is NF-κB [1]. To initiate NF-κB signaling, TLRs induce a downstream kinase cascade that results in activation of IKK, which phosphorylates IκBα, the negative regulator of NF-κB[1]. Ubiquitination and degradation of IκBα frees NF-κB to translocate into the nucleus and activate downstream transcriptional programming to promote inflammation and immune responses [1].

Salmonella engagement of TLRs and activation of NF-κB serves primarily to alert the host of invading pathogens. However, *Salmonella* recognition by TLRs may result in at least two potentially deleterious downstream effects in host cells. First, it has been shown that *Salmonella* capitalizes on host TLR activation to induce bacterial virulence factor expression, indicating that the bacteria have evolved mechanisms to increase their virulence in response to detection by the host cell [2]. Second, NF-κB activation leads to pro-proliferative signaling in host cells, and over-activation of these pro-proliferative signals has been linked to cancer [3]. Indeed, chronic bacterial infections, including

those by *Salmonella* species, have been linked to carcinogenesis [3, 4]. Therefore, a better understanding of the signaling pathways specifically induced during *Salmonella* colonization is necessary to fully understand how to best combat infection.

In this work, we have identified flagellin as the predominant immunostimulatory PAMP of *Salmonella*-induced activation of NF-κB signaling in HCT116 colon carcinoma cells. We then utilized a high-throughput approach to search for previously unidentified host modulators of *Salmonella*-induced NF-κB signaling. We identified NME3, a eukaryotic kinase, as an important regulator of NF-κB signaling activity.

4.3 Methods

Cell lines and culture conditions: HCT116 cells were a gift of Bert Vogelstein and cultured according to ATCC directions. All stably transfected HCT116 cells were cultured in 0.5 μg/ml puromycin.

Salmonella *strains*: *Salmonella* Typhimurium strain SL1344 was used for all experiments, except where noted. All mutants (*fliC-*, *fljB-* and *fliC-fljB-*) were constructed using a lambda red recombinase strategy [5]. First, primers were designed to amplify the kanamycin- or chloramphenicol-resistance cassette in pKD4 or pKD3 with tails flanking the targeted locus of the *Salmonella* genome to be deleted. PCR fragments were then electroporated into SL1344 bacteria expressing plasmid-encoded red recombinase. Following electroporation, growth on kanamycin or chloramphenicol plates at 37°C selected for strains that had lost the temperature-sensitive recombinase plasmid and inserted the chloramphenicol-resistance cassette into the targeted genomic loci. The double mutant strain was created in a step wise manner, by individually deleting each gene. Deletion of the genes was confirmed by PCR.

Creation of a κB5→IκBαFLuc*-expressing HCT116 stable cell line*: HCT116 cells at 95% confluency were co-transfected with 10 µg of *pκB5→IκBαFLuc* and 3 µg of *pIRES-puro* plasmid DNA using Fugene 6 in 10 cm dishes. After 24 hours, the media was replaced with fresh cell media. Twenty-four hours later, the cells were split at multiple dilutions into media containing 0.5µg/ml puromycin to select for stable transformants. After two weeks, isolated cell colonies were imaged to check for reporter gene expression and bioluminescent colonies were harvested and expanded. The cells were continuously cultured in the presence of 0.5µg/ml puromycin to maintain expression of the reporter plasmid.

Transient transfections of HCT116 cells: HCT116 cells were transiently transfected where noted. Cells were plated in 24-well (50,000-60,000 cells/well) or 96-well (10,000 cells/well) plates and transfected with Fugene 6 (Roche) and 200 ng of plasmid DNA(24-well) or 50 ng of plasmid DNA (96-well) per well. In the case of NME3 over-expression experiments, 100 ng of reporter plasmid and 200 ng of over-expression (*pCMV6:NME3*) or vector control (*pCMV6*) plasmid were used in each well of a 24-well plate. Cells were allowed to recover for 48 hours prior to imaging.

Dynamic imaging of NF-κB signaling: Thirty minutes prior to imaging, cell media were aspirated and replaced with colorless DMEM supplemented with 10% heat-inactivated FBS and 150 µg/ ml luciferin. To image, cells were stimulated as indicated and imaging was performed in an IVIS 100 imaging system (except where noted), with images being acquired every 5 minutes for 6 hours, unless otherwise indicated. The cells were maintained in the imaging chamber by a heated stage (37ºC) and 5% CO_2 air flow. Stimuli included: SL1344 *Salmonella* Typhimurium , or indicated mutants, confluent

culture (final dilution 1:100 in well) or matched for OD_{600}, heat-killed by boiling 10 minutes and diluted 1:10 into each well (where noted), lipopolysaccharide (1µg/ml) (Sigma), peptidoglycan (Sigma), ie-DAP(10µg/ml) (InvivoGen), MDP (10µg/ml) (InvivoGen), TNFα (20 ng/ml) (R & D systems), or flagellin (100 ng/ml) (InvivoGen). Acquisition parameters are noted in the figure legends.

High-throughput screen: siRNA screening was performed in white, clear-bottomed, 96-well culture plates using a Beckman-Coulter Core robotics system, including an FX liquid handler, controlled by the Sagian graphical method development tool (SAMI scheduling software). HCT116 cells stably expressing *pκB5→IκBαFLuc* were seeded at 15,000 cells per well in a 96 well plate and cells were allowed to attach for 24 hours. Forward transfection was performed with a 96 multichannel head on the FX liquid handler, adding 0.5 µl/well of media-complexed R1 Transpass (NEB) to the aliquotted siRNA library (Kinase siRNA set v2; Qiagen Inc.) in a 96-well reaction plate and allowed to incubate for 15 minutes. Experimental siRNA oligos were arrayed in columns 2-11 of each plate and individual controls comprising vehicle-treated wells, a non-targeting control sequence (Qiagen Allstar Negative control), TLR5-targetting siRNA sequences (IDT), and a firefly luciferase-targeting PGL3 siRNA (Dharmacon Research Inc.) were placed manually in columns 1 and 12. After incubation of siRNA complexes, 100 µl was added to each well of a plate with cells (x3 plates) using the FX liquid handler, yielding a final concentration of ~50 nM siRNA/well. Plates were maintained at 37ºC and 5% CO_2 for 48 hrs. At this time, media were aspirated and replaced with 180 µl imaging media (colorless DMEM supplemented with 10% heat inactivated FBS and 150 µg/ml d-luciferin) and the cells were allowed to equilibrate for 45 minutes. After

equilibrating, 20 µl of stimulus (1:100 dilutions of heat-killed *Salmonella* cultures) or control (LB broth) were added to each well. Bioluminescent readings were obtained on an EnVision plate reader (PerkinElmer) immediately following the stimulus, at 45 minutes post-stimulation and at 245 minutes post-stimulation. After the final luminescent reading, 20 µl of rezasurin dye was added to all wells, allowed to incubate for 2 hours at 37^0C and monitored on a FLUOstar OPTIMA fluorescence reader for cell viability (BMG Labtech; excitation, 544 nm, emission, 590 nm).

Data analysis: Initially, the signal in each well was normalized to a plate-matched control well containing a non-targeting siRNA sequence at each time point to facilitate experiment-wide analysis. Then, the differences in the $\log_2$ values of the normalized data between 0 minutes and 45 or 245 minutes were averaged across triplicate siRNA experimental replicates. Then, screening hits were selected by quartile analysis of the normalized kinase library data. To perform the quartile analysis, median (Q2), first (Q1) and third (Q3) quartile values were calculated. From these values, the upper and lower boundaries for hit selection were calculated as Q3 + 2c(Q3 –Q2) and Q1 – 2c(Q2-Q1), respectively, for c = 1.2245 corresponding to a high-stringency targeted error rate (α = 0.02) and for c = 0.7193 corresponding to a low-stringency targeted error rate ($\alpha = 0.1$) [6].

siRNA knockdown: siRNA knockdown of NME3 was performed utilizing 4 separate targeting sequences. Stably-transfected HCT116 cells were plated in 96-well plates at 15,000 cells/well and allowed to incubate overnight. Twenty-four hours later, cells were transfected with R1 Transpass (NEB) and 25 nM siRNA (Qiagen) as per R1 Transpass instructions. Cells were incubated for 72 hours prior to imaging.

shRNA lentiviral knockdown cell line construction: Lentivirus, expressing constructs (pLKO.1 puro), were obtained pre-synthesized from the Genome Sequencing Center at Washington University. The targeting sequences for the 3 shNME3 constructs are as follows:

#7 - 5' GAGGTTGGCAAGAACCTGATT

#8 - 5' GCCTTGTCAAGTATATGGCCT

#9 - 5'CGAGAGGAAGGGCTTCAAGTT

Additionally, a scrambled shRNA construct was utilized as a negative control. To generate lentivirus containing hairpins, 500,000 293T cells were pre-plated in 60 mm dishes and co-transfected the following day with 1 μg of hairpin construct, 900 ng packaging plasmid p*CMV-ΔR8.2*, and 100 ng of envelope plasmid p*VSVG* using Fugene 6. Two days after transfection, virus containing supernatant was collected from 293T cells and filtered through a 0.45μm filter, mixed with 5ug/ml protamine sulfate, and added to HepG2 cells at 50% confluency in a $10cm^2$ dish. Media was replenished 12 hrs post-transduction, and cells were subsequently maintained in media supplemented with 500 ng/ml puromycin hydrochloride to retain expression of the hairpins. Following transduction, shNME3 or shSCRAMBLED cells were plated in parallel for mRNA knockdown confirmation and transient transfection and subsequent imaging measurements with the $\kappa B_5 \rightarrow$IκBα-FLuc reporter or the $\kappa B_5 \rightarrow$FLuc reporter as previously described.

Semi-quantitative RTPCR: HCT116 cells transduced with shNME3 or shSCRAMBLED hairpins were lysed and total RNA was purified using the Qiagen RNeasy kit (Qiagen Inc, Valencia, CA). Samples were then treated with DNase I at room temperature for 15

minutes, after which EDTA was added and samples were incubated for 10 minutes at 65°C to inactivate the DNase. Samples were then ethanol precipitated and resuspended in water. For reverse transcriptase PCR, 1 μg of total RNA was used as a template and reverse transcribed using Superscript II Reverse Transcriptase and 300 ng random primers as per the manufacturer's instructions (Invitrogen, Carlsbad, CA). To perform semi-quantitative PCR, samples were amplified using 2 μL or RT reaction and primers specific to NME3 or GAPDH. PCR cycling conditions were: 95°C for 5 minutes, 35 cycles (or 25 cycles for GAPDH reactions) of denaturation at 95°C for 45 seconds, annealing at 55°C for 45 seconds and extension at 72°C for 1 minute. PCR products were fractionated on a 1% agarose gel.

4.4 Results

To study IKK-induced activation of NF- κB by *Salmonella* in real time in living cells, we utilized a bioluminescent $\kappa B_5 \rightarrow$IκBα-FLuc fusion reporter. This reporter consists of the negative inhibitor of NF-κB, IκBα, directly fused to firefly luciferase. When the upstream kinase, IKK, is activated, it phosphorylates IκBα proteins in the host cell, targeting them for ubiquitination and proteasomal degradation. In this case the reporter fusion protein serves as a direct readout of IKK activity [7]. As activated IKK phosphorylates IκBα, the reporter fusion is phosphorylated, ubiquitinated, and targeted for degradation as well. This results in a reduction in bioluminescent reporter activity that can be followed in real time [7]. Liberation of NF-κB from its inhibitor frees it to translocate to the nucleus and activate transcription at NF-κB response elements. The reporter fusion is linked on its 5' end to five of these response elements in tandem,

allowing it to report on NF-κB nuclear transactivation ability as well by measuring an increase in bioluminescent signal [7]. Stimulation of HCT116 cells with heat-killed *Salmonella* robustly activates degradation and resynthesis of the reporter fusion, which can be imaged periodically to visualize the changes in reporter photon output following stimulation (**Figure 4-1a**). Heat-killed bacteria were preferred as a stimulus over live bacteria. When performing the assay with live *Salmonella*, replication by the bacteria quickly changed the media conditions, ultimately leading to complete attenuation of the luciferase signal (data not shown). The data obtained from imaging HCT116 cells stimulated with heat-killed *Salmonella* can also be represented graphically to demonstrate the dynamics of the reporter in the system (**Figure 4-1b**). After stimulation with bacteria, the reporter signal initially decreased to 60% of its steady state level prior to activation. Following this decrease, which corresponds to IκBα degradation, the *Salmonella*-induced reporter activity rebounds to greater than three times the original bioluminescence levels, corresponding to transcriptional activation of the IκBα-FLuc fusion protein. In comparison, TNFα, a common stimulus of NF-κB signaling, elicits more degradation and less transcriptional activation of the reporter. Additionally, the dynamics of the HCT116 cellular response to TNFα differ from those observed when HCT116 cells respond to *Salmonella*. The peaks of reporter degradation and resynthesis both occur earlier following stimulation with TNFα, indicating differences in the signal transduction following the different stimuli.

To understand how the HCT116 colon cancer cells are recognizing *Salmonella* and activating pro-inflammatory signaling, we set out to isolate the specific NF-κB -activating moiety of the bacteria. To accomplish this, we tested the NF-κB stimulatory

activity of individual known immunostimulatory components of bacteria. When tested in HCT116 cells stably expressing the $\kappa B_5 \rightarrow$IκBα-FLuc reporter, purified peptidoglycan, NOD ligands (ieDAP and MDP), and bacterial LPS were all incapable of inducing significant bioluminescent reporter activity changes (**Figure 4-2a-c**). Because bacterial flagellin is noted for its immunostimulatory activity, we chose to investigate its contribution to NF-κB activation by *Salmonella*. To better determine the contribution of the two *Salmonella* flagellin proteins to NF-κB stimulation, we constructed *Salmonella* strains mutated singly or in both flagellin genes *fliC* and *fljB*. Both single mutants were still able to activate NF-κB signaling, albeit to a lesser extent than that of wild type bacteria, but the *Salmonella* double mutant was incapable of activating NF-κB signaling in HCT116 cells. This indicated that flagellin was the predominant ligand inducing NF-κB signaling in HCT116 colon carcinoma cells (**Figure 4-3**). Further, purified *Salmonella* flagellin also activates NF-κB signaling in this system although to a lesser extent than heat-killed *Salmonella* (data not shown). This may reflect a difference in the amount of flagellin produced by bacteria compared to the concentration of purified flagellin used, a difference in solubility between bacterially-produced and purified recombinant flagellin, or a difference in the relative amounts of monomeric versus polymerized flagellin in the two preparations. Alternatively, perhaps heat-killed bacteria provide an additional co-activating ligand, in which case flagellin is necessary, but not sufficient to fully induce NF-κB signaling.

With the knowledge that HCT116 cells are robustly activating proinflammatory signaling in response to *Salmonella* flagellin, we set out to identify novel host kinases involved in immunodetection of *Salmonella*. We utilized an siRNA screen to all known and predicted

human kinases to test the involvement of each in *Salmonella*-induced activation of NF-κB. The screen consisted of utilizing HCT116 cells colon carcinoma cells stably expressing the *$\kappa B_5 \rightarrow$IκBα-FLuc* construct. Cells were plated and transfected with siRNA targeting 691 host kinases arrayed in the 10 center columns of 96-well plates with each well containing two sequences targeting a single host kinase. Forty-eight hours following siRNA transfection, cells were stimulated with heat-killed *Salmonella* and the reporter signal was measured immediately, at 45 minutes and at 245 minutes following the onset of *Salmonella* exposure (**Figure 4-4**). Normalized bioluminescence signal data at 45 and 245 minutes were plotted individually (**Figure 4-5**), or as x-y coordinates being the normalized signals at 45 and 245 minutes respectively (**Figure 4-6**).

High-throughput screening hits were determined using a quartile-based analysis. **Figure 4-5** displays the quartile-identified values for low- and high-stringency hit selection. Wells in which kinases that positively affect NF-κB signaling targeted by siRNA will demonstrate reduced responsiveness to *Salmonella*. In contrast, wells containing siRNA targeting a negative regulator of NF-κB signaling will show enhanced reporter response. Statistically significant hits and their predicted regulatory activity on NF-κB signaling are listed in **Table 4-1**. **Figure 4-6** demonstrates the four possible effects kinases in the screen may have had on reporter activity. Kinase knockdowns reducing the photon flux signal at 45 minutes, i.e., increasing IκBα degradation, indicate a negative regulator of NF-κB signaling has been targeted. Meanwhile, kinase knockdowns with relatively greater photon flux signals at 45 minutes indicate siRNA targeted a positive regulator of NF-κB signaling. Conversely, at the 245 minute time point smaller values represent a low signal during the resynthesis phase, which indicates a lack of full NF-κB

transactivation and therefore siRNA knockdown of a positive regulator of NF-κB induced transcription. Greater photon flux values correspond to over-activation of NF-κB transcriptional activity, and therefore siRNA treatment targeted a negative transcriptional regulator. Therefore, in **Figure 4-6**, an siRNA that acts on a positive regulator of both the degradation and resynthesis phases will fall in the lower right quadrant, while a negative regulator of both phases will be found in the upper left portion of the scatter plot. The positive control well containing siRNA targeting TLR5, for example, should prevent IκBα degradation at 45 minutes, which in turn, will inhibit reporter transcriptional activation at 245 minutes. This is shown by the blue triangle corresponding to TLR5 siRNA-treated wells falls in the lower right quadrant of the scatter plot. IRAK1 and AKT, both known activators of the NF-κB signaling pathway, were identified as hits in the screen, further verifying the validity of the results. The screen also identified MAP2K2 and MAP2K3, among others, as kinases involved in regulating the pathway.

In the screen, knockdown of NME3 caused reduced transcriptional activation by NF-κB at 245 minutes, indicating NME3 was behaving as a positive regulator of NF-κB (**Figure 4-6**). Knockdown of NME3 by four individual siRNA sequences recapitulated the data in the primary screen, although sequence 3 shows less inhibition of NF-κB signaling, likely due to incomplete knockdown of NME3 (**Figure 4-7**). Conversely, over-expression of plasmid-encoded NME3 in HCT116 cells induced higher levels of transcriptional activation by NF-κB, demonstrating that NME3 behaves as a positive regulator of NF-κB signaling in conditions of over-expression as well as under-expression (**Figure 4-8**).

To better measure the contribution of NME3 in *Salmonella*-induced activation of NF-κB, we constructed stable knockdowns of NME3 in HCT116 cells using shRNA lentiviral constructs. Knockdown of NME3 by shRNA in wildtype HCT116 cells did indeed interfere with NF-κB signaling pathways (**Figure 4-9a**). Compared to cells expressing a scrambled shRNA sequence, cells expressing shRNA targeted to NME3 show slightly less reporter degradation and much less resynthesis of the reporter during the transcriptional activation phase. The responsiveness of a purely transcriptional reporter fusion was also tested in these cell lines. As seen in NME3 knockdown cells expressing the κB5→IκBαFLuc reporter, cells expressing a κB5→FLuc construct show considerably less NF-κB-driven transcriptional activation following *Salmonella* stimulation (**Figure 4-9b**). Finally, semi-quantitative PCR confirms that NME3 mRNA in targeted shRNA-expressing cells is indeed reduced to much lower levels compared to cells containing a non-targeting shRNA construct (**Figure 4-9c**).

4.5 Discussion

The NF-κB pathway specifically relies on kinases to effectively transmit signals from the extracellular space into activation of transcription in the nucleus. Kinases, which phosphorylate other proteins, often have an activating role in a signal transduction pathway, and this holds true for the NF-κB signaling pathway as well. For instance, the IκB kinase IKK, is rapidly phosphorylated in response to innate immune stimuli and downstream signaling requires such IKK activation. The mechanism of IKK phosphorylation is not fully understood, but multiple kinases have been proposed, including RIP, TAK1, MAP3K14 and MAP3K1 as well as IKK itself through autophosphorylation [8]. Perhaps each of these kinases has a distinct role in IKK

activation. As there are multiple upstream stimuli capable of activating IKK, i.e., TNFα, LPS, flagellin, multiple kinases likely exist to transmit these signals. NF-κB can also be directly phosphorylated [9]. Cyclic AMP-dependent protein kinase (PKA) phosphorylates the p65 subunit of NF-κB on a specific serine residue, which activates transcriptional activity of NF-κB by enhancing DNA binding and aiding in transcriptional co-activator recruitment [9].

Although not all kinases previously implicated in NF-κB signaling appeared to modulate the NF-κB signaling pathway in this high-throughput screen, multiple kinases that have been linked to the pathway did affect reporter activity in the screen. Notably, IRAK1, a kinase with a central involvement to TLR signal transduction, is revealed in the screen as a positive regulator at 45 minutes and this correlates with its known role in IKK activation [10]. At 245 minutes, AKT is identified by the screen as a positive regulator of NF-κB, and indeed, Akt has been shown to play a role in full NF-κB activation and to promote nuclear NF-κB transactivation [11, 12]. Still, numerous kinases with well-accepted important functions in the NF-κB pathway did not appear as hits in the high-throughput screen. In the cases of these kinases, such as IKKβ, there are several possible reasons for lack of detection. First, the specific kinase may be expressed in such high levels, that siRNA knockdown is insufficient to reduce the protein levels enough to affect signaling. Alternatively, if loss of a specific kinase is toxic the host cell may have compensating pathways to cope with loss of the kinase, thus preventing any phenotypic change. Third, not all physiologically important kinases necessarily appear as high stringency hits in published screens, revealing the complexity of systems and their regulation.

Interestingly, one hit uncovered by the high-throughput siRNA screen was the kinase PTK6. PTK6 is a tyrosine kinase linked to over-expression in multiple tumor types[13, 14]. Recent research has demonstrated that plasma membrane-localized PTK6 enhances cellular proliferation, survival and migration – all downstream effects of NF-κB transcriptional activation[13]. Additionally, research has linked PTK6 to AKT activation through ERBB3, all kinases identified in the screen as positive regulators of NF-κB signaling. In this work, EGF signaling to AKT was enhanced by PTK6 overexpression and mediated by ERBB3[15]. TLRs also have been shown to activate EGFR[16]. Perhaps, in this case, TLR may be activating EGFR, which in turn transmits the proinflammatory signals downstream through PTK6, ERBB3 and AKT. This may indicate a novel mechanism by which TLR5 may activate NF-κB signaling.

Although siRNA-mediated knockdown of both MAP2K2 and MAP2K3 gave reproducible modulation of NF-κB, targeting known downstream MAP kinases via chemical inhibitor showed no effect in my system (data not shown). This could be explained by the identified kinases acting on other downstream proteins, as opposed to their typical MAP kinase targets. Additionally, recent work identified MAP kinases as important modulators of NF-κB-induced cytokine production in intestinal epithelial cells with constitutively active NF-κB [17]. Because intestinal cancers often display high levels of active NF-κB, MAPK activation in these cells may be required for full inflammatory-mediated NF-κB transcriptional activation [18]. Perhaps this effect is the underlying reason for the seemingly important contribution of MAP2K2 and MAP2K3 in HCT116 colon carcinoma cells seen here.

Targeted siRNA sequences to the nucleotide diphosphate kinase NME3 had a drastic effect on NF-κB activation. NME3 is one of eight human nucleotide diphosphate kinase genes [19]. These genes are capable of utilizing ATP to form non-ATP NTPs through their catalytic kinase domain, but have also been attributed with a large variety of potential functions from apoptosis regulation to cell migration to transcriptional activation [20]. Two homologues of NME3, NME1 and NME2, have been studied in much more detail than NME3 [20]. NME2 has demonstrated transcriptional activation of cMyc, a noted oncogene [21]. NME3 shows about 65% homology with NME2, and has an additional 17 amino acid N-terminal tail [20, 22]. NME3 has also been shown to activate integrin expression and adhesion characteristics– a known downstream target of NF-κB [23]. Perhaps, like NME2, NME3 acts as a transcription factor, and potentiates the action of NF-κB. Follow-up analysis on NME3 would likely include investigating the role of NME3 in co-activating NF-κB-dependent transcription downstream of other stimuli, such as TNFα or IL-1β. Also, DNA-binding studies may help clarify whether NME3 binds DNA to help co-activate transcription, similar to its homolog, NME2.

4.6 Tables

Table 4-1 Kinases Modulating the NF-κB Pathway

Gene name	Gene function	NF-κB regulatory activity, 45 min α=0.1	NF-κB regulatory activity, 45 min α=0.02	NF-κB regulatory activity, 245 min α=0.1	NF-κB regulatory activity, 245 min α=0.02
ACVR1	activin A receptor, type I	NS	NS	NEGATIVE	NS
ACVR1B	activin A receptor, type IB	NS	NS	NEGATIVE	NS
ADRBK2	adrenergic, beta, receptor kinase 2	NEGATIVE	NS	NS	NS
AK5	adenylate kinase 5	NEGATIVE	NS	NS	NS
AKAP3	A kinase (PRKA) anchor protein 3	NEGATIVE	NS	NS	NS
AKAP9	A kinase (PRKA) anchor protein (yotiao) 9	NS	NS	NEGATIVE	NS
AKT1	v-akt murine thymoma viral oncogene homolog 1	NS	NS	POSITIVE	POSITIVE
ALPK2	alpha-kinase 2	POSITIVE	POSITIVE	NS	NS
ALS2CR7	amyotrophic lateral sclerosis 2 (juvenile) chromosome region, candidate 7	POSITIVE	NS	NS	NS
APEG1	aortic preferentially expressed protein 1	NEGATIVE	NS	NS	NS
ARK5	AMP-activated protein kinase family member 5	NEGATIVE	NS	NS	NS
BLK	B lymphoid tyrosine kinase	POSITIVE	POSITIVE	NS	NS
BMX	BMX non-receptor tyrosine kinase	NS	NS	NEGATIVE	NEGATIVE
BTK	Bruton agammaglobulinemia tyrosine kinase	NS	NS	NEGATIVE	NEGATIVE
CALM3	calmodulin 3 (phosphorylase kinase, delta)	POSITIVE	NS	NS	NS
CAMK2B	calcium/calmodulin-dependent protein kinase (CaM kinase) II beta	NS	NS	NEGATIVE	NS
CAMK2G	calcium/calmodulin-dependent protein kinase (CaM kinase) II gamma	NEGATIVE	NS	NS	NS
CAMK4	calcium/calmodulin-dependent protein kinase IV	POSITIVE	POSITIVE	NS	NS

CCRK	cell cycle related kinase	POSITIVE	NS	POSITIVE	POSITIVE
CaMKIINalpha	calcium/calmodulin-dependent protein kinase II	POSITIVE	NS	POSITIVE	NS
CDK10	cyclin-dependent kinase (CDC2-like) 10	POSITIVE	POSITIVE	NS	NS
CDK3	cyclin-dependent kinase 3	NEGATIVE	NS	NS	NS
CDK4	cyclin-dependent kinase 4	NS	NS	NEGATIVE	NS
CDK5R2	cyclin-dependent kinase 5, regulatory subunit 2 (p39)	NEGATIVE	NEGATIVE	NS	NS
CDK6	cyclin-dependent kinase 6	NS	NS	NEGATIVE	NEGATIVE
CDKN1B	cyclin-dependent kinase inhibitor 1B (p27, Kip1)	NS	NS	POSITIVE	NS
CDKN2A	cyclin-dependent kinase inhibitor 2A (melanoma, p16, inhibits CDK4)	POSITIVE	NS	NS	NS
CKB	creatine kinase, brain	NS	NS	NEGATIVE	NS
CKMT1	creatine kinase, mitochondrial 1 (ubiquitous)	NS	NS	NEGATIVE	NS
CNKSR1	connector enhancer of kinase suppressor of Ras 1	NEGATIVE	NS	NS	NS
CSK	c-src tyrosine kinase	POSITIVE	NS	NS	NS
CSNK1A1	casein kinase 1, alpha 1	POSITIVE	NS	NS	NS
CSNK1D	casein kinase 1, delta	NS	NS	NEGATIVE	NEGATIVE
CSNK1G2	casein kinase 1, gamma 2	NS	NS	NEGATIVE	NEGATIVE
CSNK2A1	casein kinase 2, alpha 1 polypeptide	NS	NS	NEGATIVE	NS
CSNK2A2	casein kinase 2, alpha prime polypeptide	POSITIVE	NS	NS	NS
DGKA	diacylglycerol kinase, alpha 80kDa	NS	NS	NEGATIVE	NS
DGKB	diacylglycerol kinase, beta 90kDa	POSITIVE	NS	NS	NS
DGKE	diacylglycerol kinase, epsilon 64kDa	NS	NS	NEGATIVE	NS
DGKQ	diacylglycerol kinase, theta 110kDa	NS	NS	POSITIVE	NS
DGUOK	deoxyguanosine kinase	POSITIVE	POSITIVE	NS	NS
DMPK	dystrophia myotonica-protein kinase	NS	NS	NEGATIVE	NEGATIVE
EGFR	epidermal growth factor receptor (erythroblastic	NEGATIVE	NS	NS	NS

	leukemia viral (v-erb-b) oncogene homolog, avian)				
EPHA1	EPH receptor A1	NEGATIVE	NS	POSITIVE	NS
EPHA2	EPH receptor A2	NS	NS	POSITIVE	NS
EPHA3	EPH receptor A3	POSITIVE	POSITIVE	NS	NS
EPHA4	EPH receptor A4	POSITIVE	NS	NS	NS
EPHA5	EPH receptor A5	POSITIVE	NS	NS	NS
EPHA7	EPH receptor A7	NEGATIVE	NS	NS	NS
EPHA8	EPH receptor A8	NS	NS	POSITIVE	NS
EPHB2	EPH receptor B2	POSITIVE	POSITIVE	POSITIVE	POSITIVE
ERBB3	v-erb-b2 erythroblastic leukemia viral oncogene homolog 3 (avian)	POSITIVE	POSITIVE	NS	NS
ERN2	endoplasmic reticulum to nucleus signalling 2	NS	NS	NEGATIVE	NS
FASTK	FAST kinase	NS	NS	POSITIVE	NS
FER	fer (fps/fes related) tyrosine kinase (phosphoprotein NCP94)	POSITIVE	NS	POSITIVE	NS
FES	feline sarcoma oncogene	NS	NS	NEGATIVE	NS
FGFR2	fibroblast growth factor receptor 2 (bacteria-expressed kinase, keratinocyte growth factor receptor, craniofacial dysostosis 1, Crouzon syndrome, Pfeiffer syndrome, Jackson-Weiss syndrome)	POSITIVE	POSITIVE	POSITIVE	NS
FGFR4	fibroblast growth factor receptor 4	NS	NS	NEGATIVE	NS
FLT3LG	fms-related tyrosine kinase 3 ligand	NEGATIVE	NS	NS	NS
GK	glycerol kinase	NS	NS	NEGATIVE	NS
GK2	glycerol kinase 2	NS	NS	POSITIVE	NS
GNE	glucosamine (UDP-N-acetyl)-2-epimerase/N-acetylmannosamine kinase	NEGATIVE	NS	NS	NS

GRK5	G protein-coupled receptor kinase 5	NEGATIVE	NS	NS	NS
GSK3A	glycogen synthase kinase 3 alpha	POSITIVE	POSITIVE	POSITIVE	POSITIVE
GSK3B	glycogen synthase kinase 3 beta	NS	NS	NEGATIVE	NS
HK1	hexokinase 1	NS	NS	NEGATIVE	NS
HUNK	hormonally upregulated Neu-associated kinase	POSITIVE	NS	NS	NS
IHPK3	inositol hexaphosphate kinase 3	POSITIVE	POSITIVE	NS	NS
IKBKAP	inhibitor of kappa light polypeptide gene enhancer in B-cells, kinase complex-associated protein	NS	NS	POSITIVE	POSITIVE
IRAK1	interleukin-1 receptor-associated kinase 1	POSITIVE	POSITIVE	NS	NS
IRAK2	interleukin-1 receptor-associated kinase 2	POSITIVE	NS	NS	NS
ITK	IL2-inducible T-cell kinase	NEGATIVE	NS	NS	NS
ITPKA	inositol 1,4,5-trisphosphate 3-kinase A	POSITIVE	POSITIVE	NS	NS
KDR	kinase insert domain receptor (a type III receptor tyrosine kinase)	POSITIVE	POSITIVE	NS	NS
KHK	ketohexokinase (fructokinase)	NS	NS	NEGATIVE	NS
LCK	lymphocyte-specific protein tyrosine kinase	POSITIVE	POSITIVE	NS	NS
LOC375449	similar to microtubule associated testis specific serine/threonine protein kinase	NS	NS	NEGATIVE	NS
LOC400301	similar to protein kinase CHK2 isoform b; checkpoint-like protein CHK2; serine/threonine-protein kinase CHK2; CHK2 (checkpoint, S.pombe) homolog	NEGATIVE	NS	NS	NS
LRRK2	leucine-rich repeat kinase 2	POSITIVE	NS	NS	NS
LTK	leukocyte tyrosine kinase	POSITIVE	NS	NS	NS
LYN	v-yes-1 Yamaguchi sarcoma viral related oncogene homolog	POSITIVE	NS	NS	NS
MAP2K2	mitogen-activated protein kinase kinase 2	POSITIVE	POSITIVE	POSITIVE	POSITIVE

MAP2K3	mitogen-activated protein kinase kinase 3	POSITIVE	POSITIVE	POSITIVE	POSITIVE
MAP2K6	mitogen-activated protein kinase kinase 6	POSITIVE	NS	NS	NS
MAP2K7	mitogen-activated protein kinase kinase 7	NEGATIVE	NS	NS	NS
MOS	v-mos Moloney murine sarcoma viral oncogene homolog	POSITIVE	NS	NS	NS
MAP3K12	mitogen-activated protein kinase kinase kinase 12	NS	NS	POSITIVE	NS
MAP3K3	mitogen-activated protein kinase kinase kinase 3	POSITIVE	NS	NS	NS
MAPK10	mitogen-activated protein kinase 10	NS	NS	POSITIVE	NS
MAPK14	mitogen-activated protein kinase 14	POSITIVE	NS	NEGATIVE	NEGATIVE
MAPK6	mitogen-activated protein kinase 6	NS	NS	POSITIVE	POSITIVE
MAPK7	mitogen-activated protein kinase 7	NS	NS	POSITIVE	NS
MAPKAP1	mitogen-activated protein kinase associated protein 1	NS	NS	POSITIVE	NS
MAPKBP1	mouse mitogen-activated protein kinase binding protein 1-like	NS	NS	POSITIVE	NS
MET	met proto-oncogene (hepatocyte growth factor receptor)	POSITIVE	NS	NS	NS
MGC40579	hypothetical protein MGC40579	POSITIVE	POSITIVE	NS	NS
NEK1	NIMA (never in mitosis gene a)-related kinase 1	POSITIVE	NS	NS	NS
NEK2	NIMA (never in mitosis gene a)-related kinase 2	NS	NS	NEGATIVE	NS
NEK3	NIMA (never in mitosis gene a)-related kinase 3	NS	NS	POSITIVE	NS
NEK8	NIMA (never in mitosis gene a)- related kinase 8	POSITIVE	NS	NS	NS
NME2	non-metastatic cells 2, protein (NM23B) expressed in	POSITIVE	NS	NS	NS
NME3	non-metastatic cells 3, protein expressed in	NS	NS	POSITIVE	POSITIVE
PACSIN2	protein kinase C and casein kinase substrate in neurons 2	NEGATIVE	NS	NS	NS
PANK2	pantothenate kinase 2 (Hallervorden-Spatz	NS	NS	POSITIVE	NS

	syndrome)				
PBK	PDZ binding kinase	POSITIVE	POSITIVE	POSITIVE	POSITIVE
PCTK3	PCTAIRE protein kinase 3	NS	NS	POSITIVE	POSITIVE
PDGFRA	platelet-derived growth factor receptor, alpha polypeptide	NS	NS	NS	NS
PDGFRB	platelet-derived growth factor receptor, beta polypeptide	NS	NS	NEGATIVE	NS
PDK1	pyruvate dehydrogenase kinase, isoenzyme 1	NEGATIVE	NEGATIVE	NEGATIVE	NS
PDK2	pyruvate dehydrogenase kinase, isoenzyme 2	POSITIVE	POSITIVE	NS	NS
PDK3	pyruvate dehydrogenase kinase, isoenzyme 3	NEGATIVE	NS	NEGATIVE	NS
PDLIM5	PDZ and LIM domain 5	NEGATIVE	NS	NS	NS
PFKFB2	6-phosphofructo-2-kinase/fructose-2,6-biphosphatase 2	POSITIVE	NS	NS	NS
PHKA1	phosphorylase kinase, alpha 1 (muscle)	NS	NS	NEGATIVE	NS
PHKG1	phosphorylase kinase, gamma 1 (muscle)	POSITIVE	NS	NS	NS
PIK3CD	phosphoinositide-3-kinase, catalytic, delta polypeptide	POSITIVE	POSITIVE	POSITIVE	POSITIVE
PIK3CG	phosphoinositide-3-kinase, catalytic, gamma polypeptide	NS	NS	POSITIVE	POSITIVE
PIK3R2	phosphoinositide-3-kinase, regulatory subunit 2 (p85 beta)	NEGATIVE	NS	NS	NS
PIK3R4	phosphoinositide-3-kinase, regulatory subunit 4, p150	NS	NS	NEGATIVE	NS
PIK4CB	phosphatidylinositol 4-kinase, catalytic, beta polypeptide	POSITIVE	POSITIVE	NS	NS
PIM1	pim-1 oncogene	NEGATIVE	NEGATIVE	NS	NS
PIM2	pim-2 oncogene	NS	NS	NEGATIVE	NS
PKN2	protein kinase N2	POSITIVE	POSITIVE	NS	NS

PKN3	protein kinase N3	NS	NS	POSITIVE	NS
PLK1	polo-like kinase 1 (Drosophila)	POSITIVE	NS	POSITIVE	NS
PRKAG1	protein kinase, AMP-activated, gamma 1 non-catalytic subunit	NEGATIVE	NS	NS	NS
PRKAR1B	protein kinase, cAMP-dependent, regulatory, type I, beta	NEGATIVE	NS	NS	NS
PRKAR2A	protein kinase, cAMP-dependent, regulatory, type II, alpha	NEGATIVE	NEGATIVE	POSITIVE	NS
PRKAR2B	protein kinase, cAMP-dependent, regulatory, type II, beta	NEGATIVE	NS	NS	NS
PRKCABP	protein kinase C, alpha binding protein	NEGATIVE	NS	NS	NS
PRKCDBP	protein kinase C, delta binding protein	NS	NS	POSITIVE	NS
PRKD1	protein kinase D1	POSITIVE	NS	POSITIVE	NS
PRKG2	protein kinase, cGMP-dependent, type II	NS	NS	POSITIVE	NS
PRKX	protein kinase, X-linked	NS	NS	POSITIVE	NS
PRKY	protein kinase, Y-linked	NS	NS	POSITIVE	NS
PSKH1	protein serine kinase H1	NS	NS	NEGATIVE	NS
PTK6	PTK6 protein tyrosine kinase 6	POSITIVE	NS	NS	NS
RAF1	v-raf-1 murine leukemia viral oncogene homolog 1	NEGATIVE	NS	NS	NS
RPS6KA1	ribosomal protein S6 kinase, 90kDa, polypeptide 1	POSITIVE	NS	NS	NS
DCAMKL1	doublecortin and CaM kinase-like 1	NEGATIVE	NEGATIVE	NS	NS
RPS6KB1	ribosomal protein S6 kinase, 70kDa, polypeptide 1	NS	NS	NEGATIVE	NS
RPS6KB2	ribosomal protein S6 kinase, 70kDa, polypeptide 2	POSITIVE	NS	NS	NS
RPS6KL1	ribosomal protein S6 kinase-like 1	POSITIVE	NS	NS	NS

RYK	RYK receptor-like tyrosine kinase	NS	NS	POSITIVE	NS
SNF1LK	SNF1-like kinase	NS	NS	NEGATIVE	NS
STK22D	serine/threonine kinase 22D (spermiogenesis associated)	POSITIVE	POSITIVE	POSITIVE	NS
STK25	serine/threonine kinase 25 (STE20 homolog, yeast)	POSITIVE	NS	NS	NS
STK32C	serine/threonine kinase 32C	NS	NS	NEGATIVE	NS
STK11	serine/threonine kinase 11 (Peutz-Jeghers syndrome)	POSITIVE	NS	NS	NS
TAOK1	TAO kinase 1	NS	NS	POSITIVE	NS
TEK	TEK tyrosine kinase, endothelial (venous malformations, multiple cutaneous and mucosal)	NEGATIVE	NS	NS	NS
TESK1	testis-specific kinase 1	POSITIVE	POSITIVE	POSITIVE	NS
TGFBR2	transforming growth factor, beta receptor II (70/80kDa)	NEGATIVE	NEGATIVE	POSITIVE	POSITIVE
TIE1	tyrosine kinase with immunoglobulin-like and EGF-like domains 1	NEGATIVE	NS	NS	NS
TNK2	tyrosine kinase, non-receptor, 2	NEGATIVE	NS	NS	NS
TYRO3	TYRO3 protein tyrosine kinase	NEGATIVE	NEGATIVE	NS	NS
ULK2	unc-51-like kinase 2 (C. elegans)	NEGATIVE	NS	NS	NS

4.7 Figures

Figure 4-1

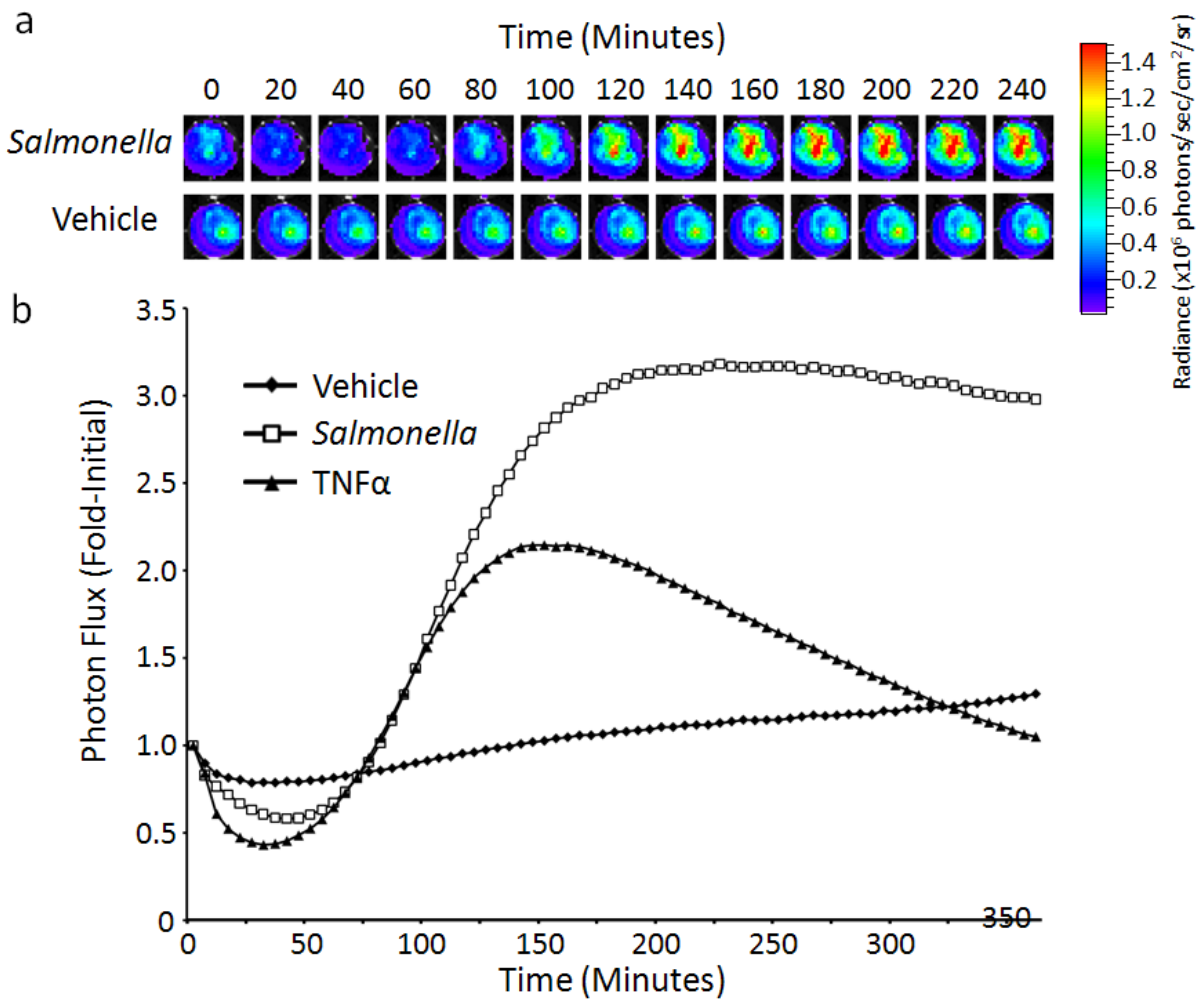

Figure 4-1: Real-time activation of NF-κB signaling by *Salmonella* Typhimurium. HCT116 cells transiently transfected with *pκB5→IκBαFLuc* were stimulated with heat-killed *Salmonella* at T=0 and imaged for reporter activity every 5 minutes for 6 hours. (a) Photon flux images obtained every 20 minutes are shown. (b) Data are displayed as the fold-initial photon flux values. Imaging parameters: acquisition time, 60 sec; binning, 4; filter, open; f stop, 1; FOV, 23 cm.

Figure 4-2

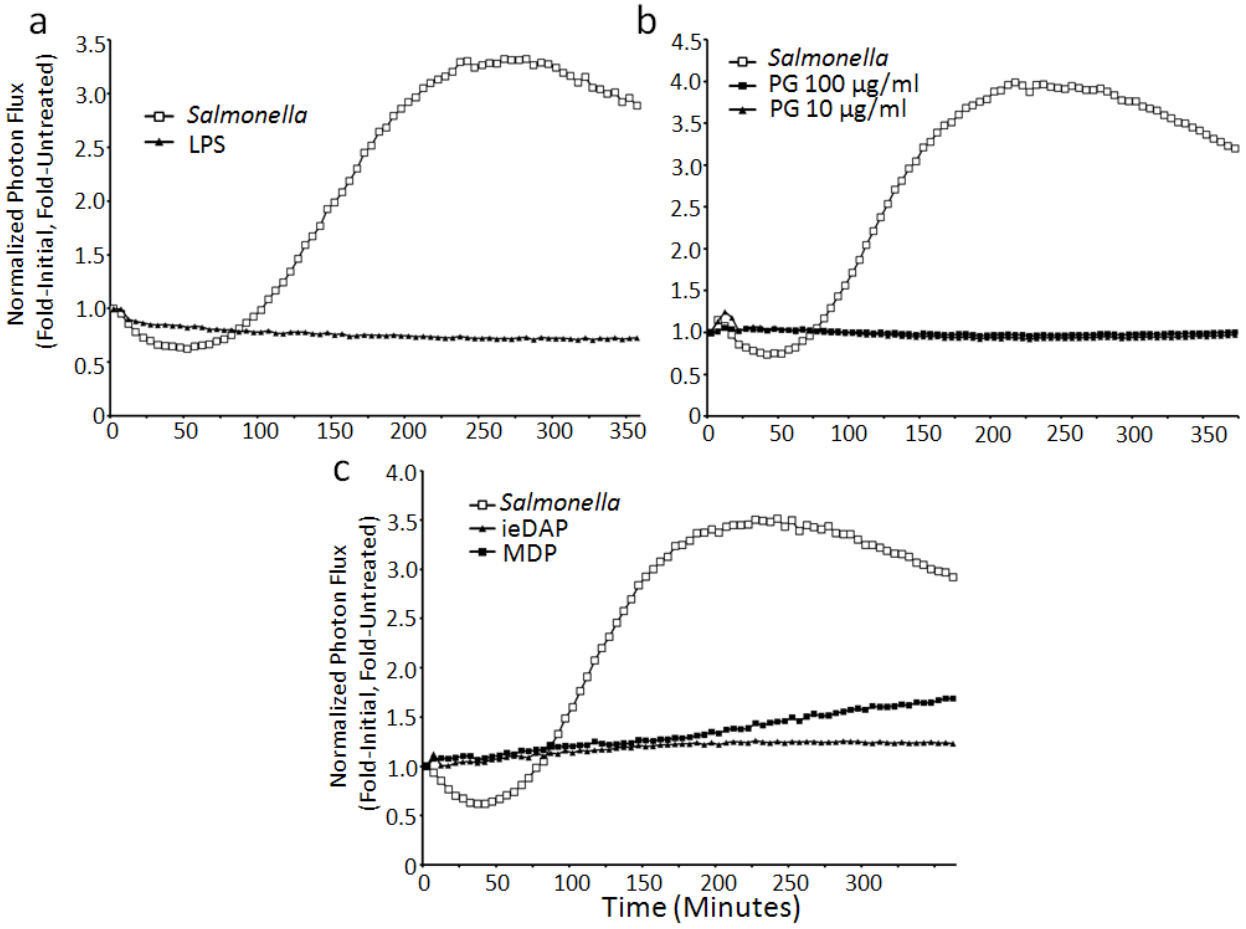

Figure 4-2: LPS, Peptidoglycan and NOD ligands do not significantly contribute to NF-κB activation in HCT116 cells in response to *Salmonella*. HCT116 cells stably expressing κB5→IκBαFLuc were stimulated with the indicated ligand at T=0 and imaged for reporter activity every 5 minutes for 6 hours. Data is displayed as normalized photon flux values (Fold-initial, fold-vehicle). Imaging parameters: acquisition time, 60 sec; binning, 8; filter, open; f stop, 1; FOV, 20 cm(a,c) 15 cm(b).

Figure 4-3

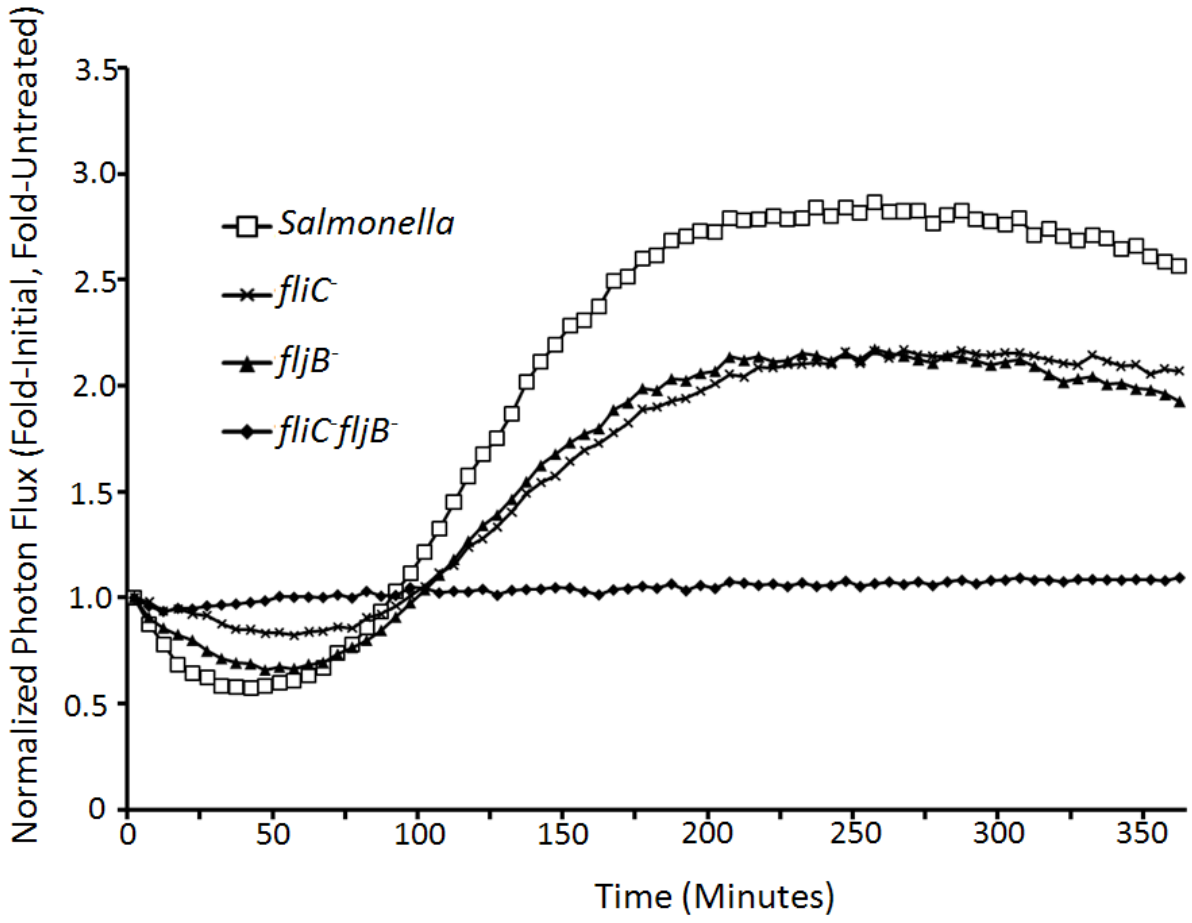

Figure 4-3: *Salmonella* flagellin activates NF-κB signaling in HCT116 colon carcinoma cells. HCT116 cells stably expressing κB5→IκBαFLuc were stimulated with heat-killed wild-type *Salmonella*, *fliC*$^-$, *fjB*$^-$, or *fliC*$^-$/*fjB*$^-$ at T=0 and imaged for reporter activity every 5 minutes for 6 hours. Data is displayed as normalized photon flux values (Fold-initial, fold-vehicle). Imaging parameters: acquisition time, 60 sec; binning, 8; filter, open; f stop, 1; FOV, 20 cm.

Figure 4-4

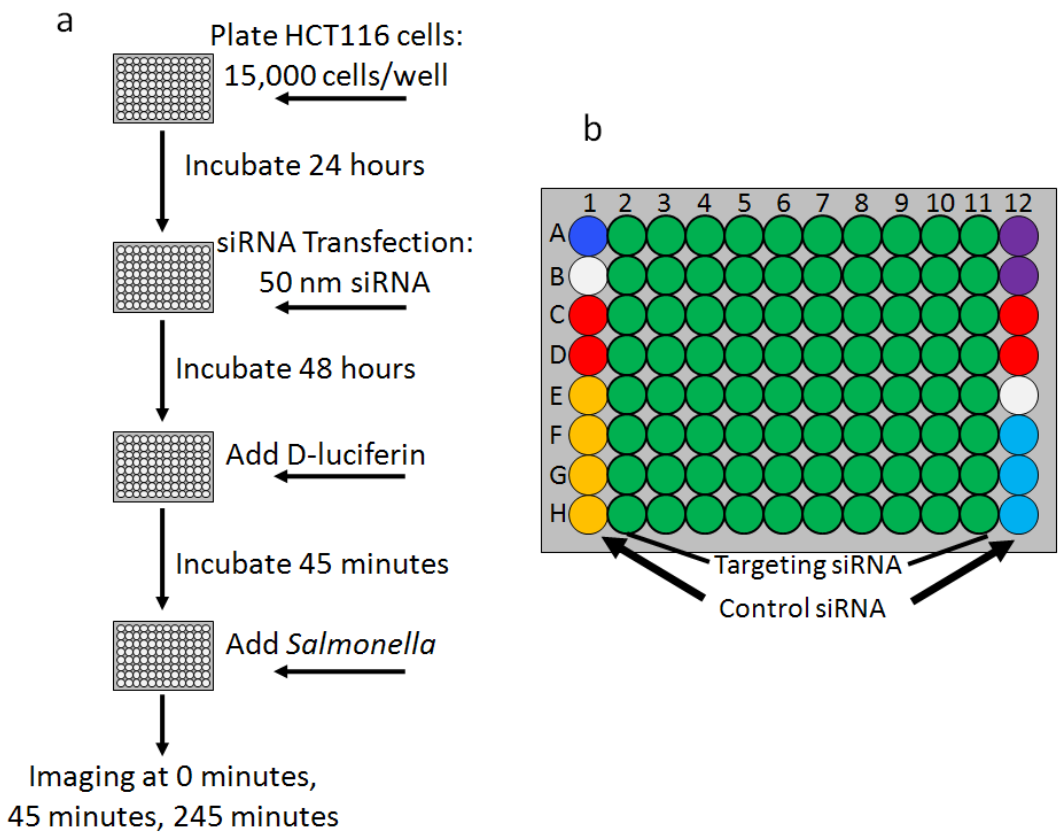

Figure 4-4: A schematic of the high-throughput screening technique. (a)HCT116 cells stably expressing κB5→IκBαFLuc were plated into 96-well plates. After a 24-hour incubation, cells were transfected with siRNA and incubated for 48 hours more. To image, cells were transferred into d-luciferin-containing media, allowed to equilibrate for 45 minutes, stimulated with heat-killed *Salmonella* and imaged for reporter activity at 0, 45 and 245 minutes. (b) Each siRNA library plate contained targeting siRNA in columns 2-11 and control siRNA constructs in columns 1 and 12, as indicated. Control wells included: mock-transfected cells (blue, A1), vehicle-treated wells (yellow; E1, F1, G1, H1), three non-targeting control sequences (turquoise, Qiagen Allstar Negative control,

F12; Qiagen scrambled siRNA, G12; Qiagen GFP siRNA, H12), TLR5-targetting siRNA sequences (red, IDT, C1, C12, D1, D12), and a firefly luciferase-targeting PGL3 siRNA (purple, Dharmacon Research Inc, A12, B12).

Figure 4-5

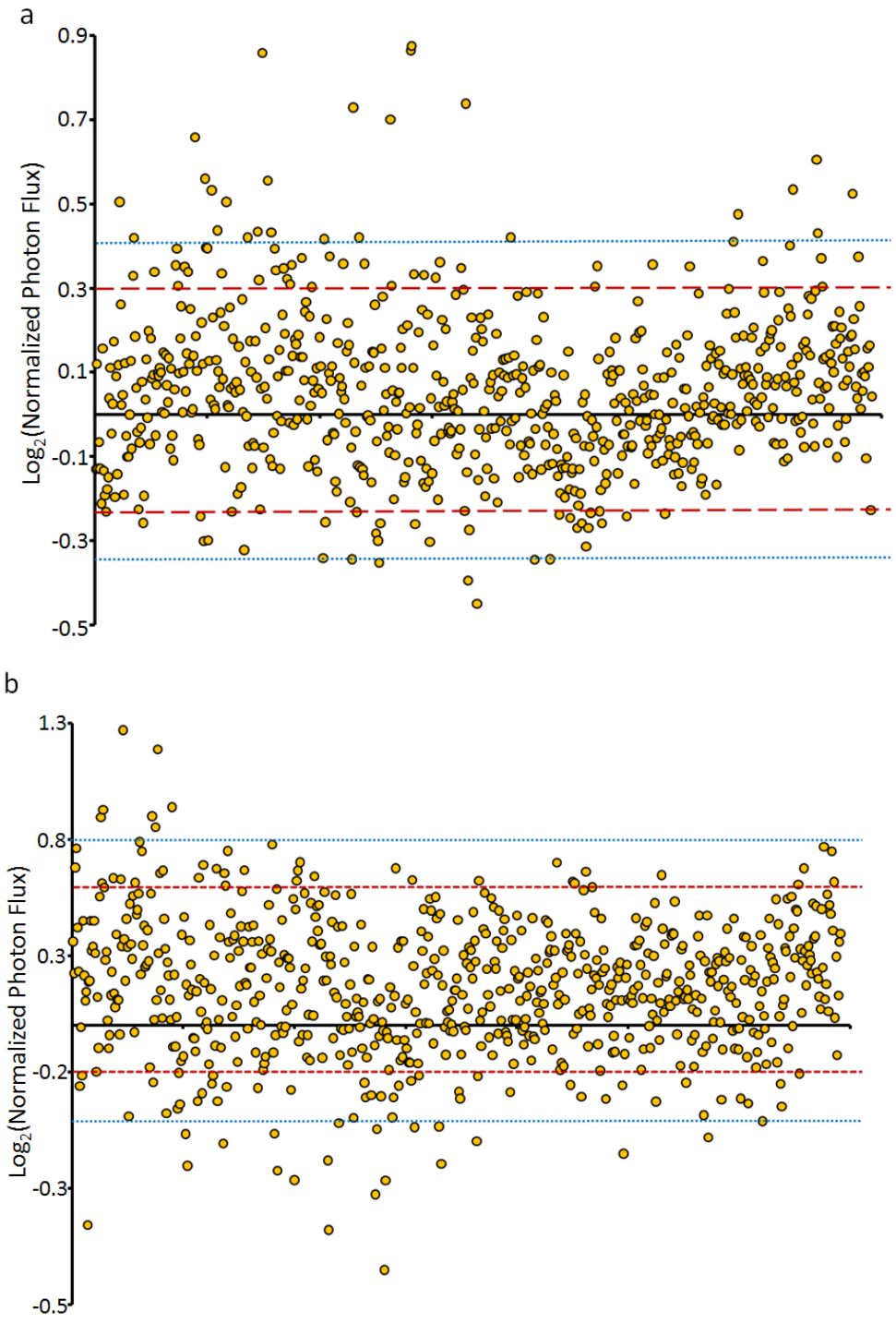

Figure 4-5: High-throughput screening data. Normalized photon flux data for 691 targeted kinases is shown at 45(a) and 245(b) minutes after *Salmonella* situation. Data is

the average of three replicates. Dotted blue and dashed red lines show significance cut-offs for low ($\alpha = 0.1$) and high ($\alpha = 0.02$) stringency targeted error rates, respectively.

Figure 4-6

a

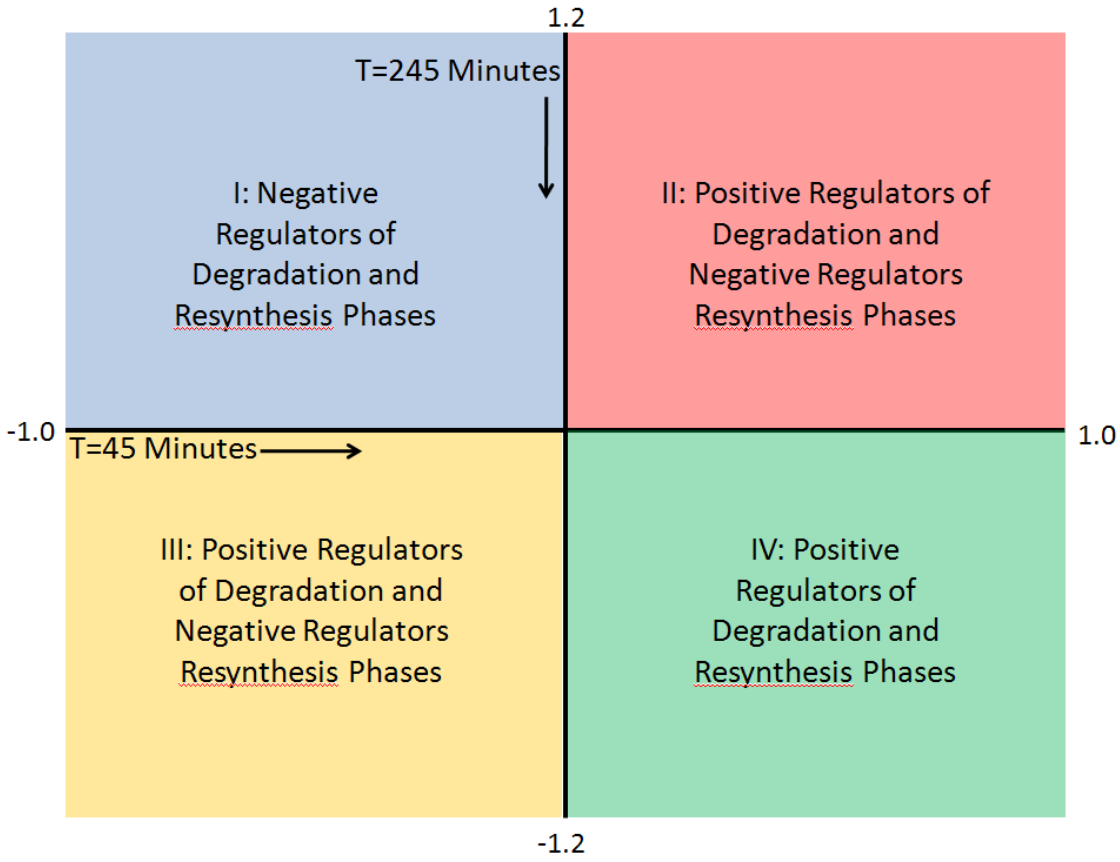
1.2
T=245 Minutes
I: Negative Regulators of Degradation and Resynthesis Phases
II: Positive Regulators of Degradation and Negative Regulators Resynthesis Phases
-1.0
T=45 Minutes
1.0
III: Positive Regulators of Degradation and Negative Regulators Resynthesis Phases
IV: Positive Regulators of Degradation and Resynthesis Phases
-1.2

b

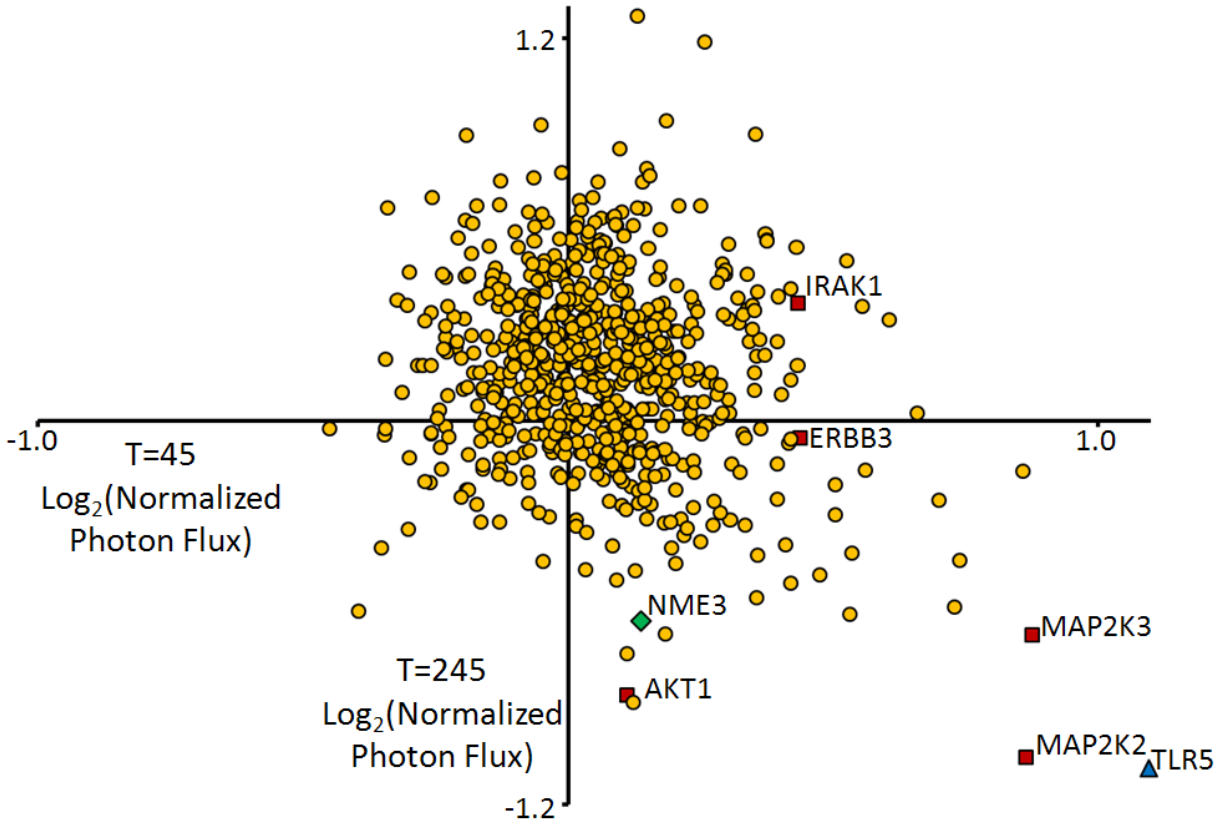

Figure 4-6: MAP2K2, MAP2K3 and NME3 act as positive regulators of *Salmonella*-induced NF-κB pathways. (a) A schematic diagram shows the proposed regulatory activity on NF-κB by kinase targets in each of four quadrants in the plot. (b) The normalized photon flux data from the primary screen at 45 minutes and 245 minutes are plotted on the x- and y- axes, respectively. Highlighted points show data from specific screening hits and TLR5 control wells.

Figure 4-7

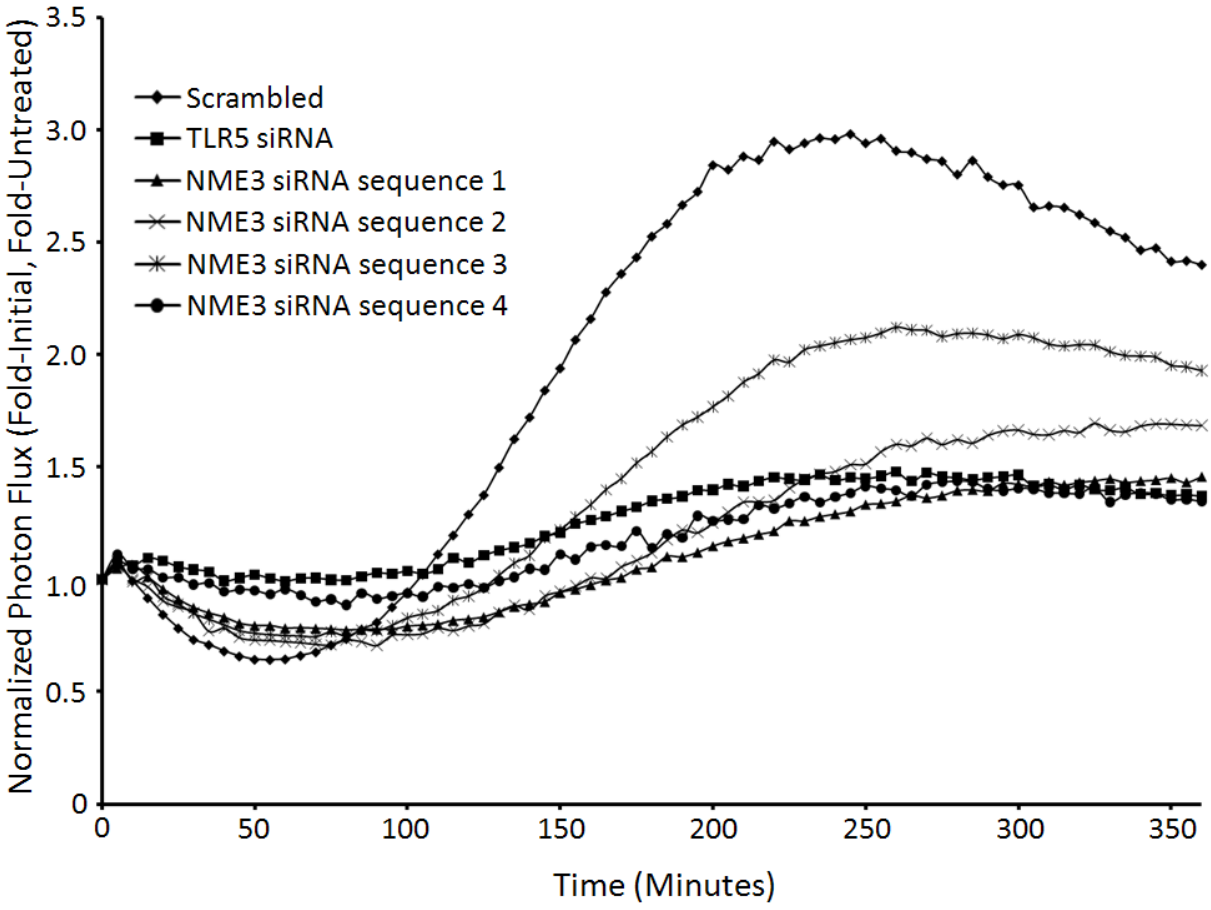

Figure 4-7: NME3 knockdown inhibits NF-κB. HCT116 cells stably expressing κB5→IκBαFLuc and transfected with the indicated siRNA constructs were stimulated with heat-killed *Salmonella* and imaged for reporter activity every 5 minutes for 6 hours. Data is displayed as normalized photon flux values (fold-initial, fold-untreated). Individual siRNA sequences targeting NME3 show reduced IκBαFLuc reporter responsiveness. Imaging parameters: acquisition time, 60 sec; binning, 8; filter, open; f stop, 1; FOV, 12 cm.

Figure 4-8

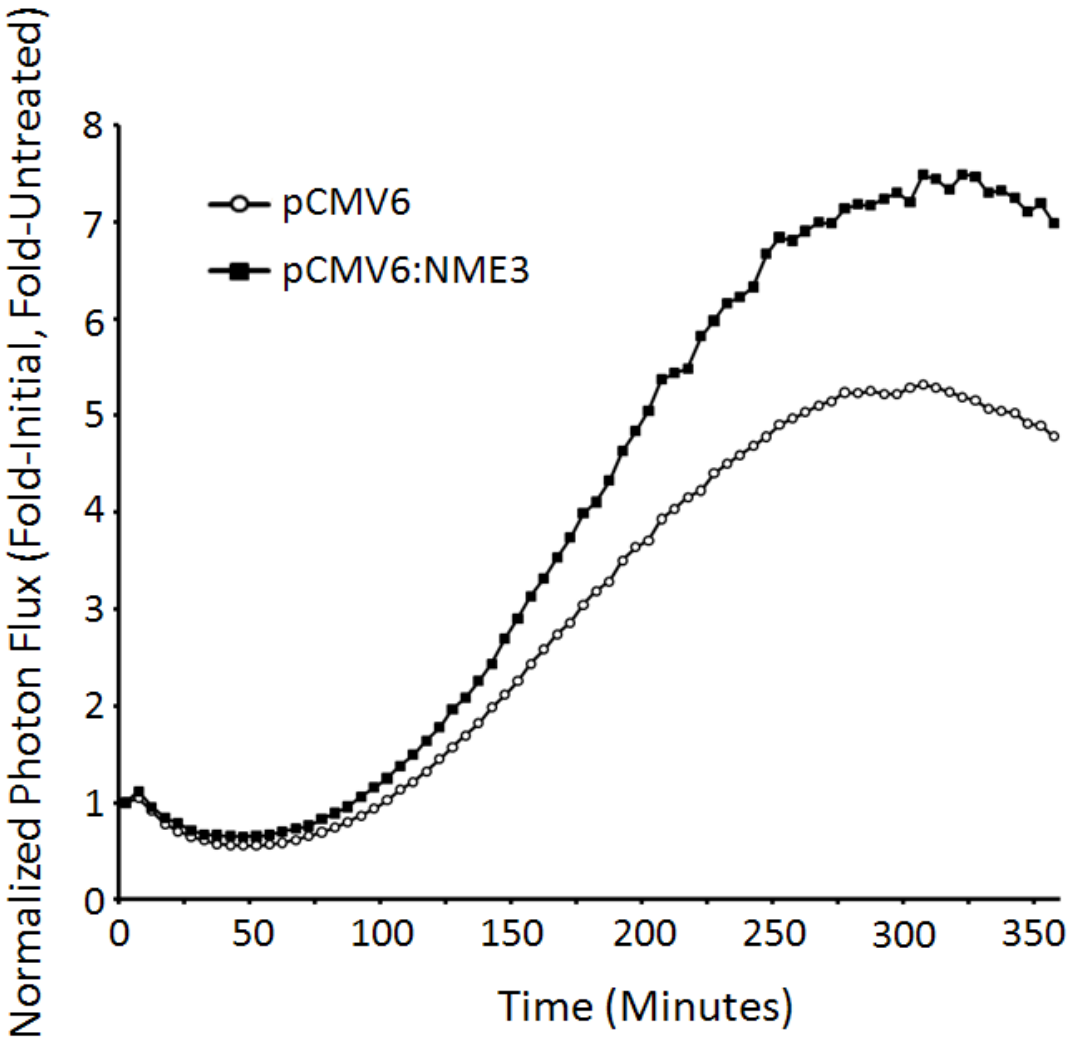

Figure 4-8: NME3 over-expression induces NF-κB transcriptional activation. HCT116 cells were transfected with *pκB5→IκBαFLuc* and the indicated plasmid constructs and stimulated with heat-killed *Salmonella* and imaged for reporter activity every 5 minutes for 6 hours. Data is displayed as normalized photon flux values (fold-initial, fold-untreated). Plasmid-based over-expression of NME3 induces over-expression of NF-κB transcriptional targets. Imaging parameters: acquisition time, 60 sec; binning, 8; filter, open; f stop, 1; FOV, 12 cm.

Figure 4-9

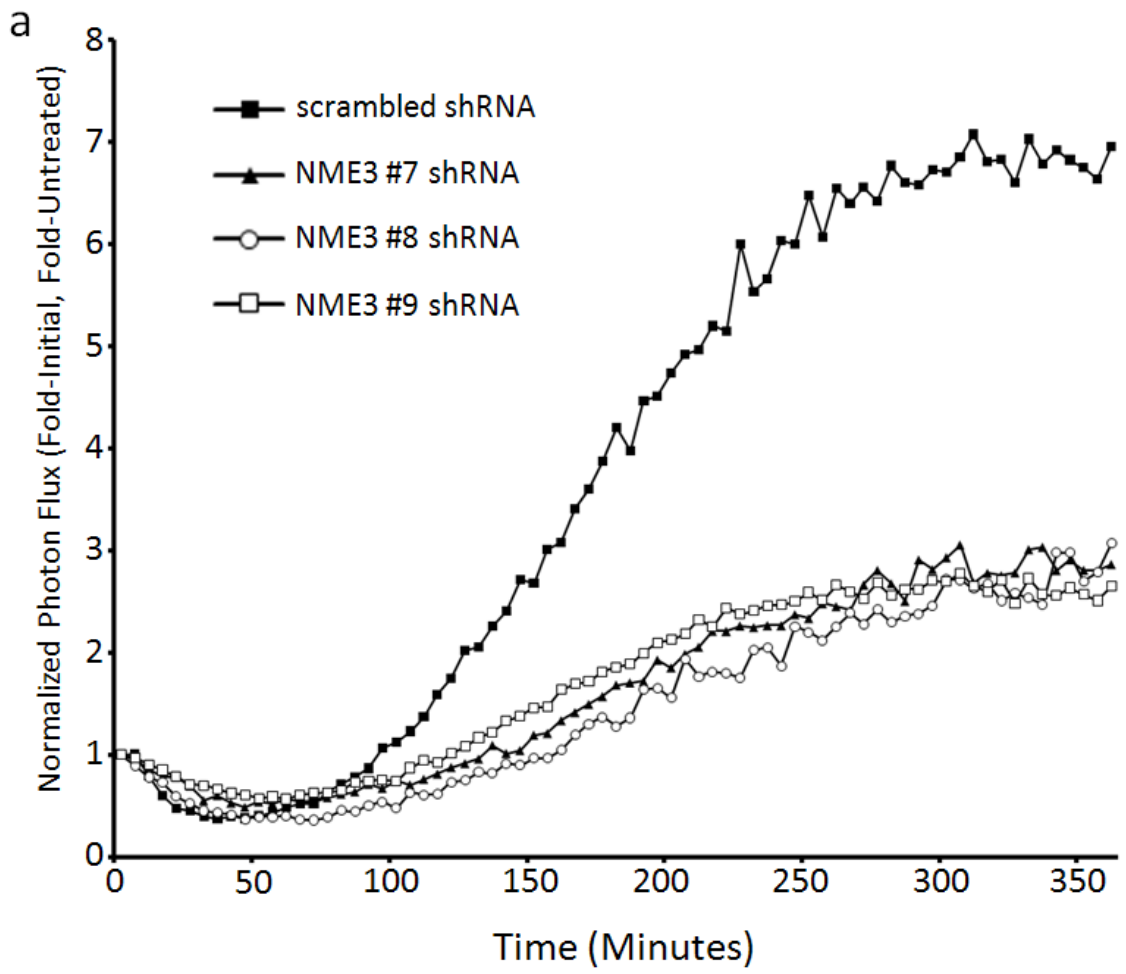
a
Normalized Photon Flux (Fold-Initial, Fold-Untreated)
scrambled shRNA
NME3 #7 shRNA
NME3 #8 shRNA
NME3 #9 shRNA
0
1
2
3
4
5
6
7
8
0
50
100
150
200
250
300
350
Time (Minutes)

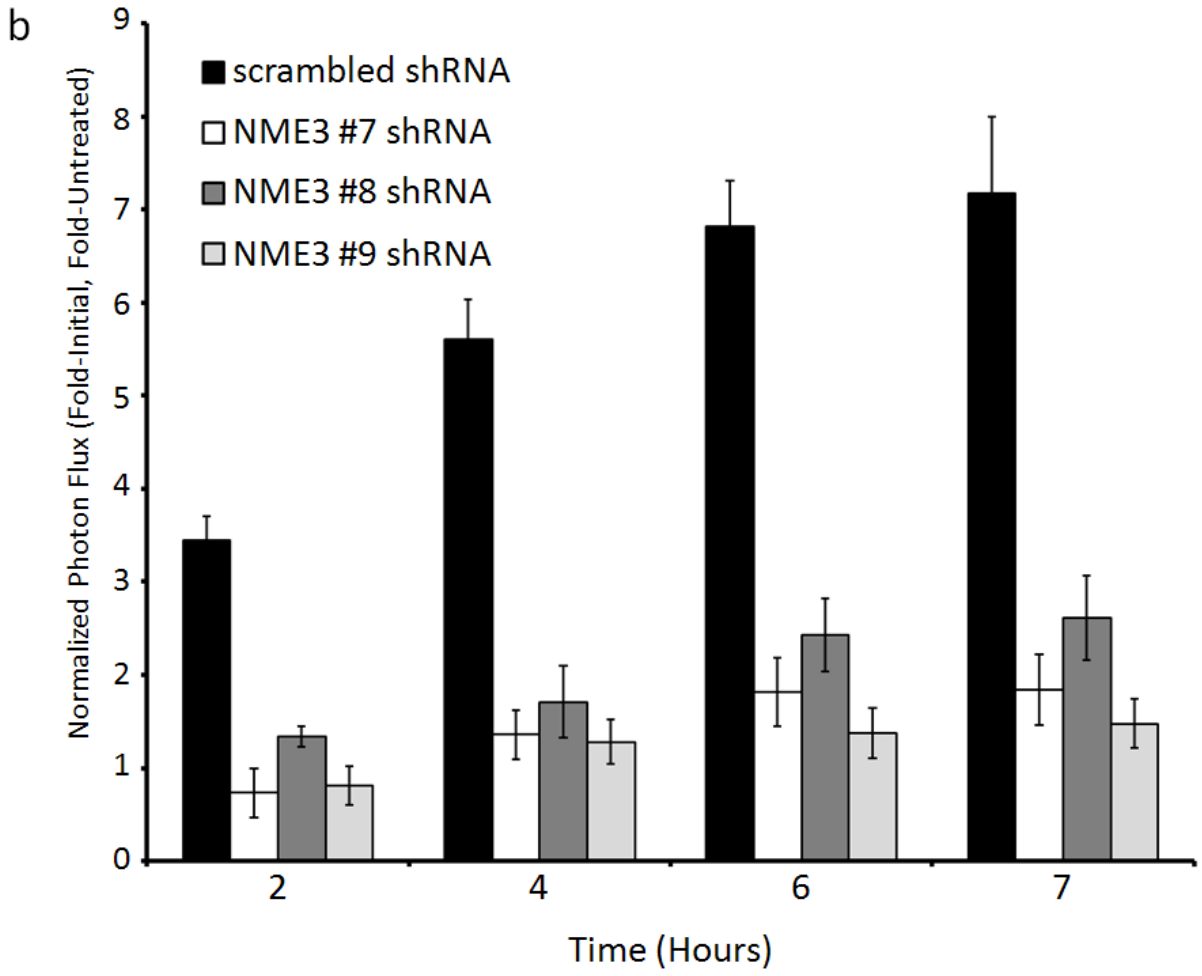
b
scrambled shRNA
NME3 #7 shRNA
NME3 #8 shRNA
NME3 #9 shRNA
Normalized Photon Flux (Fold-Initial, Fold-Untreated)
0
1
2
3
4
5
6
7
8
9
2
4
6
7
Time (Hours)

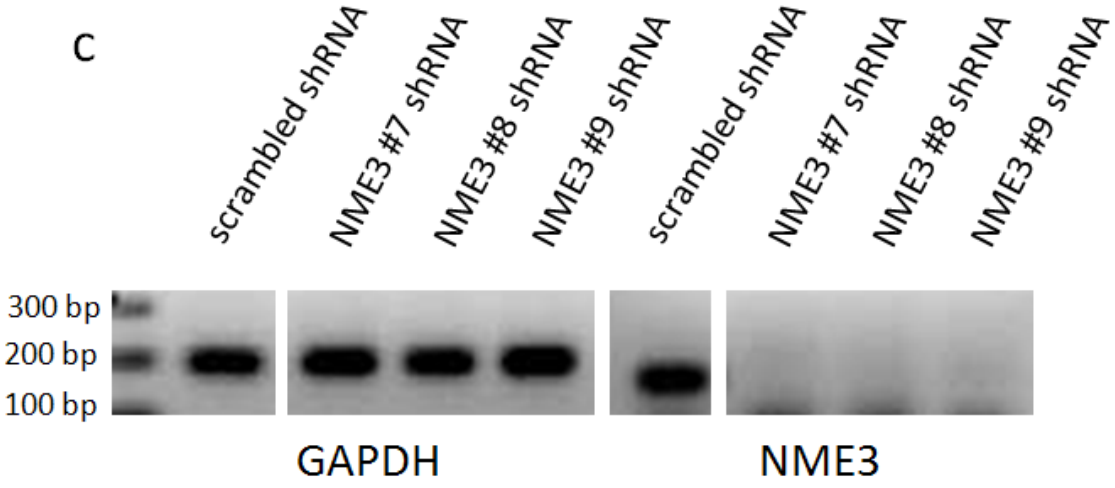
c
scrambled shRNA
NME3 #7 shRNA
NME3 #8 shRNA
NME3 #9 shRNA
scrambled shRNA
NME3 #7 shRNA
NME3 #8 shRNA
NME3 #9 shRNA
300 bp
200 bp
100 bp
GAPDH
NME3

Figure 4-9: Targeting NME3 by shRNA reduces NF-κB responsiveness. (a) HCT116 cells were subjected to lentiviral knockdown with the indicated shRNA constructs and transfected with the *pκB5→IκBαFLuc* plasmid. Cells were then stimulated with heat-killed *Salmonella* and imaged for reporter activity every 5 minutes for 6 hours. Data is displayed as normalized photon flux values (fold-initial, fold-untreated). Imaging parameters: acquisition time, 30 sec; binning, 8; filter, open; f stop, 1; FOV, 15 cm. (b) HCT116 cells were subjected to lentiviral knockdown with the indicated shRNA constructs and transfected with the *pκB5→FLuc* plasmid. Imaging was performed at 0, 2, 4, 6, and 7 hours following stimulation with *Salmonella.* Data is displayed as normalized photon flux values (fold-initial, fold-untreated). IVIS 50 Imaging parameters: acquisition time, 10 sec; binning, 8; filter, open; f stop, 1; FOV, 12 cm. (c) Semi-quantitative PCR verifies knockdown of NME3 mRNA in shRNA-expressing HCT116 cells. GAPDH mRNA levels are shown as a control.

4.8 References

1. Akira, S. and K. Takeda, *Toll-like receptor signalling.* Nat Rev Immunol, 2004. **4**(7): p. 499-511.

2. Arpaia, N., et al., *TLR signaling is required for Salmonella typhimurium virulence.* Cell. **144**(5): p. 675-88.

3. Karin, M., *NF-kappaB as a critical link between inflammation and cancer.* Cold Spring Harb Perspect Biol, 2009. **1**(5): p. a000141.

4. Nath, G., H. Singh, and V.K. Shukla, *Chronic typhoid carriage and carcinoma of the gallbladder.* Eur J Cancer Prev, 1997. **6**(6): p. 557-9.

5. Datsenko, K.A. and B.L. Wanner, *One-step inactivation of chromosomal genes in Escherichia coli K-12 using PCR products.* Proc Natl Acad Sci U S A, 2000. **97**(12): p. 6640-5.

6. Zhang, X.D., et al., *Robust statistical methods for hit selection in RNA interference high-throughput screening experiments.* Pharmacogenomics, 2006. **7**(3): p. 299-309.

7. Moss, B.L., et al., *Identification of a ligand-induced transient refractory period in nuclear factor-kappaB signaling.* J Biol Chem, 2008. **283**(13): p. 8687-8698.

8. Hacker, H. and M. Karin, *Regulation and function of IKK and IKK-related kinases.* Sci STKE, 2006. **2006**(357): p. re13.

9. Zhong, H., R.E. Voll, and S. Ghosh, *Phosphorylation of NF-kappa B p65 by PKA stimulates transcriptional activity by promoting a novel bivalent interaction with the coactivator CBP/p300.* Mol Cell, 1998. **1**(5): p. 661-71.

10. Gottipati, S., N.L. Rao, and W.P. Fung-Leung, *IRAK1: a critical signaling mediator of innate immunity.* Cell Signal, 2008. **20**(2): p. 269-76.

11. Madrid, L.V., et al., *Akt stimulates the transactivation potential of the RelA/p65 Subunit of NF-kappa B through utilization of the Ikappa B kinase and activation of the mitogen-activated protein kinase p38.* J Biol Chem, 2001. **276**(22): p. 18934-40.

12. Ozes, O.N., et al., *NF-kappaB activation by tumour necrosis factor requires the Akt serine-threonine kinase.* Nature, 1999. **401**(6748): p. 82-5.

13. Ie Kim, H. and S.T. Lee, *Oncogenic functions of PTK6 are enhanced by its targeting to plasma membrane but abolished by its targeting to nucleus.* J Biochem, 2009. **146**(1): p. 133-9.

14. Aubele, M., et al., *Prognostic value of protein tyrosine kinase 6 (PTK6) for long-term survival of breast cancer patients.* Br J Cancer, 2008. **99**(7): p. 1089-95.

15. Zheng, Y., et al., *Protein tyrosine kinase 6 directly phosphorylates AKT and promotes AKT activation in response to epidermal growth factor.* Mol Cell Biol. **30**(17): p. 4280-92.

16. Koff, J.L., et al., *Multiple TLRs activate EGFR via a signaling cascade to produce innate immune responses in airway epithelium.* Am J Physiol Lung Cell Mol Physiol, 2008. **294**(6): p. L1068-75.

17. Guma, M., et al., *Constitutive intestinal NF-{kappa}B does not trigger destructive inflammation unless accompanied by MAPK activation.* J Exp Med.

18. Kojima, M., et al., *Increased nuclear factor-kB activation in human colorectal carcinoma and its correlation with tumor progression.* Anticancer Res, 2004. **24**(2B): p. 675-81.

19. Venturelli, D., et al., *The nucleoside diphosphate kinase activity of DRnm23 is not required for inhibition of differentiation and induction of apoptosis in 32Dcl3 myeloid precursor cells.* Exp Cell Res, 2000. **257**(2): p. 265-71.

20. Lacombe, M.L., et al., *The human Nm23/nucleoside diphosphate kinases.* J Bioenerg Biomembr, 2000. **32**(3): p. 247-58.

21. Postel, E.H., et al., *Human c-myc transcription factor PuF identified as nm23-H2 nucleoside diphosphate kinase, a candidate suppressor of tumor metastasis.* Science, 1993. **261**(5120): p. 478-80.

22. Boissan, M., et al., *The mammalian Nm23/NDPK family: from metastasis control to cilia movement.* Mol Cell Biochem, 2009. **329**(1-2): p. 51-62.

23. Amendola, R., et al., *DR-nm23 gene expression in neuroblastoma cells: relationship to integrin expression, adhesion characteristics, and differentiation.* J Natl Cancer Inst, 1997. **89**(17): p. 1300-10.

CHAPTER FIVE

A High-Throughput siRNA Screen to Identify Novel Host Phosphatases Involved in Regulation of *Salmonella* Induction of Inflammation

5.1 Introduction

NF-κB is a key transcription factor and mediator of human innate immunity and stress-response pathways. The protein can be activated by a number of different stimulatory signals, including cytokines, microbial PAMPs and reactive oxygen species (ROS). One major outcome of activated NF-κB signaling is the activation of genes involved in promoting cellular survival and inhibiting apoptosis. Unregulated NF-κB signaling, therefore, can lead to increased levels of cellular proliferation and has been linked to cancer and other chronic inflammatory diseases [1].

Phosphatases are key players in many host signal transduction pathways and are known to specifically modulate the NF-κB pathway at several instances. For example, the phosphatase PP-2A acts to dephosphorylate IKKβ [2]. Also, WIP1 phosphatase acts to directly dephosphorylate an activating serine phosphorylation on the p65 subunit of NF-κB, thereby inhibition NF-κB activity [3].

Although other studies have identified novel phosphatase modulators of NF-κB signaling, these studies most often utilize TNFα as the NF-κB-stimulating ligand. Yet, the NF-κB pathway is activated by multiple other stimuli that lead to different downstream signaling intermediates. For example, many of the proteins directly downstream of TLR activation are not required for TNFα-induced signaling and different TLRs recruit different adapters

to transduce their signals. Therefore, novel phosphatase actions may be discovered by studying the NF-κB pathway downstream of TLR signaling as well.

To investigate the contribution of individual phosphatases to *Salmonella*-induced activation of NF-κB, I performed an siRNA screen. By imaging the degradation and resynthesis of an NF-κB-driven IκBα-FLuc reporter, I could study the individual contributions of each phosphatase in two separate phases of NF-κB pathway activation.

5.2 Methods

Cell lines and culture conditions: HCT116 cells were a gift of Bert Vogelstein and cultured according to ATCC directions. All stably transfected HCT116 cells were cultured in 0.5 μg/ml puromycin.

Salmonella *strains*: *Salmonella* Typhimurium strain SL1344 was used for all experiments.

Creation of a κB5→IκBαFLuc-expressing HCT116 stable cell line: HCT116 cells at 95% confluency were co-transfected with 10 μg of pκB5→IκBαFLuc and 3 μg of pIRES-puro plasmid DNA using Fugene 6 in 10 cm dishes. After 24 hours the media was replaced with fresh cell media. Twenty-four hours later the cells were split at multiple dilutions into media containing 0.5μg/ml puromycin to select for stable transformants. After two weeks, isolated cell colonies were imaged to check for reporter gene expression and bioluminescent colonies were harvested and expanded. The HCT116 stable cells were continuously cultured in the presence of 0.5μg/ml puromycin to maintain expression of the reporter plasmid.

High-throughput screen: siRNA screening was performed in white, clear-bottomed, 96-well culture plates using a Beckman-Coulter Core robotics system, including an FX

liquid handler, controlled by the Sagian graphical method development tool (SAMI scheduling software). HCT116 cells stably expressing pκB5→IκBαFLuc were seeded at 15,000 cells per well and allowed to attach for 24 hours. Forward transfection was performed with a 96 multichannel head on the FX liquid handler, adding 0.5 µl/well of media-complexed R1 Transpass (NEB) to the aliquotted siRNA library (Kinase siRNA set v2; Qiagen Inc.) in a 96-well reaction plate and allowed to incubate for 15 minutes. Experimental siRNA oligos were arrayed in columns 2-11 of each plate and individual controls comprising vehicle-treated wells, a non-targeting control sequence (Qiagen Allstar Negative control), TLR5-targetting siRNA sequences (IDT), and a firefly luciferase-targeting PGL3 siRNA (Dharmacon Research Inc.) were placed manually in columns 1 and 12. After incubation of siRNA complexes, 100 µl was added to each well of a plate with cells (x3 plates) using the FX liquid handler, yielding a final concentration of ~50 nM siRNA/well. Plates were maintained at 37ºC and 5% CO_2 for 48 hours. At this time, media were aspirated and replaced with 180 µl imaging media (colorless DMEM supplemented with 10% heat inactivated FBS and 150 µg/ml d-luciferin) and the cells were allowed to equilibrate for 45 minutes. After equilibrating, 20 µl of stimulus (1:100 dilutions of heat-killed *Salmonella* cultures) or control (LB broth) were added to each well. Bioluminescent readings were obtained on an EnVision plate reader (PerkinElmer) immediately following stimulus, at 45 minutes post-stimulation and at 245 minutes post-stimulation. After the final luminescent reading, 20 µl of rezasurin dye was added to all wells, allowed to incubate for 2 hours at 37ºC and monitored on a FLUOstar OPTIMA fluorescence reader (BMG Labtech; excitation, 544 nm, emission, 590 nm).

Data analysis: Initially, the signal in each well was normalized to a plate-matched control well containing a non-targeting siRNA sequence to facilitate experiment-wide analysis. Then, the differences in the $\log_2$ values of the normalized data between 0 minutes and 45 or 245 minutes were averaged across triplicate siRNA experimental replicates. Screening hits were selected by quartile analysis of the normalized kinase library data. To perform the quartile analysis, median (Q2), first (Q1) and third (Q3) quartile values were calculated. From these values, the upper and lower boundaries for hit selection were calculated as Q3 + 2c(Q3 –Q2) and Q1 – 2c(Q2-Q1), respectively, for c = 0.9529 corresponding to a targeted error rate ($\alpha = 0.05$).

5.3 Results

To identify novel host factors involved in *Salmonella*-induced activation of innate immunity, an siRNA screen targeting all known and predicted host phosphatases was performed in HCT116 colon carcinoma cells. The HCT116 colon carcinoma cells were stably transfected with a plasmid containing five tandem NF-κB binding sites driving an IκBα-FLuc fusion reporter construct. This reporter permitted imaging two separate stages in the activation of the NF-κB pathway. The first stage is the early degradation of the fusion reporter, representing degradation of IκBα, the negative regulator NF-κB, which preceeds nuclear translocation NF-κB. Then, the second stage represents the transcriptional activation mediated by NF-κB, which drives reporter synthesis, due to the five tandem NF-κB binding sites. These two stages can be measured by an initial decrease in bioluminescence, followed by a large increase in bioluminescent signal, respectively. HCT116 cells stably expressing this reporter were treated with siRNA constructs (2 sequences per well) targeting individual host phosphatases for 48 hours.

Then, heat-killed preparations for *Salmonella* were added to stimulate NF-κB signaling. The normalized data obtained from imaging at 45 minutes and 245 minutes are shown in **Figures 5-1a** and **b**. Additionally, to combine the information acquired for each targeted phosphatase, the data can be plotted with the 45-minute signals on the x-axis and the 245 minute signals on the y-axis (**Figure 5-2**). In this plot, positive values along the x-axis correspond to phosphatase knockdowns that induced less reporter degradation than control, indicating phosphatases that positively modulate the degradation phase of NF-κB signaling. Conversely negative x-values represent wells that induced more reporter degradation and therefore represent phosphatses with a negative regulatory role in NF-κB signaling. At 245 minutes, represented by y-values, positive and negative values represent negative and positive regulators of NF-κB signaling, respectively. In this case, data representing a phosphatase acting as a positive regulator of NF-κB signaling at both time points will fall in the lower right quadrant of the plot, as in the case of the TLR-5 control siRNA. A summary of all statistically significant hits and their predicted regulatory activity on NF-κB signaling are listed in **Table 5-1**.

5.4 Discussion

Salmonella is known to activate NF-κB signaling through activation of Toll-like receptors in host cells. In order to identify potential novel phosphatases involved in *Salmonella*-induced activation of host NF-κB signaling through bacterial flagellin, we utilized a high-throughput siRNA screen. Interestingly, phosphatases are often credited as negative regulatory proteins in signal transduction pathways, and the global high-throughput screening data obtained here seem to confirm this role. At both the 45 and

245 minute time points, the majority of assayed phosphatases are negatively regulating NF-κB signaling.

Several of the phosphatases identified as hits in the high throughput screen belong to the PP2C family of phosphatases. PPM1A, PPM1G, and PPM1L are all phosphatases in the PP2C family, a group of serine/threonine phosphatases found in eukaryotes that have been shown to have roles in negative regulation of stress responses [4, 5]. WIP1 phosphatase also belongs to the PP2C family and has previously been shown to modulate NF-κB signaling, but was not a hit in this high-throughput screen [3]. However the experiments with WIP1 demonstrated its role in TNFα and IL-1β-induced signaling, and perhaps WIP1 is less relevant to TLR-induced NF-κB signaling as studied here [3]. PPM1A has been shown to negatively regulate NF-κB signaling, and in previous work, knockdown of PPM1A induced enhanced NF-κB nuclear translocation and downstream gene activation, similar to the results in this high-throughput screen [4]. PPM1L and PPM1G have demonstrated opposing roles in regulation of cellular stress response pathways in previous work, verifying the data from this screen [5]. However, these studies have demonstrated negative regulation of TNFα-induced activation of MAP kinase and pro-apoptotic signaling by PPM1L and positive regulation by PPM1G, the opposite of the effects observed in this screen [5]. Because NF-κB activation by TNFα serves to prevent apoptosis, it could be reasoned that while PPM1L negatively regulates TNFα induction of apoptosis, it effectively positively regulates TNFα induction of NF-κB signaling, thereby creating roles for PPM1L and PPM1G in positive and negative regulation of NF-κB signaling, respectively, as demonstrated here [6].

Another phosphatase identified in the screen, PTPNS1, has also been shown to play an important role in AKT activation following treatment with TNFα or IL-1β [7]. Because AKT is likely involved in activation of NF-κB signaling, PTPNS1 may be required for full activation of NF-κB downstream of TLR signaling as well [8]. Finally, in a study of host lipid compounds called resolvins that regulate host inflammatory pathways, ALP1 was linked to cellular resolution of inflammation [9]. In this work, resolvin treatment induce ALP1 expression, which reduced NF-κB activation and promoted resolution of inflammation[9]. However, the researchers in the study claim the anti-inflammatory role of ALP1 lies in its dephosphorylation of LPS, which detoxifies the bacterial product. However, based on the data from the high-throughput screen performed here, the role of ALP1seems more likely to be dephosphorylation of a common intermediate in TLR4 and TLR5 signal transduction. It would be interesting to determine where ALP1 negatively regulates NF-κB activation downstream of cytokine receptors, such as TNFR, as well. The phosphatases identified here warrant further functional studies to better understand their roles in modulation of NF-κB. ALP1 is of particular interest based on its hypothesized role as a mediator of resolution of inflammation. Through further research on ALP1 we may discover new ways to target over-active inflammatory responses.

5.5 Tables

Table 5-1 Phosphatases Modulating the NF-κB Pathway

Gene name	Gene function	NF-κB regulatory activity, 45 min α=0.1	NF-κB regulatory activity, 45 min α=0.02	NF-κB regulatory activity, 245 min α=0.1	NF-κB regulatory activity, 245 min α=0.02
ALPI	alkaline phosphatase, intestinal	NEGATIVE	NS	NS	NS
CTDSP2	CTD (carboxy-terminal domain, RNA polymerase II, polypeptide A) small phosphatase 2	NS	NS	POSITIVE	NS
DOLPP1	dolichyl pyrophosphate phosphatase 1	POSITIVE	POSITIVE	NS	NS
DUSP12	dual specificity phosphatase 12	NS	NS	NEGATIVE	NS
DUSP7	dual specificity phosphatase 7	NS	NS	POSITIVE	NS
ENPP1	ectonucleotide pyrophosphatase/phosphodiesterase 1	NS	NS	NEGATIVE	NS
FBP1	fructose-1,6-bisphosphatase 1	NS	NS	NEGATIVE	NEGATIVE
G6PC	glucose-6-phosphatase, catalytic (glycogen storage disease type I, von Gierke disease)	NS	NS	NEGATIVE	NS
G6PC3	glucose 6 phosphatase, catalytic, 3	POSITIVE	POSITIVE	POSITIVE	NS
INPP5B	inositol polyphosphate-5-phosphatase, 75kDa	NS	NS	POSITIVE	NS
LHPP	phospholysine phosphohistidine inorganic pyrophosphate phosphatase	POSITIVE	POSITIVE	NS	NS
LOC387870	similar to protein tyrosine phosphatase, receptor type, Q isoform 1 precursor; glomerular mesangial cell receptor protein-tyrosine phosphatase; glomerular mesangial cell receptor protein-tyrosine phosphatase precursor	NS	NS	POSITIVE	POSITIVE

PHPT1	phosphohistidine phosphatase 1	POSITIVE	POSITIVE	POSITIVE	NS
PLIP	PTEN-like phosphatase	NS	NS	POSITIVE	NS
PNKP	polynucleotide kinase 3'-phosphatase	POSITIVE	NS	POSITIVE	NS
PPFIA4	protein tyrosine phosphatase, receptor type, f polypeptide (PTPRF), interacting protein (liprin), alpha 4	POSITIVE	NS	NS	NS
PPM1A	protein phosphatase 1A (formerly 2C), magnesium-dependent, alpha isoform	NS	NS	NEGATIVE	NS
PPM1G	protein phosphatase 1G (formerly 2C), magnesium-dependent, gamma isoform	NS	NS	NEGATIVE	NEGATIVE
PPM1L	protein phosphatase 1 (formerly 2C)-like	POSITIVE	NS	POSITIVE	NS
PPP1CB	protein phosphatase 1, catalytic subunit, beta isoform	NS	NS	NEGATIVE	NEGATIVE
PPP1CC	protein phosphatase 1, catalytic subunit, gamma isoform	NS	NS	NEGATIVE	NEGATIVE
PPP1R12C	protein phosphatase 1, regulatory (inhibitor) subunit 12C	POSITIVE	POSITIVE	NS	NS
PPP1R15B	protein phosphatase 1, regulatory (inhibitor) subunit 15B	POSITIVE	POSITIVE	NS	NS
PPP1R2	protein phosphatase 1, regulatory (inhibitor) subunit 2	NEGATIVE	NS	NS	NS
PPP1R3B	protein phosphatase 1, regulatory (inhibitor) subunit 3B	POSITIVE	NS	NS	NS
PPP1R3D	protein phosphatase 1, regulatory subunit 3D	NS	NS	NEGATIVE	NS
PPP1R3F	protein phosphatase 1, regulatory (inhibitor) subunit 3F	NS	NS	NS	NS
PPP1R8	protein phosphatase 1, regulatory (inhibitor) subunit 8	NEGATIVE	NS	NEGATIVE	NS

PPP2R2C	protein phosphatase 2 (formerly 2A), regulatory subunit B (PR 52), gamma isoform	NS	NS	NEGATIVE	NEGATIVE
PTPDC1	protein tyrosine phosphatase domain containing 1	POSITIVE	POSITIVE	POSITIVE	POSITIVE
PTPN22	protein tyrosine phosphatase, non-receptor type 22 (lymphoid)	POSITIVE	POSITIVE	NS	NS
PTPNS1	protein tyrosine phosphatase, non-receptor type substrate 1	POSITIVE	POSITIVE	POSITIVE	POSITIVE
PTPRB	protein tyrosine phosphatase, receptor type, B	NS	NS	NEGATIVE	NS
PTPRR	protein tyrosine phosphatase, receptor type, R	NEGATIVE	NS	NS	NS
PTPRV	protein tyrosine phosphatase, receptor type, V	POSITIVE	NS	NS	NS
RNGTT	RNA guanylyltransferase and 5'-phosphatase	NEGATIVE	NS	NS	NS
SKIP	skeletal muscle and kidney enriched inositol phosphatase	NS	NS	NEGATIVE	NS

5.6 Figures

Figure 5-1

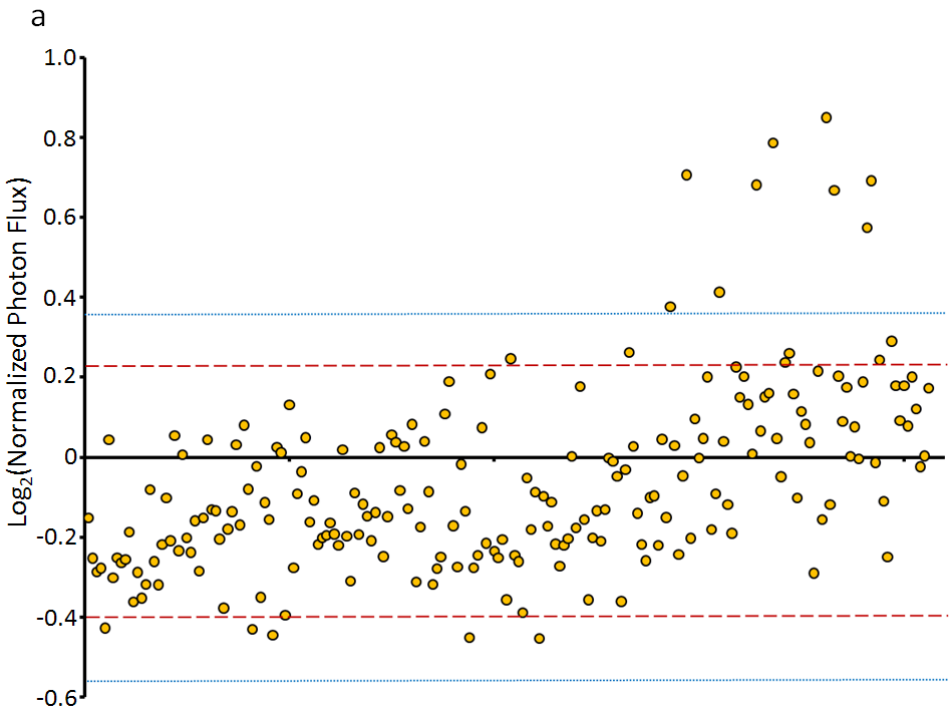

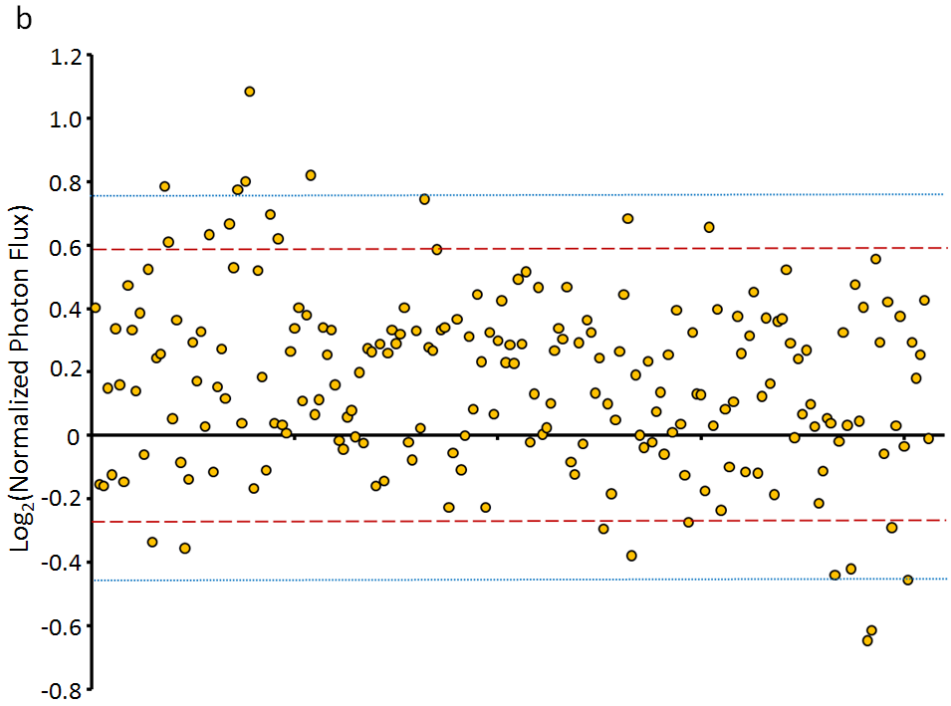

Figure 5-1: High-throughput screening data. Normalized photon flux data for 206 targeted phosphatases is shown at 45(a) and 245(b) minutes after *Salmonella* stimulation. Data is the average of three replicates. Dotted blue and dashed red lines show significance cut-offs for low ($\alpha = 0.1$) and high ($\alpha = 0.02$) stringency targeted error rates, respectively.

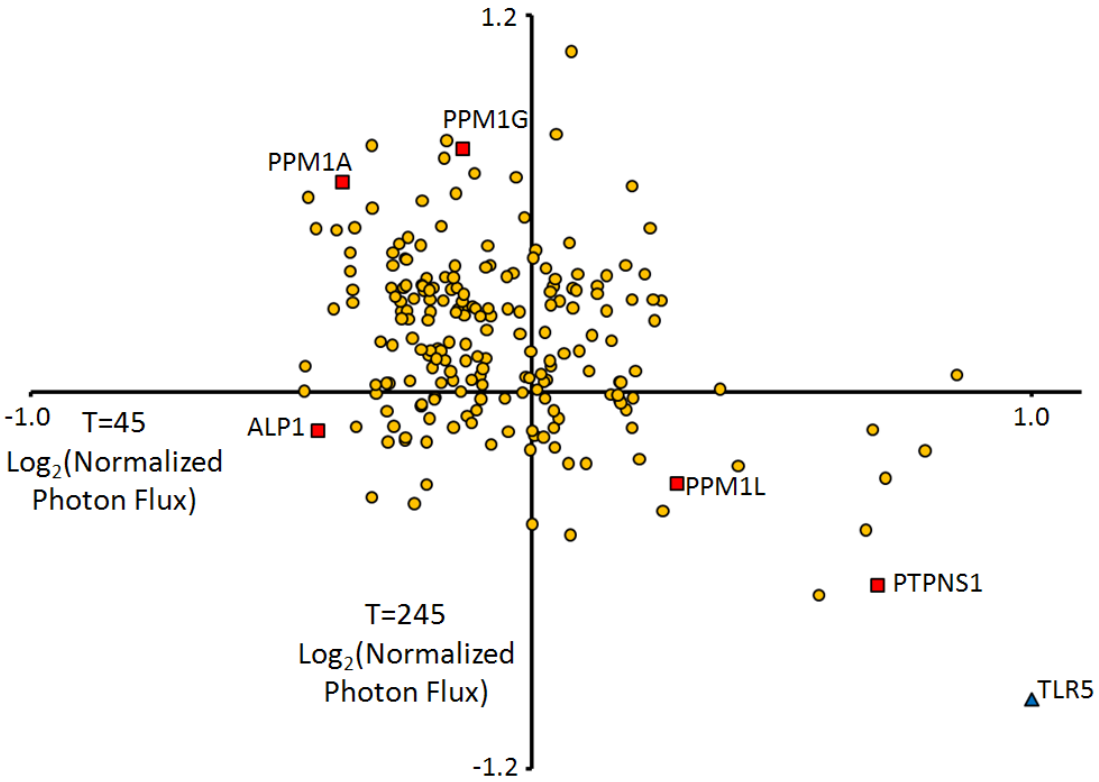

Figure 5-2: PTPNS1, PPM1L, ALP1, PPM1A and PPM1G modulate *Salmonella*-induced NF-κB pathways. The normalized photon flux data from the primary screen at 45 minutes and at 245 minutes are plotted on the x- and y- axes, respectively. Highlighted points show data from specific screening hits and TLR5 control wells.

5.7 References

1. Karin, M., *Nuclear factor-kappaB in cancer development and progression.* Nature, 2006. **441**(7092): p. 431-6.

2. Witt, J., et al., *Mechanism of PP2A-mediated IKK beta dephosphorylation: a systems biological approach.* BMC Syst Biol, 2009. **3**: p. 71.

3. Chew, J., et al., *WIP1 phosphatase is a negative regulator of NF-kappaB signalling.* Nat Cell Biol, 2009. **11**(5): p. 659-66.

4. Sun, W., et al., *PPM1A and PPM1B act as IKKbeta phosphatases to terminate TNFalpha-induced IKKbeta-NF-kappaB activation.* Cell Signal, 2009. **21**(1): p. 95-102.

5. Tamura, S., et al., *PP2C family members play key roles in regulation of cell survival and apoptosis.* Cancer Sci, 2006. **97**(7): p. 563-7.

6. Van Antwerp, D.J., et al., *Suppression of TNF-alpha-induced apoptosis by NF-kappaB.* Science, 1996. **274**(5288): p. 787-9.

7. Ruhul Amin, A.R., et al., *A role for SHPS-1/SIRPalpha1 in IL-1beta- and TNFalpha-dependent signaling.* Oncogene, 2002. **21**(57): p. 8871-8.

8. Ozes, O.N., et al., *NF-kappaB activation by tumour necrosis factor requires the Akt serine-threonine kinase.* Nature, 1999. **401**(6748): p. 82-5.

9. Campbell, E.L., et al., *Resolvin E1-induced intestinal alkaline phosphatase promotes resolution of inflammation through LPS detoxification.* Proc Natl Acad Sci U S A. **107**(32): p. 14298-303.

CHAPTER 6

Conclusions and Future Directions

6.1 *Salmonella* Interactions with Neoplastic Cells

In this work, *Salmonella* demonstrated invasion of cancer cells *in vitro*. However, whether *Salmonella* are capable of invading host cells in a tumor *in vivo* remains to be proven definitively. Existing data does seem to indicate, that in a tumor microenvironment, the majority individual bacteria remain in the extracellular space [1]. This may prove to be an advantage, though, when using bacteria to deliver toxins to tumors *in vivo*. The promoters identified in this work are regulated by a low pH environment. While the intracellular pH in tumors is similar to that of normal cells, the extracellular pH in the tumor microenvironment is particularly acidic [2]. Therefore, a pH-regulated promoter would be specifically activated by extracellular bacteria in the tumor microenvironment, but not by bacteria that had invaded tumor cells. This does pose a problem since the toxin utilized to target the tumor must work on the surface of the tumor cells or be internalized readily by tumor cells in the area. In this interest, Shiga toxin is an ideal choice for cargo of a therapeutic bacterial vector. It can be produced readily by bacteria and binds the glycosphingolipid globotriaosylceramide (Gb3) cellular surface receptor. Gb3 levels are relatively low in normal tissues, but noted to be highly expressed in multiple cancers [3]. By exploiting tumor -targeting bacteria expressing a tumor-specific toxin under the control of a tumor microenvironment-induced promoter, a highly specific bacterial-based therapeutic could be developed.

Studies have also shown that *Salmonella* may be forming a biofilm in the tumor microenvironment [4]. In recent work, microscopic analysis demonstrates bacterial biofilm formation at the site of a tumor *in vivo* [4]. In addition, deletion of genes known to be involved in *Salmonella* biofilm formation enhanced bacterial uptake into tumor cells and immune cells [4]. The authors posited that perhaps bacteria are forming biofilms in the tumor microenvironment to resist phagocytosis [4]. This work may indicate bacterial biofilm genes are an additional set of tumor microenvironment-induced promoters that could also be exploited in bacterial tumor-targeting studies.

Finally, it would be worthwhile to further characterize the regulation of the *Salmonella* genes uncovered in this screen. For instance, other stimuli bacteria encounter during transit through the acidic environments of the stomach and intestines may also induce activation of the identified promoters. Other conditions bacteria may respond to during a typical infection include oxygen concentration, osmolarity and acetate concentration , all conditions that may also be relevant to growth in the tumor microenvironment [5].

6.2 How Neoplastic Cells Respond to *Salmonella*

Bacterial adaptation to the tumor microenvironment addresses only half of the *Salmonella*-host interaction. Also at play are the host cells comprising a tumor likely respond to the presence of a foreign organism by activating proinflammatory signaling. In this work, I demonstrate the response of HCT116 colon carcinoma cells to *Salmonella*. HCT116 cells respond predominantly to bacterial flagellin with a robust activation of NF-κB signaling. Interestingly, the dynamics and amplitude of *Salmonella*-induced NF-κB signaling differ from that of TNFα-induced signaling. *Salmonella* stimulation of HCT116 cells induced less degradation of IκBα, but more and sustained NF-κB

transcriptional activation compared to TNFα stimulation. Perhaps Salmonella and TNFα are activating different downstream transcriptional programs of NF-κB. Microarray analysis of *Salmonella*-treated versus TNFα-treated cells would provide a way to interrogate the differences in downstream gene activation.

To identify novel kinases and phosphatases involved in detection of *Salmonella* and activation of proinflammatory signaling, an siRNA high-throughput screen was utilized. One striking observation from the screening data is that most kinases and phosphatases have some effect on NF-κB signaling. This observation serves to highlight the vast amount of interconnectivity between intracellular signaling pathways and must be considered when analyzing screen data and selecting candidates for follow-up. Another potential caveat of this high-throughput screen was the use of siRNA for target knockdown, a known ligand of TLR3 [6]. While normalizing to negative control, non-targeting siRNA should account for this effect, TLR3 is also known to activate NF-κB signaling, and therefore its potential effect should be acknowledged when choosing candidate hits for further study. Additionally, TLR5-positive, TLR3-negative cell lines may serve as a useful tool for follow-up studies.

In the high-throughput screen, two of the most significant hits at both phases of the pathway tested (degradation and resynthesis) were MAP kinase kinases. Intriguingly, IKK has a similar role to MAP kinase kinases in its signal transduction pathway in that its activity is one kinase removed from proteins thought to act at the intracellular domain of the activated cell surface receptor. It is tempting, therefore, to consider a model where all pathways downstream of an activated TLR are interconnected and interdependent. Perhaps proper progression of all signaling pathways downstream of a receptor is

required for appropriate signal transduction in any singular pathway. For instance, blocking the activation of MAP2K2 or MAP2K3 may reprogram all downstream and parallel intracellular signaling pathways, thus preventing IKK activation as well. This indicates future studies of intracellular signaling should embrace a global view of cellular pathways to fully understand the role of specific proteins.

6.3 References

1. Pawelek, J.M., K.B. Low, and D. Bermudes, *Bacteria as tumour-targeting vectors.* Lancet Oncol, 2003. **4**(9): p. 548-56.

2. Tannock, I.F. and D. Rotin, *Acid pH in tumors and its potential for therapeutic exploitation.* Cancer Res, 1989. **49**(16): p. 4373-84.

3. Engedal, N., et al., *Shiga toxin and its use in targeted cancer therapy and imaging.* Microb Biotechnol, 2010. **4**(1): p. 32-46.

4. Crull, K., et al., *Biofilm formation by Salmonella enterica serovar Typhimurium colonizing solid tumours.* Cell Microbiol, 2011. **13**(8): p. 1223-33.

5. Altier, C., *Genetic and environmental control of salmonella invasion.* J Microbiol, 2005. **43 Spec No**: p. 85-92.

6. Kleinman, M.E., et al., *Sequence- and target-independent angiogenesis suppression by siRNA via TLR3.* Nature, 2008. **452**(7187): p. 591-7.